

論文 / 著書情報
Article / Book Information

題目(和文)	水熱処理と水洗処理を組み合わせたパーム椰子房からの低カリウム含有ペレット燃料の製造
Title(English)	Low-potassium Content Pellet Fuel Production from Palm Empty Fruit Bunch by Hydrothermal and Washing Co-treatment
著者(和文)	SrikandiNovianti
Author(English)	SRIKANDI NOVIANTI
出典(和文)	学位:博士(工学), 学位授与機関:東京工業大学, 報告番号:甲第10202号, 授与年月日:2016年3月26日, 学位の種別:課程博士, 審査員:吉川 邦夫,高橋 史武,竹下 健二,加茂 徹,時松 宏治
Citation(English)	Degree:., Conferring organization: Tokyo Institute of Technology, Report number:甲第10202号, Conferred date:2016/3/26, Degree Type:Course doctor, Examiner:,,,,,
学位種別(和文)	博士論文
Type(English)	Doctoral Thesis

**LOW-POTASSIUM CONTENT PELLET FUEL
PRODUCTION FROM PALM EMPTY FRUIT BUNCH
BY HYDROTHERMAL AND WASHING
CO-TREATMENT**

Doctoral Dissertation

Srikandi Novianti



Department of Environmental Science and Technology
Interdisciplinary Graduate School of Science and Engineering
Tokyo Institute of Technology
February 2016

Acknowledgement

In the name of Allah the merciful. The author wishes to praise Allah for His guidance to finish this research.

This doctoral dissertation is a partial requirement for graduating from the Department of Environmental Science and Technology, Tokyo Institute of Technology. It would not be completed without full support of many people; therefore the author gratefully acknowledges:

1. My beloved parents, my big family, especially my husband Muhammad Fadlil, and our “baby”, who always give endless support on *everything* and during my study in Japan.
2. Professor Kunio Yoshikawa, as the supervisor, for giving me the best opportunity in my life, and for his kind guidance and assistance throughout my study in Japan.
3. Associate Professor Fumitake Takahashi, as the co-advisor, and Associate Professor Koji Tokimatsu, for valuable advices during the study.
4. Mrs. Eriko Ohno, for administrative support, and all supportive staffs in Department of Environmental Science and Technology, Tokyo Institute of Technology.
5. Japanese Government Monbukagakusho Scholarship scheme for its financial support during my study.
6. Dr. Pandi Prawisudha for valuable discussions and support during research in Mechanical Engineering, Institut Teknologi Bandung.
7. Professor Hiroaki Sumida from Nihon University and Associate Professor Akiko Nakagawa-izumi from Tsukuba University for their kind help and support in this research (Chapter 3 and 4).
8. HT- fuel group members, Ms. Anissa Nurdiawati and Mr. Ilman Nuran Zaini, for their remarkably support and silly discussions during experiments.
9. All friendly members of Yoshikawa-Takahashi-Tokimatsu Laboratory for their close friendship.
10. Friends and colleagues in PPI-Tokodai and Japan who makes me always feel at home.

Comments, suggestions, and criticisms concerning some errors would be greatly appreciated as they will contribute to further improvement of this research

Srikandi Novianti

Summary

In Southeast Asia, one kind of biomass that being considered as the most potential for energy production is empty fruit bunch (EFB), a byproduct of palm oil industry. This byproduct is poorly utilized yet causing many problems associated with the improper disposal practices of EFB. Hence, the utilization of EFB as a source of renewable energy is considered to be crucial. Despite of the abundant resource of EFB, as like other biomass, it also faces several limitations in its use. The bulk density is low and the moisture content of fresh EFB is approximately 65%. It also contains high ash and potassium content that promotes slagging and fouling problems in boilers. Currently, several different approaches have been considered to improve the fuel properties of biomass. In this study, the combination of hydrothermal treatment (HTT), washing pre-treatment and pelletization were employed in order to mitigate the issues.

The lab scale investigation on HTT of waste EFB was performed in order to upgrade the fuel qualities of the biomass into value added solid fuel. The HTT experiments were conducted using a batch type autoclave reactor. Four reaction temperatures were investigated at 100, 150, 180, and 220°C with the holding time of 30 minutes. The results indicated that the fuel qualities of the product was improved after HTT; such as a higher carbon content, a higher energy density, a lower O/C and H/C ratios compared with the raw feedstock. The calorific value of the EFB was increased from 17 MJ/kg to approximately 20 MJ/kg after HTT, which is equal to low-grade sub-bituminous coal. The mechanism of HTT was also investigated by the Van Krevelen diagram and the FTIR analysis. The main reaction pathways that might occur during the HTT process at a mild temperature were the dehydration and the hydrolysis. Considering the energy consumption and fuel property, HTT at 180°C is found to be most favorable for large-scale production of solid fuel from EFB.

High potassium content in EFB leads to the high slagging and fouling tendency in furnaces. Hence, the removal of the potassium content by combination of HTT and the water washing is also investigated. After HTT, the treated product was subjected to water washing experiments that were conducted using a batch-washing system. The samples were mixed with the ratios of 1:5, 1:8, 1:10, 1:20 and 1:50 of distilled water at the washing temperature of 60°C for 15 min. The results indicated that the major removal of potassium was attributed to the HTT process, with 92% potassium removal

can be obtained after HTT combined with the water washing. The combination also lowered the ash content and the chlorine content of EFB down to averagely 0.9% and 0.19%, respectively. According to the results, it was found that 180°C was the optimum HTT temperature for the effective potassium removal. Combination of HTT and the water washing improved the slagging and fouling indices, exhibiting positive results in the term of the deposition tendency, thus clarified that the removal of potassium may lead to the lower deposition tendency.

The comparison of the pellets produced from raw EFB, and the hydrothermally treated EFB (hydrochar) as well as the washed hydrochar were investigated. Pelletization of biomass has been practiced widely to produce homogenous products with a high density. However, the study on the pelletization of the washed hydrothermally treated biomass is currently limited. The pelletization was conducted using a single pellet making device and performed in the room temperature and the pressure of 150 MPa with the holding time of 30 s. From the results, washed HTT-EBF pellets showed a high mechanical strength, and high durability compared to HTT-EBF and raw EFB pellets. The pellets also showed the hydrophobic nature against the moisture exposure. However, washed HTT EFB pellets required higher energy for making pellet. From the analysis, it was found that the changes in the composition of EFB biomass by HTT and the washing process regulate the pelletization behavior and affect the bonding mechanism during the pelletization.

The possibility to use the leachate from the washing process of HTT-EBF for the agricultural purpose was studied. The analysis of the properties of the leachate and the phytotoxicity test were performed to decide the safety approach when applying the leachate back to the palm oil plantation. Considering the macronutrients amount, the leachate could not be used as an universal fertilizer, but primarily as an organic nutrient supplement. A proper dilution factor was found to reduce the phytotoxicity effect of the leachates to the plant growth.

Overall, the combination of the pelletization, HTT, and the washing co-treatment is promising for upgrading abundant EFB biomass into clean, energy dense, homogenous, friable, durable, and hydrophobic solid fuel that is ready for domestic and international markets, while dealing with the waste EFB problem in the plantation.

Table of Contents

List of Figures	iii
List of Tables.....	v
Chapter 1. Introduction.....	1
1.1 Biomass as a renewable energy source	1
1.2 Lignocellulosic biomass.....	2
1.2.1 Chemical composition.....	2
1.2.2 Conversion technologies.....	4
1.3 Oil palm residues: Empty Fruit Bunch.....	6
1.3.1 Biomass composition.....	7
1.3.2 EFB Potential in Indonesia.....	8
1.3.3 Challenges in utilizing EFB for thermo-chemical conversion.....	9
1.4 Biomass pretreatment process	10
1.4.1 Hydrothermal treatment	10
1.4.2 Water washing	12
1.4.3 Pelletization	13
1.5 Research objectives.....	14
1.6 Thesis structure	15
References	17
Chapter 2. Hydrothermal upgrading of Empty Fruit Bunches.....	21
2.1 Background	21
2.2 Material and method.....	22
2.2.1 Biomass material	22
2.2.2 HTT	22
2.2.3 Analytical method.....	22
2.2.4 Process analysis	25
2.3 Result and Discussions	27
2.3.1 Mass yield and energy value of hydrochars	27
2.3.2 Physicochemical characteristics of hydrochars.....	28
2.3.3 Mass balance and energy balance	32
2.3.4 Combustion characteristics	36
2.3.5 Mechanism of HTT	39
2.3.6 Treatment of the liquid HTT residue.....	46
2.4 Summary.....	50
References	51
Chapter 3. Low potassium fuel from EFB via hydrothermal treatment and water washing.....	54
3.1 Background	54
3.2 Material and methods.....	55
3.2.1 Biomass material	55
3.2.2 HTT experiments	55
3.2.3 Washing experiments.....	56
3.2.4 Analytical methods.....	56
3.2.5 Data Analysis	57
3.3 Results and discussion	58
3.3.1 Fuel properties of washed hydrochar	58
3.3.2 Effect of HTT and washing on potassium content	59

3.3.3	Potassium balance.....	63
3.3.4	Ash composition and slagging fouling tendency.....	64
3.3.5	Effect of washing on combustion characteristics.....	66
3.3.6	FTIR Analysis.....	68
3.4	Summary.....	70
	References.....	71
Chapter 4.	Pelletized fuel from EFB hydrochar and washed EFB hydrochar.....	74
4.1	Introduction.....	74
4.2	Material and methods.....	75
4.2.1	Fuel preparation.....	75
4.2.2	Pelletization technique.....	75
4.2.3	Characterization methods.....	76
4.2.3.1	Physical characterization.....	76
4.2.3.2	Durability test.....	77
4.2.3.3	Compressive test.....	77
4.2.3.4	Equilibrium moisture content.....	78
4.2.3.5	SEM analysis.....	78
4.2.3.6	Lignocellulosic component analysis.....	79
4.3	Results and discussion.....	79
4.3.1	Lignocellulosic chemical composition of the pelletization feedstock.....	79
4.3.2	Pellet characteristics.....	80
4.3.2.1	Appearance.....	80
4.3.2.2	Particle size distribution.....	81
4.3.2.3	Mass and energy density of pellets.....	82
4.3.3	Mechanical strength and durability of pellets.....	84
4.3.3.1	Compressive strength.....	84
4.3.3.2	Durability.....	86
4.3.4	Hydrophobicity.....	88
4.3.5	Morphology of pellet and bonding mechanism.....	89
4.3.6	Energy input of compression of pellet.....	92
4.3.7	High HTT temperature consideration.....	93
4.4	Summary.....	95
	References.....	96
Chapter 5.	Evaluation of the leachate for agricultural purpose.....	99
5.1	Introduction.....	99
5.2	Material and methods.....	99
5.2.1	Washing treatment.....	99
5.2.2	Analysis.....	100
5.3	Results and discussion.....	102
5.3.1	pH and EC of the leachate.....	102
5.3.2	Macronutrient of the leachate.....	103
5.3.3	C/N ratio.....	104
5.3.4	Phytotoxicity.....	105
5.4	Summary.....	107
	References.....	108
Chapter 6.	Conclusions and Recommendation.....	109
6.1	Conclusions.....	109
6.2	Recommendations.....	110

List of Figures

Figure 1-1. Lignocellulosic biomass.....	2
Figure 1-2. Conversion routes for dry biomass	4
Figure 1-3. Conversion routes for wet biomass	5
Figure 1-4. Palm oil utilization diagram for oil production.....	6
Figure 1-5. Palm oil	7
Figure 1-6. Global distribution of oil palm cultivation.....	8
Figure 1-7 Effect of thermal pre-treatments on biomass structure	11
Figure 1-8. Outline of this research	15
Figure 2-1. Lab scale hydrothermal apparatus.....	22
Figure 2-2. The SEM images of EFB hydrochars	29
Figure 2-3. Mapping of the chlorine content on the hydrochar surface	31
Figure 2-4. Mass balance for HTT of EFB at the temperature of 180°C	32
Figure 2-5. TG and DTG curves of raw EFB and hydrochars.....	37
Figure 2-6. Van Kravelen diagram of raw EFB and its resulting hydrochar	40
Figure 2-7. FTIR spectra of raw EFB and its derived hydrochar.	42
Figure 2-8. GC/MS chromatogram of the EFB liquid products of HTC.....	43
Figure 2-9. Pathways of cellulose and hemicellulose degradation	45
Figure 2-10. Main reaction pathway of hemicelluloses hydrolysis	45
Figure 2-11. Main reaction pathways of cellulose hydrolysis	45
Figure 2-12. Macronutrient in liquid product	47
Figure 2-13. N, P, K solubilization ratios	47
Figure 2-14. C/N ratios of HTT liquids at different temperatures.....	49
Figure 3-1. Lab scale hydrothermal apparatus.....	55
Figure 3-2. Potassium concentration of EFB after HTT and washing.....	60
Figure 3-3. Potassium removal efficiency of EFB after HTT and washing	60
Figure 3-4. Potassium concentration and potassium removal efficiency	61
Figure 3-5. Potassium distribution in the product after HTT and washing	63
Figure 3-6. Slagging and fouling indices for raw- EFB and pretreated products	66
Figure 3-7. TGA profiles of unwashed and washed HTT-180 hydrochars	67
Figure 3-8. DTG profiles of unwashed and washed HTT-180 hydrochars	67
Figure 3-9. FTIR spectra of unwashed and washed HTT-180 hydrochar	70
Figure 4-1. The pelletization unit set up	76
Figure 4-2. The tumbler can set up in the laboratory.....	77
Figure 4-4. Static desiccators technique	78
Figure 4-5. The appearance of the pellets.....	81
Figure 4-6. Particle size distribution of raw EFB and hydrochars.....	82
Figure 4-7. Initial, final density and expansion of all the pellet samples	82
Figure 4-8. Mass and energy densities of all the pellet samples.....	83
Figure 4-9. The compressive force versus displacement curves of the pellets.....	85

Figure 4-10. The compressive strength of the pellets	85
Figure 4-11. The appearance of the pellets after tumbling	86
Figure 4-12. The durability index of pellets.	87
Figure 4-13. The moisture uptake of pellets at 26-28°C and 75-80% RH.....	88
Figure 4-14. SEM images of the cross section of pellets.....	90
Figure 4-15. The magnification of SEM images of HTW-180 pellet.....	91
Figure 4-16. The magnification of SEM images of HTT-220 pellet.....	91
Figure 4-17. The typical force-displacement plot during the compression	92
Figure 4-18. The compression energy required for making each pellet	93
Figure 4-19. Effect of pre-treatment on the durability and strength of pellets	94
Figure 5-1. pH meter.....	100
Figure 5-2. TOC-L with unit TNM-L.....	100
Figure 5-3. Seed germination test	101
Figure 5-4. The C/N ratio of all the leachate samples	104
Figure 5-5. Seed germinated using leachates from washed hydrochars	106
Figure 6-1. Outline of this research	109

List of Tables

Table 1-1 Compositions of EFB	7
Table 2-1. HHV, mass, energy yields of the raw EFB and the hydrochars	28
Table 2-2. Chemical characteristics and properties of the raw EFB, and the hydrochars	28
Table 2-3. Elemental metal analysis of hydrochar by SEM-EDX.....	31
Table 2-4 Mass balance in the HTT process of EFB	33
Table 2-5. Estimated energy produced and utilized	34
Table 2-6. Tank Dimensions and Operational Data	35
Table 2-7 Re-calculated energy balance	36
Table 2-8. The combustion characteristic parameters for the raw EFB and its corresponding hydrochars	39
Table 2-9. Products detected in liquid extract after the HTC process at 180, 200 dan 220 °C for t = 22 h	44
Table 2-10. Micronutrient and heavy metal in liquid residue.....	48
Table 2-11. Effect of the HTT liquid product from EFB on the germination of Komatsuna seedlings.	50
Table 3-1. Slagging, fouling, alkali, and ratio-slag indices, Cl content, definition and their limits	58
Table 3-2. Ultimate analysis and HHV of the raw-EFB and resulting hydrochar at various HTT and washing conditions*	58
Table 3-3. Comparison between the advantage of washing treatment and combination of HTT and washing	62
Table 3-4. Ash composition of raw-EFB and pretreated EFB.....	65
Table 3-5. Ash element in the untreated and treated EFB.	66
Table 3-6. Combustion characteristics of the washed and unwashed HTT-180 hydrochar	68
Table 4-1. The lignocellulosic chemical composition of the raw EFB and treated hydrochars.....	80
Table 5-1. The pH and EC values of leachates obtained from washing of hydrochars.....	103
Table 5-2. The macronutrients and the TC values of the hydrochar leachates.....	104
Table 5-3. Effect of leachates from washed hydrochars on the germination of Komatsuna seedlings	105

Chapter 1. Introduction

1.1 Biomass as a renewable energy source

Renewable energy is energy which comes from natural resources such as sunlight, wind, rain, tides, waves, and geothermal heat, which are renewable (naturally replenished), as the International Energy Agency explains [1]:

Renewable energy is derived from natural processes that are replenished constantly. In its various forms, it derives directly from the sun, or from heat generated deep within the earth. Included in the definition is electricity and heat generated from solar, wind, ocean, hydropower, biomass, geothermal resources, and biofuels and hydrogen derived from renewable resources.

The use of renewable energy sources is becoming increasingly necessary, if we are to achieve the changes required to address the impacts of global warming [2]. Several problems associated with the fossil fuel exploitation also change the current energy scheme to move towards a more sustainable model. In the transition to cleaner technologies, biomass stands out as one of most important renewable energy sources. Moreover, the high cost of fossil fuels and technological progress have made the appearance of energy development of biomass systems possible to allow us to obtain energy directly or indirectly by means of combustion, pyrolysis or gasification processes. These development systems are becoming more and more efficient, reliable and clean. Due to this fact, biomass is currently being taken into account as a total or partial alternative to fossil fuels.

Biomass energy, or “bioenergy,” is the energy of sunlight that was stored in chemical bonds of organic material which is produced by green plants converting sunlight into plant material through photosynthesis. Biomass has always been a major source of energy for mankind. Biomass is a fourth largest source of energy and providing at about 14 percent of the world’s total energy consumption[3, 4]. Biomass is the only renewable energy resource that can be converted into any form of fuel including solid, liquid and gaseous[5].

The life cycle of biomass as a renewable material has a neutral effect on CO₂ emission. It also offers the possibilities of a closed mineral and nitrogen cycle. The environmentally hazardous sulfur dioxide (SO₂), which is produced during combustion of fossil fuels, leading to acid deposition, is not a major problem in biomass systems due to the low sulfur content of biomass (< 1% compared to 1 to 5% for coal)[6]. Biomass is widely used to meet wide variety of energy requirements such as heat and electricity generation, and producing biofuels for vehicles. Biomass can readily be used in boilers to produce directly heat and/or steam to generate electricity. Co-firing with

coal is an attractive option with a relatively low need for additional investments [7]. Moreover, using biomass as a fuel can also be an opportunity to empower rural communities.

Although it is a common source of energy (especially in developing countries), biomass is not such an ideal fuel due to its fibrous nature, low density, and low heating value. The transportation and handling of solid biomass is expensive considering its low fuel value. Furthermore, lack of developed conversion technologies and high costs limit the scope of biomass usage to energy. Nonetheless, biomass is still attractive feedstock for renewable energy and the price of biomass is relatively stable and less than the fluctuating fossil fuel price. Consequently, to ease the biomass conversion into energy, biomass should be converted to a more hydrophobic, energy dense fuel, with better handling characteristics compare to its raw conditions.

1.2 Lignocellulosic biomass

Lignocellulosic biomass covers most plants that have three main components: cellulose, hemicelluloses and lignin as shown in Figure 1-1. The term lignocellulosic is coming from the chemical composition of the plants. Terrestrial biomass, like farm crops, woody trees from forest, agricultural residues are considered lignocellulosic biomass. The composition can differs from one plant species to another, for example most softwoods have more cellulose than grassy type biomass, whereas wheat straw and leaves contain more hemicelluloses [8]. The three main components are chemically bonded by non-covalent forces, and cross-linked together to provide structure and rigidity in the biomass.

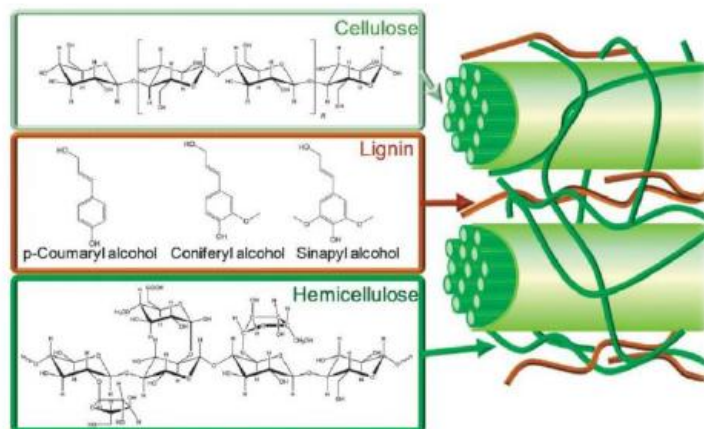


Figure 1-1. Lignocellulosic biomass

1.2.1 Chemical composition

The chemical compositions of lignocellulosic biomass mainly consist of about 95% of three biopolymers of cellulose, hemicelluloses, and lignin. The remaining contents is composed of a profusion of associated materials called extractives; such as resins, fats, tanning agents, starch, sugar, proteins, and minerals. The proportions of the chemical components vary in accordance with their species types.

1.2.1.1 Cellulose

Cellulose is a high-molecular-weight (10⁶ or more) linear chain of glucose linked by β -glycosidic linkage forming long chains (elemental fibrils) linked together by the hydrogen bonds and van der Waals forces. This chain is highly stable and resistant to chemical attack because of the presence of high degree of intra and intermolecular hydrogen bonding [9]. The strong hydrogen bonding provides a strong and rigid structure of the polymer. The chains tend to arrange in parallel and form a crystalline structure that cause the thermal degradation of cellulose starting in the temperature range of 300 - 400°C [10]. Due to its high degree of crystallization, in spite of owing a relatively high number of hydrophilic groups, cellulose is not water soluble but acts hygroscopically (water-absorbing).

1.2.1.2 Hemicelluloses

Hemicelluloses have a complex carbohydrate structure consisting of short, highly branched chains of sugars (five-carbon sugars such as D-xylose and L-arabinose, and six-carbon sugars such as D-galactose, D-glucose, and D-mannose) and uronic acid. It has lower molecular weight than cellulose. Hemicelluloses always appear as a substance associated with cellulose. Because of its low molecular weight and amorphous structure, the hemicelluloses is a highly soluble polymer in water. It is the least thermally stable polymer among all three lignocellulosic polymers, followed by cellulose and lignin. The thermal degradation of cellulose starts at 200 - 300°C [10], while its solubilization in water starts at about 180°C under hydrothermal conditions [11, 12]. The hemicelluloses is relatively easy to be hydrolyzed into basic sugars.

1.2.1.3 Lignin

Lignin is a biopolymer rich in three-dimensional, highly branched polyphenolic constituents that provide structural integrity to plants. Lignin found as the most abundant polymer in the nature and is present in the cell wall of biomass. Lignin is amorphous hetero-polymer with no exact structure and highly hydrophobic in nature. Lignin is more difficult to be dehydrated than cellulose and hemicelluloses and is the most thermally stable polymer with the thermal degradation starting at 600°C under atmospheric conditions [10]. Nonetheless, its degradation under hydrothermal conditions starts at lower temperature of 220°C [11]. Lignin is the polymer in biomass that shows glass temperature transition behavior in the temperature range of 135 -

165°C where it melts and acts as natural binding agent during the densification process [13, 14].

1.2.1.4 Extractives

Extractives are the minor constituents in the plants, the organic substances which have low molecular weight and soluble in neutral solvents. Their mass related concentration is typically 4 – 10% and the contents of extractives may vary among wood species, location, and season. Extractives include resin (combination of terpenes, lignans, and another aromatics), fats, waxes, fatty acids and alcohols, terpenes, tannins, minerals and flavonoids. Although extractives constitute only minor portions of the molecular substance of plants, they can determine significant characteristics of the raw materials; such as the resistivity against fungi and insects, the odor, the water-repellent, the impregnability and the flammability [15].

1.2.2 Conversion technologies

There are several conversion techniques available for the conversion of biomass. Nevertheless, the choice of the pre-treatments is very limited depending on the type of feedstock (wet biomass or dry biomass, desired output products (solid, liquid, and gas), distribution and properties of the product for different applications.

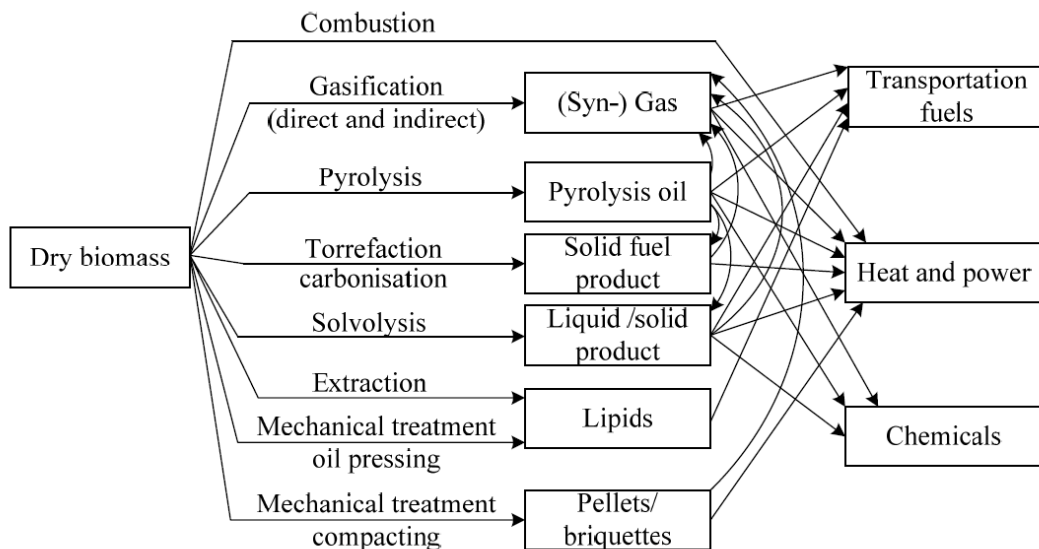


Figure 1-2. Conversion routes for dry biomass [16]

Biomass with the moisture less than 30 wt% is categorized as dry biomass [16]. Examples of dry biomass are wood, straw, and other sun dried waste. The conversion pathways for the dry biomass are depicted in Figure 1-2. The most common method used for conversion of dry biomass is the direct combustion to produce heat and power.

However, the inferior physicochemical properties of the biomass causes the direct combustion of biomass to be considered as not eco-friendly route for biomass conversion, since it produces smoke and other harmful gaseous. Mechanical treatment like compaction or densification is widely used method where biomass is compacted in regular shaped product such as pellets or briquettes [4]. Oil pressing from the oil rich seeds is also one of mechanical methods for the production of biodiesels. Both of mechanical treatment can be applied in the plantation site and can support the development of rural communities. Apart from combustion, fast and slow pyrolysis can be applied to produce bio-oil, char and gas. The gasification is also one possible route to convert biomass to fuel gas or to syngas for production of synthetic fuel. Solvolysis is another conversion process where the biomass is mixed with hot compressed water to recover sugar and liquid intermediate compounds [17].

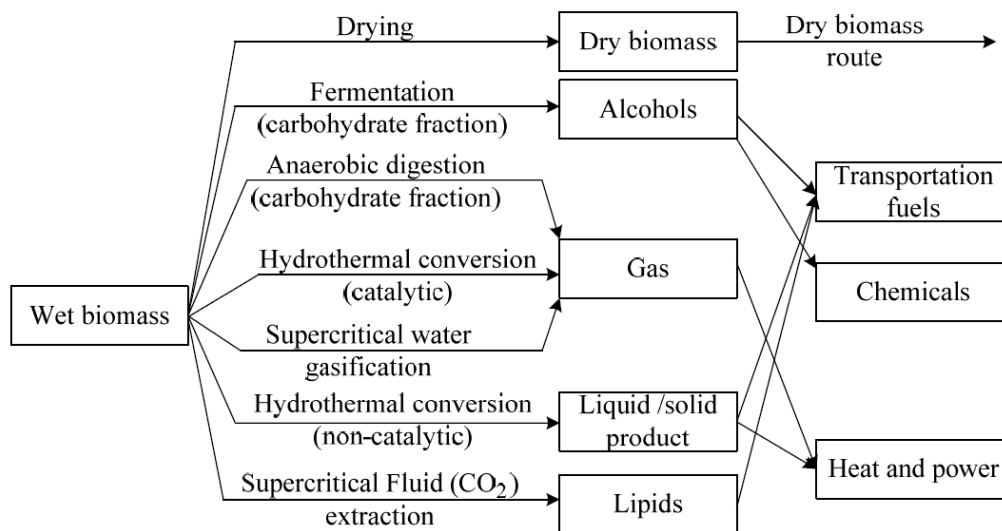


Figure 1-3. Conversion routes for wet biomass [16]

Wet biomass includes sewage sludge, sugar solutions, algae suspensions and waste animal manure from biomass processing or from biorefineries. The conversion pathways for the wet biomass are shown in Figure 1-3. Wet biomass can be dried with drying processes; however this is not the most efficient and economical way to operate. The conversion of wet biomass into a fuel can be processed via biological methods like anaerobic digestion or fermentation. Generally, biological routes are limited to certain carbohydrate fractions in biomass. However, for second generation conversion processes, enzymes and pretreatment options are being developed that target the lignocellulosic biomass in broader sense [16]. The next conversion is conversion in hot compressed water (both sub- and super-critical) that aimed at the production of hydrophobic liquids, solids and gases [18]. Presence of water in hot compressed water treatment like the hydrothermal conversion eliminates the pre-drying requirement of wet biomass which is energy extensive and costly for the processing of wet biomass when performed under conventional dry thermal pretreatments like pyrolysis and

torrefaction [19]. The thermochemical conversion methods are more preferable than biological conversions since they offer significant merits like shorter reaction time and higher product yields [20].

By combining dry and wet conversion routes, a wide spectrum of interconnected thermochemical biomass conversion routes toward final products is possible and may be used in a biorefinery. In such complex concepts, the hydrothermal conversion can be applied to produce intermediate energy carriers, in primary conversion steps like gasification, or it can be used for working up of side/ waste streams from conversion processes of biomass to food, fuel, and chemicals [16].

1.3 Oil palm residues: Empty Fruit Bunch

Empty fruit bunch (EFB) is a major waste generated from the processing of palm oil at the mills. In general, fresh fruit bunch contains only 21% palm oil (See Figure 1-4), while the rest are fiber (14-15%), palm kernel (6-7%), shell (6-7%) and EFB (22%) which left as biomass residue [21]. Palm oil fresh fruit bunch and empty fruit bunch are depicted in Figs. 1-5.b and 1-5.c, respectively. For every 100 tons of fresh fruit bunches (FFBs) processed, 20 - 25 tons of EFB is produced.

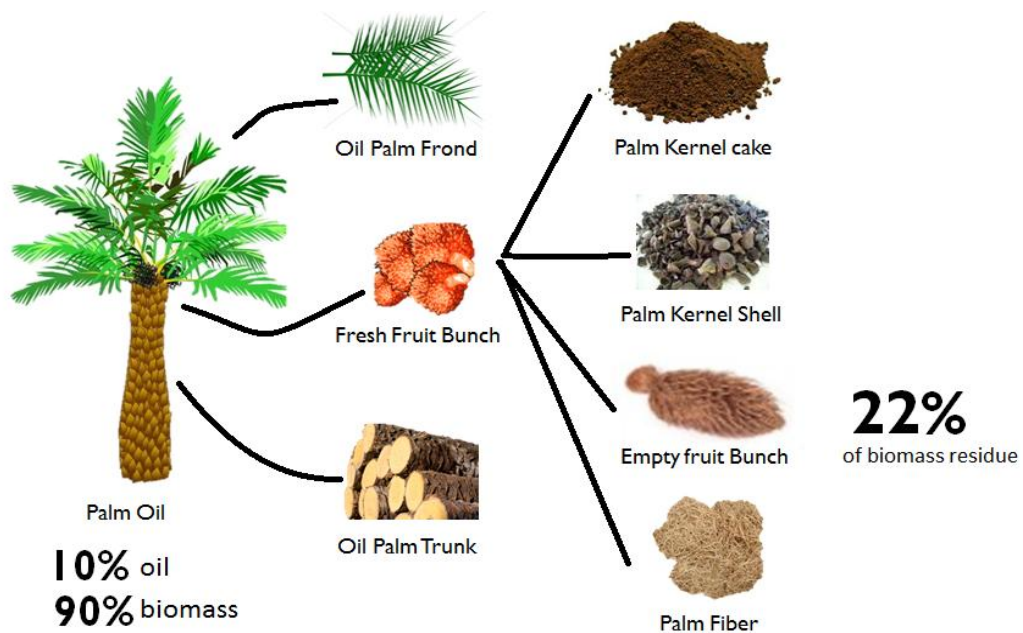


Figure 1-4. Palm oil utilization diagram for oil production

EFB is a bunch of foliage surrounding the oil palm fruit. EFB is generated when sterilizing fresh fruits and pericarp along with bunches. The sterilization is needed to inactivate the enzymatic process, avoiding an excessive production of free fatty acids. EFB is then separated from the fruit by rotary drum or fixed drum after sterilization. The value of EFB is commercially low and posing a disposal problem because of its

large quantity [22]. Purified palm oil only represents, approximately, 20 wt% of the harvested material and consequently, many palm oil manufacturers face with problems associated with increasing waste streams, such as insufficient dumping spaces and bad odor and hazardous methane gas from the decomposition processes [23]. Conventionally in Indonesia, EFB is burned, disposed of in landfills, or composted to organic fertilizer [22]. The burning of EFB is for steam and power generation for factories and the ash is utilized as potassium fertilizer. However, burning EFB may cause environmental problems, such as air pollution due to incomplete combustion and very fine size of ash particles which may harm respiratory system of human [24].

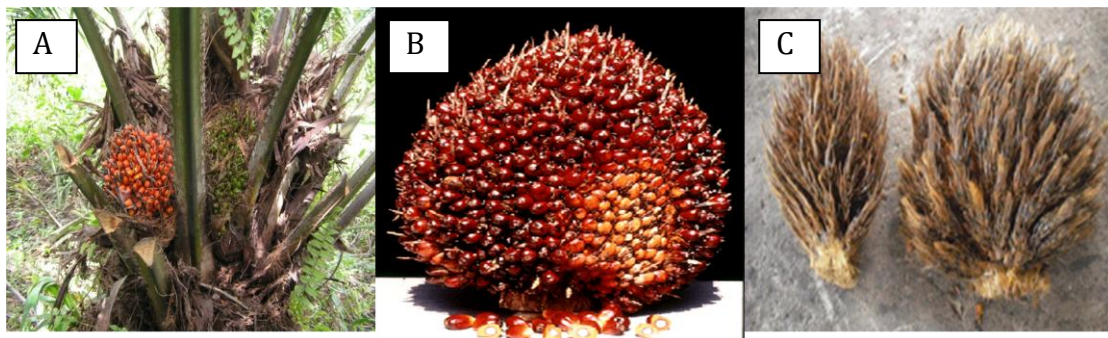


Figure 1-5. Palm oil (a) tree, (b) fresh fruit bunch (FFB), and (c) empty fruit bunch (EFB)

The other utilizations of EFB have also been investigated, such as for natural fiber reinforced composites [25, 26], filler material in polypropylene (PP) composite [27], and bioethanol production [24]. EFB pellets exhibit high energy content due to decrease in the moisture content, uniform size, and superior combustion performance and high mechanical strength [28].

1.3.1 Biomass composition

EFB as lignocellulosic material comprises of three major sugar-based polymeric components; cellulose, hemicelluloses and lignin. Table 1-1 shows the typical chemical composition of oil palm EFB. This variation of the chemical composition gives impact on the thermal decomposition behavior of EFB during the hydrothermal treatment and also during densification process. Special attention should be drawn on the potassium and chlorine content in the raw EFB that will heavily affect the ash melting behavior in the furnace, causing some technical problems when combusting it in the furnace.

Table 1-1 Compositions of EFB [29]

Properties	Raw EFB
Proximate Analysis* (wt%)	
Volatiles	78.7
Fixed Carbon	15.3
Ash	5.9

Ultimate analysis**	
Carbon	43.56
Hydrogen	5.34
Nitrogen	0.56
Chlorine	0.67
Oxygen (diff)	44.86
Potassium (%DM)	3.24
HHV (MJ/kg)	16.8
Component analysis (wt%)	
Hemicellulose	35.0 ^a
Cellulose	43.8 ^a
Lignin	16.0 ^a
Extractives	4.8 ^a

*dry basis. **dry ash-free basis.

1.3.2 EFB Potential in Indonesia

The oil palm provides one of the leading vegetable oils produced globally, accounting for one-quarter of global consumption and approximately 60 per cent of international trade in vegetable oils. Oil palm is grown across more than 13.5 million ha of tropical, high-rainfall, low-lying areas. Malaysia and Indonesia produce more than 80% of all palm oil [30] (see Figure 1-6). Global palm oil production increased by 55% between 2001 and 2006, and will be further promoted by increases in demand for biofuels generally.

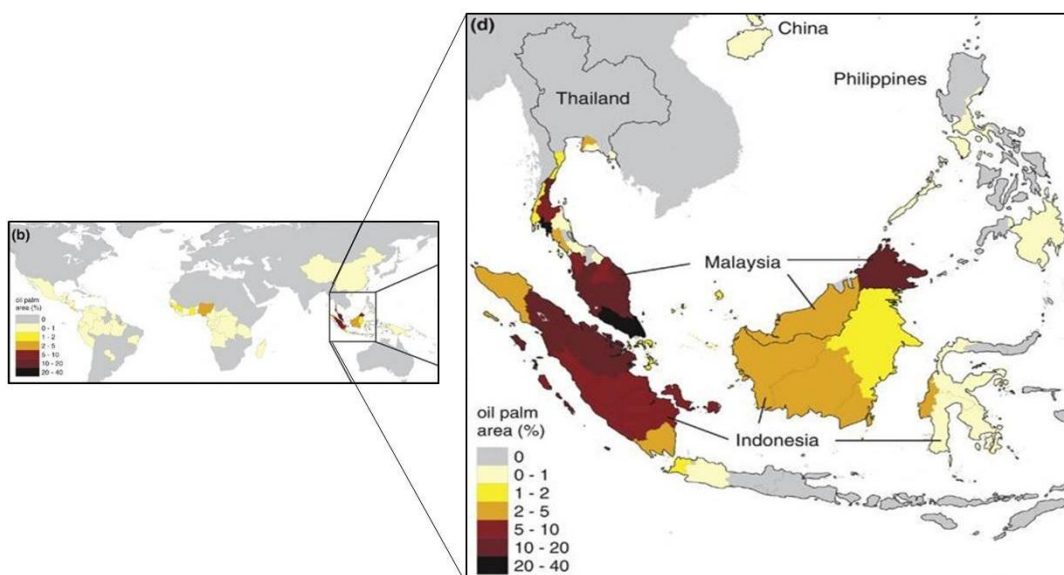


Figure 1-6. Global distribution of oil palm cultivation (harvested area as percentage of country area) (adapted from [30])

Indonesia, the world's largest palm oil producer, plans to double its current production of crude palm oil to 40 million tons by 2020, expecting the growing amount of EFB byproduct in each year [31]. The Indonesian palm oil industry has experienced significant growth in recent years with approximately 1.3 million ha of new area dedicated to palm oil plantations since 2005, reaching almost 5 million ha in 2007 (representing 10.3 percent of the 48.1 million ha of agricultural land)[31]. Indonesia has a great potential for the utilization of oil palm empty fruit bunch (EFB) as it is the waste in the palm oil industry, which disposes approximately 1.1 ton of EFB for every ton of crude palm oil (CPO) produced [25]. EFB is a lignocellulosic residual remains from the extraction of oil palm fruits at the mills [22]. The value of EFB is commercially low and posing a disposal problem because of its large quantity [22]. On the other hand, the large energy potential of 138.3 million GJ/year [32] from EFB waste has gained government attention to utilize this kind of agricultural waste as a solid fuel for supplying electricity to either national and local grids.

A palm oil mill processing 200,000 ton/year fresh fruit bunches (i.e. producing 40,000 ton/year crude palm oil) could supply a power plant with 44,000 ton/year fresh EFB (65 % moisture content). As the heating value of dry EFB is around 16 MJ/kg then, at 25 % energy conversion efficiency, this amount of EFB is equivalent to the generating capacity of 1.9 MWe. According to Directorate General of Estate Crops, Indonesia Ministry of Agriculture, 5.3 million tons of EFB was produced throughout Indonesia in 1997. Utilization of this amount of EFB as a power plant fuel would potentially result in generation of 229 MWe.

1.3.3 Challenges in utilizing EFB for thermo-chemical conversion

Due to its attractive and promising application of EFB as bioenergy, many technologies had been investigated to convert the EFB biomass into direct energy or fuel feedstock with improved quality for generating energy by thermo-chemical conversion. Thermo-chemical conversion processes mainly include direct combustion, pyrolysis, gasification, and liquefaction. The stored energy within biomass could be released directly as heat via combustion/co-firing, or could be transformed into solid (e.g., charcoal), liquid (e.g., bio-oils), or gaseous (e.g., synthetic gas) fuels via pyrolysis, liquefaction, or gasification with various utilization purposes. Biomass characteristics such as the moisture, the ash, the volatile matter, the inorganic elements, the structural constituents, the calorific value, the particle size and the density are of great importance in understanding the changes that occur in the chemical structure of EFBs, which will affect their performance when exposed to elevated temperatures during thermo-chemical conversion [33].

However, some inherent properties imposed by raw EFB become challenges in its thermo-chemical conversion, including high moisture, low energy density, hygroscopic nature, low heating value, and high alkali content, limiting its usage as energy resources. Raw EFB was known to have low bulk density with high moisture content, making it

difficult to be burnt or gasified with a high efficiency and low emissions [34]. Moisture in biomass generally decreases its heating value [35]. These also can lead to the difficulty in handling and transportation of this EFB biomass residue. Due to its fibrous and tenacious nature, biomass is difficult to grind into small homogenous particle. This poor grindability issue can cause serious problems especially when the biomass is used in the pulverized system such as co-firing with coal [36, 37]. Moreover, very high load of untreated biomass is required to generate an equivalent amount of energy from coal due to its relatively low carbon content [38].

The ash content in EFB, particularly the alkali content and chlorine content, poses an issue in the combustion furnace fouling and corrosion. The ash content of EFB is approximately 5.9% and the potassium content is very high at around 3.2% (see Table 1-1). The ash content itself is an important parameter directly affecting the heating value. High ash content of a plant part makes it less desirable as fuel [35]. The slagging and fouling of combustor surfaces become major issues that have played an important role in the design and operation of combustion equipment. Slagging and fouling reduce heat transfer of combustor surfaces and causes corrosion and erosion problems, which reduce the lifetime of the equipment. The main contributions to fouling come from the inorganic material in the fuel [39]. Sodium and potassium lower the melting point of ash and, thus, can increase ash deposition and fouling of boiler tubes [40]. It generally demonstrates that the alkali in general (and the potassium and sodium in particular) are more available and reactive in the bio-fuels than in the various deposits of coal. Ash deposits reduce heat transfer and may also result in severe corrosion at high temperatures. Compared with deposits generated during coal combustion, deposits from biomass fuels are denser and more difficult to remove. The high chlorine and alkali contents of some biomass, like wheat straw, raise concerns regarding corrosion. The chlorine concentration should be minimized in all cases.

1.4 Biomass pretreatment process

1.4.1 Hydrothermal treatment

The research on the hydrothermal treatment started when scientist such as Bergius, Berl, Schmidh, Leibniz and Van Kravelen tried to mimic the natural coalification process. This artificial coalification process has been called the hydrothermal carbonization (HTC) or the hydrothermal treatment (HTT). The wet biomass, agricultural waste and municipal solid waste are treated in hot compressed water at subcritical temperatures [41].

HTT refers to a pressurized thermo-chemical conversion conducted at a mild temperature of 150 - 350°C. And compared to other thermo-chemical conversion methods, such as pyrolysis and gasification, temperature used for HTT is relatively lower (450-550°C for pyrolysis and 800-1200°C for gasification)[42, 43]. Since the

process is carried out in the presence of water, the use of high moisture content feedstock is not an issue. This unique advantage of HTT eliminates the pre-drying requirement of wet biomass, which is energy and cost intensive in the biomass pre-processing when performed under the conventional thermal pretreatments like slow pyrolysis and dry torrefaction. The role of water in this process is not only as a reaction medium but also a chemical reactant for decomposition[44]. HTT is performed in subcritical water. Water in subcritical condition (below the critical point 374°C and 22.1MPa) is still in liquid phase and acts as a non-polar solvent enhancing the solubility of organic compounds in biomass. Water at high temperature and high pressure has high degree of ionization and starts dissociating into acidic hydronium ions (H_3O^+) and basic hydroxide ions (OH^-), therefore, shows both acidic and basic characteristics [45, 46]

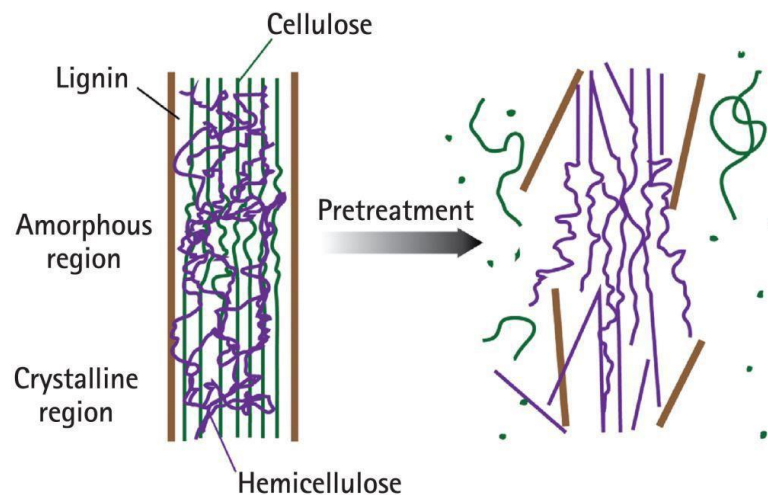


Figure 1-7 Effect of thermal pre-treatments on biomass structure (adapted from [4])

The common products yields from the HTT process are: upgraded solid (hydrochar), aqueous organics and small fractions of gases (mainly CO_2). The distribution percentage and the physicochemical properties of the hydrochar are ruled by the reaction temperature [47]. The mass yield of hydrochar during the HTT process typically varies from 40 to 70%. It has been reported that with the equivalent mass yield, the energy densification ratio (ratio of the HHV of biochar to the HHV of raw biomass) obtained via HTT is significantly higher than the one obtained under torrefaction [47, 48]. The mechanical dewatering of wet materials like sludge and paper pulp can reduce the moisture content to a range of 70 - 75%. The moisture content of the HT treated material can be achieved to a value of less than 50% just by compression, ultimately reducing the supplement energy and time consumption in drying of hydrochar [49]. Pulverization of hydrochar is much less energy intensive when compared to raw wood. The high conversion efficiency, elimination of pre-drying requirement, and relatively low operating temperature among other pretreatments, implies that HTC is a perfectly suitable conversion technique for the production of hydrochar especially from wet biomass.

For conversion of lignocellulosic biomass, the primary goal of the thermochemical pre-treatment is to breakdown the rigid structure of the biomass polymers into small and low molecular weight chains. Figure 1-7 shows the effect of the thermal pre-treatment on the physical structure of biomass. The rate of destruction of the polymeric structure of biomass typically depends upon the reaction time, the temperature and the reaction medium. In HTT, due to the presence of subcritical water, the reaction mechanism is initiated by the hydrolysis, thus it lowers the activation energy level of hemicellulose and cellulose, favoring the rapid degradation and depolymerisation of these polymers into the water soluble products like oligomers and monomers [11, 49].

1.4.2 Water washing

Washing process, also called leaching process by water, or water leaching is defined as the removal of water soluble and ion-exchangeable inorganic constituents from solid substrate using water. Water washing is reported as a low cost pre-treatment to reduce inorganic constituents in the biomass content [50, 51]. The typical inorganic constituents that can be removed during washing process are potassium, sodium, calcium, aluminum and magnesium. Those are macro- and micronutrient for biomass which are very important for plant growth. Potassium is crucial to the plant metabolism and is therefore mostly concentrated in regions where rapid growth occurs, such as leaves and plant tops; Potassium in biomass is apparently tied up as organically bound, occurs as dissolved salts inherent moisture, cations attached to carboxylic and other functional groups, complex ions, and chemisorb material [52]. It occurs as either water soluble or ion exchangeable, thus it highly mobile in water. Sodium and calcium are found with small concentrations in plants and are important for the metabolism and the structure integrity. Aluminum, one of the ingredients of many soils, is toxic to the plants. Magnesium is part of the chlorophyll and is responsible for photosynthesis.

As discussed in the previous sub-chapter, the inorganic constituents, particularly potassium and sodium, can cause fouling, slagging, agglomeration and corrosion during combustion. Fouling occurs when the inorganic constituents form ash deposit on the surfaces of the combustion furnace. Slagging, in which a glass layer rich in Fe_2O_3 and K_2O [53], is a process formed by the melting of the deposits. Agglomeration of Fe_2O_3 and K_2O leads to the increase of the thickness of the glass layer. Interaction of the deposit layers with the metal surfaces within the furnace accelerates corrosion. The potassium compound, such as potassium chloride in EFB, is reported to evolve into gas-phase condenses and deposits on low-temperature surface of the heat exchanger, causing slagging [54]. This hinders the heat transfer between the heat exchanger and also corrodes the surface [55].

Jenkins et al. [50] investigated the effect of natural rain washing technology on composition and ash fusibility of rice straw. Experiments showed that rain washing effectively removed potassium and chlorine, and delayed the onset of ash fusion, for

collected samples without soil contamination. However, water washing appears to be a more controllable manner than natural rain washing. Previous studies [50, 51, 56] demonstrated that water washing may be an effective pretreatment process to remove a large part of inherent inorganic constituents in biomass for mitigating the ash-related issues, thus improving the quality of the biomass fuel. These studies conducted water washing in conventionally batch operations, with the removal performance reported to be dependent on the properties of the biomass feedstock [57]. Jenkins et al. (1996) reported that a significant proportion of 90 % - 91 % potassium and chlorine were removed after leaching banagrass with water [50]. Wheat straw and rice straw showed a similar trend in responding to water leaching in the reduction of potassium and chlorine. A substantial reduction of soluble metal salts after water leaching in pine barks and switchgrass was reported [58]. Vamvuka and Sfakiotakis [59] also reported that after washing, the contents of potassium, phosphorus, sulfur and chlorine in ash were lowered and the kinetic parameters (pre-exponential factor and activation energy) corresponding to hemicellulose and cellulose decomposition were increased [60].

1.4.3 Pelletization

With the increasing demand of energy fuel, EFB waste biomass is considered to be potential fuel for power generation in East Asia [61]. Meanwhile, as discussed above, EFB has many drawbacks that makes very difficult to handle, transport, store, and utilize in its original form. One solution to these problems is the densification of EFB waste biomass into pellets, briquettes, or cubes [62]. Pelletization may facilitate handling and transporting of EFB for domestic and international markets.

In pelletization equipment, the raw material is pressed through a ring or a flat hollowed ring by the pressure of two or more rotating rolls. The rotating rolls push the material into the die holes from the inside of the ring towards the outside of the ring. The friction between the die holes walls and the raw materials resist the free flow of the materials and thus produces increased pressure and temperature which compress the particles against each other inside the die to form pellets. Pellets leaving the die are then cut down by one or two adjustable knife into desired lengths. The diameter of the pellets may range from 4.8 to 19.0 mm, and the length of the pellets may range from 12.7 to 15.4 mm [62]. Pelletization technology is commonly used in the U.S. and Europe for producing animal feed.

The pelletization of biomass could reduce the costs of transportation, handling and storage. Because of uniform sizes and shape, the pelletized biomass can be easily handled using the standard handling and storage equipment, and can be easily adopted in direct-combustion or co-firing with coal, gasification, pyrolysis and in other biomass-fired plants. Many researchers have been studied the pelletization of biomass [63–65], co-pelletization of biomass and sludge [66, 67], and pelletization of treated biomass [14, 68–70].

In comparison to raw biomass, biomass pellets have obviously improved fuel quality. However, biomass pellets may still not be the ideal fuels because of the high moisture affinity and the relatively weak durability, especially for the pellets made from agricultural residues [71]. A less durable pellet tends to disintegrate easily into fines during handling and storage. A low content of lignin and unavailability of other potential natural binders (starches and proteins) within the lignocellulose matrix may require additional binders to assist in forming durable pellets [68]. Conventional wood pellets tend to absorb moisture from the surrounding humid air that leads to pellets disintegration and also provides an ideal environment for microbial and biochemical activities [72]. However, previous published literature has shown that wood products made from steam-exploded ground wood become more dimensionally stable and less hygroscopic after the steam treatment [68]. Because of the increased lignin content, the pellets made from steam-exploded poplar wood resisted higher breaking forces than untreated poplar pellets [73]. Liu et al also reported that the moisture uptake of hydrochar pellets was decreased compared to raw biomass pellets showing the hydrophobic nature of treated pellets.

1.5 Research objectives

As explained in the previous section, the waste from the growing palm oil production need immediate mitigation to fully utilize the waste and extract its potential energy for energy production. Despite its promising advantages to replace fossil fuels, there are many issues regarding raw EFB biomass [33, 34, 74], such as hydrophilic nature, high moisture content and low bulk density, thus lowering its calorific value and limiting its ease of use as fuel. Therefore, improvement to obtain better characteristics is indispensable in the term of fuel use. Currently, several different approaches have been considered to improve the fuel properties of biomass. In this study, the combination of HTT, washing pre-treatment and pelletization will be employed in order to mitigate the issues.

Pelletization is one good way to deal with the handling and transporting issues of the EFB in its original form, especially when we intend to use it for domestic and international market. The pelletization of biomass could reduce the costs of transportation, handling and storage. Because of uniform sizes and shape, the pelletized biomass can be easily handled using the standard handling and storage equipment, and can be easily adopted in direct-combustion or co-firing with coal, gasification and in other biomass-fired plants. However, biomass pellets may still not be the ideal fuels because of the high moisture affinity and the relatively weak durability, especially for the pellets made from agricultural residues [71]. Therefore, the HTT and washing co-treatment is necessary before the pelletization; HTT can upgrade the raw biomass into more stable, more hydrophobic and more lignin containing feedstock; and washing

treatment can deal with the ash deposition issue. The co-treatment is effective to produce more strong, durable and clean pellets.

The previous published literatures had conducted the various pre-treatments prior to pelletization, such as steam exploded biomass pellets, torrefied biomass pellets, and including the hydrothermally-carbonized biomass pellets. The steam treatment and hydrothermal treatment studies had shown that the pellets were more dimensionally stable and less hygroscopic [68], more resisted to higher breaking forces due to increased lignin content [73], and more durable compared to untreated one [70, 71, 75]. Nevertheless, there is no research focused on the washed treated pellets was found. Therefore, this study may give more clear information and knowledge on the effect of washing on the HT treated pellets.

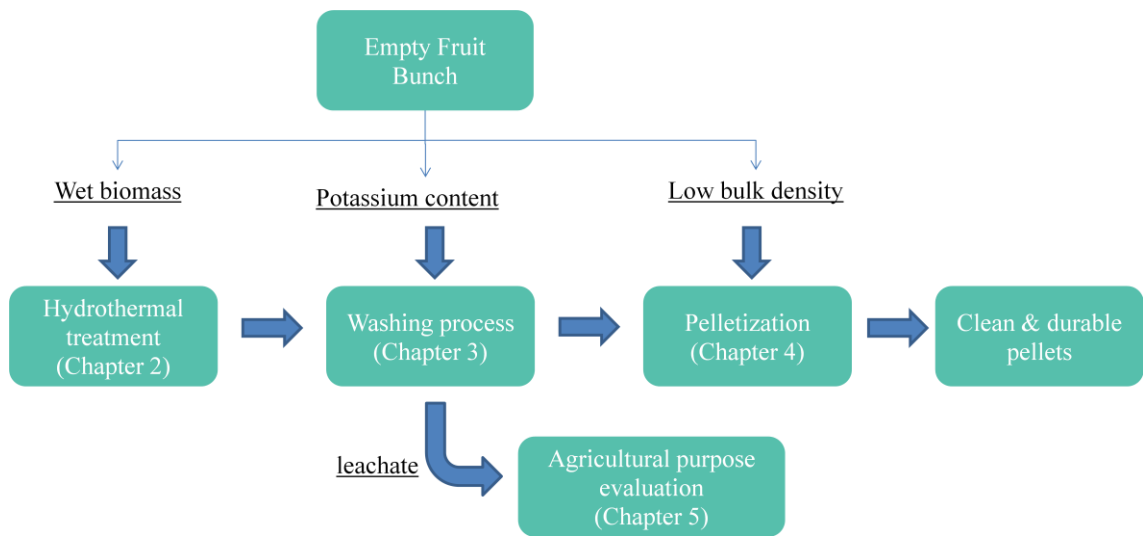


Figure 1-8. Outline of this research

In summary, the objective of this research is to produce a clean and durable pelletized fuel from palm empty fruit bunch (EFB) utilizing the combination of the hydrothermal treatment technology and washing treatment. Several steps of experiments and analyses were conducted to realize this objective. An illustration of the outline of this research is shown in Figure 1-8.

1.6 Thesis structure

This thesis presents a structured experimental results and analysis of the production of low-potassium pellets from EFB. A series of experiments on the hydrothermal upgrading of EFB, potassium removal, pelletization of treated EFB and fertilizer evaluation of leachate have been conducted. Complete explanation of the research will be presented in 6 (six) chapters. Four main chapters in this thesis are devoted to main contents of this research. They are in Chapters 2–5. Chapter 1 and 6 are the introduction and conclusion with recommendation of this research, respectively.

Chapter 1 explains the background of the research. The increasing importance of the utilization of renewable biomass energy is described along with the overview of the biomass itself. The composition, the global potential for energy production, and the thermo-chemical application challenges of palm empty fruit bunch (EFB), as the main feedstock in this research, are summarized in this chapter. Lastly, the description of each main technology that is adopted in this research to deal with the low energy density, low bulk density, and high slagging fouling tendency biomass were reviewed. Furthermore, literature reviews on the application of the technologies were covered. Finally, the objectives of this research were stated.

Chapter 2 deals with the hydrothermal upgrading of EFB waste biomass in lab-scale to investigate the improvement of the fuel qualities into value added solid fuel. The description includes the experimental method, results and analysis on the effect of varying operational condition to the product characteristic i.e the heating value, the appearance, the chemical changes, the combustion characteristics and the effect of HTT on the slagging and fouling behavior of the biomass. The mechanism of HTT is also investigated by the Van Krevelen diagram and the FTIR analysis. From the result, a preferable HTT condition is drawn for large-scale production of solid fuel from EFB.

In Chapter 3, the removal of the potassium content by combination of HTT and the water washing is described further in detail. This chapter presents the potassium removal behavior during HTT process and washing experiment, including the effect of the solid to water ratios on the potassium removal, and fuel properties after the washing process. Explanation on the improvement in its deposition tendency after both processes by calculating the slagging and fouling indices will also be included in this chapter. The combustion properties by TGA and the FTIR analysis of the washed and unwashed hydrochar were also discussed in this chapter.

Chapter 4 aims to investigate the comparison of the pellets produced from raw EFB, and the hydrothermally treated EFB (hydrochar) as well as the washed hydrochar. The physical property, the mechanical strength, the durability and the hydrophobicity of the produced pellets from each sample were evaluated. From the analysis, it was found that the changes in the composition of EFB biomass due to HTT and the washing process regulate the pelletization behavior and affect the bonding mechanism during the pelletization. In conclusion, the promising combination of the pelletization, HTT, and the washing co-treatment can be drawn from the investigation results for upgrading biomass into clean, energy dense, homogenous, friable, durable and hydrophobic solid fuel.

Chapter 5 discusses about the possibility to use the leachate from the washing process of HTT-EFB for agricultural purpose. The properties of the leachate were analyzed for its macronutrient, pH and EC. The phytotoxicity effect of the leachate on the plant

growth by means of seed germination was also performed and discussed in this chapter. The result will then be used to decide the safety approach when applying the leachate back to the palm oil plantation.

Chapter 6 will summarize the overall results, and some recommendations for further work or implementation of this research are suggested.

References

1. IEA Renewable Energy Working Party: Renewable Energy ... into the Mainstream. (2003).
2. McKendry, P.: Energy production from biomass (Part 1): Overview of biomass. *Bioresour. Technol.* 83, 37–46 (2002).
3. Saxena, R.C., Adhikari, D.K., Goyal, H.B.: Biomass-based energy fuel through biochemical routes: A review. *Renew. Sustain. Energy Rev.* 13, 167–178 (2009).
4. Tumuluru, J.S., Wright, C.T., Hess, J.R., Kenney, K.L., National, I.: A review of biomass densification systems to develop uniform feedstock commodities for bioenergy application †. 683–707 (2011).
5. Özbay, N., Pütün, a. E., Uzun, B.B., Pütün, E.: Biocrude from biomass: Pyrolysis of cottonseed cake. *Renew. Energy.* 24, 615–625 (2001).
6. Yu, Y., Lou, X., Wu, H.: Some Recent Advances in Hydrolysis of Biomass in Hot-Compressed Water and Its Comparisons with Other Hydrolysis Methods. *Energy & Fuels.* 22, 46–60 (2008).
7. Veringa, H., Alderliesten, P.: Advanced techniques for generation of energy from biomass and waste. *ECN Publ.* <http://www.ecn.nl/fileadmin/ecn/units> 1–24 (2004).
8. Kumar, P., Barrett, D.M., Delwiche, M.J., Stroeve, P.: Methods for Pretreatment of Lignocellulosic Biomass for Efficient Hydrolysis and Biofuel Production. *Ind. Eng. Chem. Res.* 48, 3713–3729 (2009).
9. Jarvis, M.: Chemistry: cellulose stacks up. *Nature.* 426, 611–612 (2003).
10. Grønli, M.G., Várhegyi, G., Di Blasi, C.: Thermogravimetric Analysis and Devolatilization Kinetics of Wood. *Ind. Eng. Chem. Res.* 41, 4201–4208 (2002).
11. Bobleter, O.: Hydrothermal degradation of polymers derived from plants. *Prog. Polym. Sci.* 19, 797–841 (1994).
12. Garrote, G., Dominguez, H., Parajo, J.C.: Hydrothermal processing of lignocellulosic materials. *Holz als Roh- und Werkst.* 57, 191–202 (1999).
13. Kaliyan, N., Morey, R.V.: Natural binders and solid bridge type binding mechanisms in briquettes and pellets made from corn stover and switchgrass. *Bioresour. Technol.* 101, 1082–90 (2010).
14. Reza, M.T., Uddin, M.H., Lynam, J.G., Coronella, C.J.: Engineered pellets from dry torrefied and HTC biochar blends. *Biomass and Bioenergy.* 63, 229–238 (2014).
15. Döring, S.: *Power from Pellets.* (2013).
16. Knezevic, D.: *Hydrothermal Conversion of Biomass.* University of Twente (2009).
17. Mok, W.S.L., Antal, M.J.: Uncatalyzed Solvolysis of Whole Biomass Hemicellulose by Hot Compressed Liquid Water. *Ind. Eng. Chem. Res.* 31, 1157–1161 (1992).
18. Goudriaan, F., Peferoen, D.G.R.: Liquid fuels from biomass via a hydrothermal process. *Chem. Eng. Sci.* 45, 2729–2734 (1990).
19. Uslu, A., Faaij, A.P.C., Bergman, P.C.A.: Pre-treatment technologies, and their effect on international bioenergy supply chain logistics. *Techno-economic evaluation of torrefaction, fast pyrolysis and pelletisation.* *Energy.* 33, 1206–1223 (2008).

20. Liu, Z., Balasubramanian, R.: Upgrading of waste biomass by hydrothermal carbonization (HTC) and low temperature pyrolysis (LTP): A comparative evaluation. *Appl. Energy.* 114, 857–864 (2014).
21. Aziz, M. a., Sabil, K.M., Uemura, Y., Ismail, L.: A study on torrefaction of oil palm biomass, (2012).
22. Isroi, Ishola, M.M., Millati, R., Syamsiah, S., Cahyanto, M.N., Niklasson, C., Taherzadeh, M.J.: Structural changes of oil palm empty fruit bunch (OPEFB) after fungal and phosphoric acid pretreatment. *Molecules.* 17, 14995–5002 (2012).
23. Alam, M.Z., Muyibi, S. a., Mansor, M.F., Wahid, R.: Activated carbons derived from oil palm empty-fruit bunches: Application to environmental problems. *J. Environ. Sci.* 19, 103–108 (2007).
24. Ria, M., Rachma, W., Titik, T.E., Nur, C.M., Claes, N.: Ethanol from Oil Palm Empty Fruit Bunch via Dilute Acid Hydrolysis and Fermentation by *Mucor indicus* and *Saccharomyces cerevisiae*, (2011).
25. Karina, M., Onggo, H., Abdullah, A.D., Syampurwadi, A.: Effect of Oil Palm Empty Fruit Bunch Fiber on the Physical and Mechanical Properties of Fiber Glass Reinforced Polyester Resin, (2008).
26. Fahma, F., Iwamoto, S., Hori, N., Iwata, T., Takemura, A.: Isolation, preparation, and characterization of nanofibers from oil palm empty-fruit-bunch (OPEFB). *Cellulose.* 17, 977–985 (2010).
27. Wirjosentono, B., Guritno, P., Ismail, H.: Oil Palm Empty Fruit Bunch Filled Polypropylene Composites. *Int. J. Polym. Mater. Polym. Biomater.* 53, 295–306 (2004).
28. Nasrin, A.B., Ma, A.N., Choo, Y.M., Mohamad, S., Rohaya, M.H., Azali, A., Zainal, Z., Institusi, P., Bangi, B.B., Tebal, N., Pinang, P.: Oil Palm Biomass As Potential Substitution Raw Materials For Commercial Biomass Briquettes Production. *Am. J. Appl. Sci.* 5, 179–183 (2008).
29. Hamzah, F., Idris, A., Shuan, T.K.: Preliminary study on enzymatic hydrolysis of treated oil palm (*Elaeis*) empty fruit bunches fibre (EFB) by using combination of cellulase and β 1-4 glucosidase. *Biomass and Bioenergy.* 35, 1055–1059 (2011).
30. FITZHERBERT, E., STRUEBIG, M., MOREL, A., DANIELSEN, F., BRUHL, C., DONALD, P., PHALAN, B.: How will oil palm expansion affect biodiversity? *Trends Ecol. Evol.* 23, 538–545 (2008).
31. PwC Indonesia: Palm Oil Plantation: Industry landscape, regulatory and financial overview. 1–12 (2012).
32. Prastowo, B.: Biomass Resource in Indonesia: Indonesia s Solid Biomass Energy Potential. *Indones. Ger. Work. Semin.* 1–15 (2012).
33. Omar, R., Idris, A., Yunus, R., Khalid, K., Aida Isma, M.I.: Characterization of empty fruit bunch for microwave-assisted pyrolysis. *Fuel.* 90, 1536–1544 (2011).
34. Lam, P.S., Lam, P.Y., Sokhansanj, S., Lim, C.J., Bi, X.T., Stephen, J.D., Pribowo, A., Mabee, W.E.: Steam explosion of oil palm residues for the production of durable pellets. *Appl. Energy.* 141, 160–166 (2015).
35. Demirbas, A.: Combustion characteristics of different biomass fuels. *Prog. Energy Combust. Sci.* 30, 219–230 (2004).
36. Arias, B., Pevida, C., Feroso, J., Plaza, M.G., Rubiera, F., Pis, J.J.: Influence of torrefaction on the grindability and reactivity of woody biomass. *Fuel Process. Technol.* 89, 169–175 (2008).
37. van der Stelt, M.J.C., Gerhauser, H., Kiel, J.H.A., Ptasinski, K.J.: Biomass upgrading by torrefaction for the production of biofuels: A review. *Biomass and Bioenergy.* 35, 3748–3762 (2011).
38. Chew, J.J., Doshi, V.: Recent advances in biomass pretreatment – Torrefaction fundamentals and technology. *Renew. Sustain. Energy Rev.* 15, 4212–4222 (2011).

39. Demirbas, A.: Potential applications of renewable energy sources, biomass combustion problems in boiler power systems and combustion related environmental issues. *Prog. Energy Combust. Sci.* 31, 171–192 (2005).
40. Khan, A.A., de Jong, W., Jansens, P.J., Spliethoff, H.: Biomass combustion in fluidized bed boilers: Potential problems and remedies. *Fuel Process. Technol.* 90, 21–50 (2009).
41. Titirici, M.-M., Antonietti, M.: Chemistry and material options of sustainable carbon materials made by hydrothermal carbonization. *Chem. Soc. Rev.* 39, 103–106 (2009).
42. Arvanitoyannis, I.S., Kassaveti, A.: Current and potential uses of composted olive oil waste. *Int. J. Food Sci. Technol.* 42, 281–295 (2007).
43. Zhang, L., Xu, C. (Charles), Champagne, P.: Overview of recent advances in thermochemical conversion of biomass. *Energy Convers. Manag.* 51, 969–982 (2010).
44. Yuliansyah, A.T., Hirajima, T., Kumagai, S., Sasaki, K.: Production of Solid Biofuel from Agricultural Wastes of the Palm Oil Industry by Hydrothermal Treatment. *Waste and Biomass Valorization*. 1, 395–405 (2010).
45. Kalinichev, A.G., Churakov, S. V: Size and topology of molecular clusters in supercritical water: a molecular dynamics simulation. *Chem. Phys. Lett.* 302, 411–417 (1999).
46. Marcus, Y.: On transport properties of hot liquid and supercritical water and their relationship to the hydrogen bonding. *Fluid Phase Equilib.* 164, 131–142 (1999).
47. Yan, W., Hastings, J.T., Acharjee, T.C., Coronella, C.J., Vásquez, V.R.: Mass and Energy Balances of Wet Torrefaction of Lignocellulosic Biomass †. *Energy & Fuels*. 24, 4738–4742 (2010).
48. Yan, W., Acharjee, T.C., Coronella, C.J., Vasquez, V.R.: Thermal pretreatment of lignocellulosic biomass. *Environ. Prog. Sustain. Energy*. 28, 435–440 (2009).
49. Funke, A., Ziegler, F.: Hydrothermal carbonization of biomass: A summary and discussion of chemical mechanisms for process engineering. *Biofuels, Bioprod. Biorefining*. 4, 160–177 (2010).
50. Jenkins, B.M., Bakker, R.R.: On the properties of washed straw. *Biomass and Bioenergy*. 10, 177–200 (1996).
51. Turn, S., Kinoshita, C., Ishimura, D., Jenkins, B., Zhou, J.: Leaching of Alkalis in Biomass Using Banagrass as a Prototype Herbaceous Species Final Report , February 1997 Leaching of Alkalis in Biomass Using Banagrass as a Prototype Herbaceous Species. (2003).
52. Baxter, L.L., Miles, T.R., Jenkins, B.M., Milne, T., Dayton, D., Bryers, R.W., Oden, L.L.: The behavior of inorganic material in biomass-fired power boilers: field and laboratory experiences. *Fuel Process. Technol.* 54, 47–78 (1998).
53. Kostakis, G.: Mineralogical composition of boiler fouling and slagging deposits and their relation to fly ashes: The case of Kardias power plant. *J. Hazard. Mater.* 185, 1012–1018 (2011).
54. Konsomboon, S., Pipatmanomai, S., Madhiyanon, T., Tia, S.: Effect of kaolin addition on ash characteristics of palm empty fruit bunch (EFB) upon combustion. *Appl. Energy*. 88, 298–305 (2011).
55. Madhiyanon, T., Sathitruangsak, P., Sungworagarn, S., Pipatmanomai, S., Tia, S.: A pilot-scale investigation of ash and deposition formation during oil-palm empty-fruit-bunch (EFB) combustion. *Fuel Process. Technol.* 96, 250–264 (2012).
56. Dayton, D.C., Jenkins, B.M., Turn, S.Q., Bakker, R.R., Williams, R.B., Hill, L.M.: Release of Inorganic Constituents from Leached Biomass during Thermal Conversion. 1977, 860–870 (1999).
57. Liaw, S.B., Wu, H.: Leaching Characteristics of Organic and Inorganic Matter from Biomass by Water : Differences between Batch and Semi-continuous Operations. (2013).
58. Liu, X., Bi, X.T.: Removal of inorganic constituents from pine barks and switchgrass. *Fuel Process. Technol.* 92, 1273–1279 (2011).

59. Vamvuka, D., Sfakiotakis, S.: Effects of heating rate and water leaching of perennial energy crops on pyrolysis characteristics and kinetics. *Renew. Energy.* 36, 2433–2439 (2011).
60. Deng, L., Zhang, T., Che, D.: Effect of water washing on fuel properties, pyrolysis and combustion characteristics, and ash fusibility of biomass. *Fuel Process. Technol.* 106, 712–720 (2013).
61. Cocchi, M., Nikolaisen, L., Junginger, M., Goh, C.S., Hess, R., Jacobson, J., Ovard, L.P., Thrän, D., Hennig, C., Deutmeyer, M., Schouwenberg, P.P.: Global wood pellet industry market and trade study. IEA Bioenergy Task. 190pp (2011).
62. Kaliyan, N., Vance Morey, R.: Factors affecting strength and durability of densified biomass products. *Biomass and Bioenergy.* 33, 337–359 (2009).
63. Garcia-Maraver, a., Rodriguez, M.L., Serrano-Bernardo, F., Diaz, L.F., Zamorano, M.: Factors affecting the quality of pellets made from residual biomass of olive trees. *Fuel Process. Technol.* 129, 1–7 (2015).
64. Castellano, J.M., Gómez, M., Fernández, M., Esteban, L.S., Carrasco, J.E.: Study on the effects of raw materials composition and pelletization conditions on the quality and properties of pellets obtained from different woody and non woody biomasses. *Fuel.* 139, 629–636 (2015).
65. Zamorano, M., Popov, V., Rodríguez, M.L., García-Maraver, a.: A comparative study of quality properties of pelletized agricultural and forestry lopping residues. *Renew. Energy.* 36, 3133–3140 (2011).
66. Li, H., Jiang, L.-B., Li, C.-Z., Liang, J., Yuan, X.-Z., Xiao, Z.-H., Xiao, Z.-H., Wang, H.: Co-pelletization of sewage sludge and biomass: The energy input and properties of pellets. *Fuel Process. Technol.* 132, 55–61 (2015).
67. Jiang, L., Liang, J., Yuan, X., Li, H., Li, C., Xiao, Z., Huang, H., Wang, H., Zeng, G.: Co-pelletization of sewage sludge and biomass: the density and hardness of pellet. *Bioresour. Technol.* 166, 435–43 (2014).
68. Lam, P.S., Sokhansanj, S., Bi, X., Lim, C.J.: Energy Input and Quality of Pellets Made from Steam-Exploded Douglas Fir (*Pseudotsuga menziesii*). 1521–1528 (2011).
69. Cao, L., Yuan, X., Li, H., Li, C., Xiao, Z., Jiang, L., Huang, B., Xiao, Z., Chen, X., Wang, H., Zeng, G.: Complementary effects of torrefaction and co-pelletization: Energy consumption and characteristics of pellets. *Bioresour. Technol.* 185, 254–262 (2015).
70. Kambo, H.S., Dutta, A.: Strength, storage, and combustion characteristics of densified lignocellulosic biomass produced via torrefaction and hydrothermal carbonization. *Appl. Energy.* 135, 182–191 (2014).
71. Liu, Z., Quek, A., Balasubramanian, R.: Preparation and characterization of fuel pellets from woody biomass, agro-residues and their corresponding hydrochars. *Appl. Energy.* 113, 1315–1322 (2014).
72. Lehtikangas, P.: Storage effects on pelletised sawdust , logging residues and bark. 19, 287–293 (2000).
73. Shaw, M.D., Karunakaran, C., Tabil, L.G.: Physicochemical characteristics of densified untreated and steam exploded poplar wood and wheat straw grinds. *Biosyst. Eng.* 103, 198–207 (2009).
74. Stemann, J., Erlach, B., Ziegler, F.: Hydrothermal Carbonisation of Empty Palm Oil Fruit Bunches: Laboratory Trials, Plant Simulation, Carbon Avoidance, and Economic Feasibility. *Waste and Biomass Valorization.* 4, 441–454 (2012).
75. Reza, M.T., Lynam, J.G., Vasquez, V.R., Coronella, C.J.: Pelletization of biochar from hydrothermally carbonized wood. *Environ. Prog. Sustain. Energy.* 31, 225–234 (2012).

Chapter 2. Hydrothermal upgrading of Empty Fruit Bunches

Abstract: The lab scale investigation on hydrothermal treatment (HTT) of waste EFB was performed in order to upgrade the fuel qualities of the biomass into value added solid fuel. The HTT experiments were conducted using a commercially available batch type autoclave reactor. Four reaction temperatures were investigated at 100, 150, 180, and 220°C with the holding time of 30 minutes. The results indicated that the fuel qualities of the product was improved after HTT; such as a higher carbon content, a higher energy density, a lower O/C and H/C ratios compared with the raw feedstock. The calorific value of the EFB was increased from 17 MJ/kg to approximately 20 MJ/kg after HTT, which is equal to low-grade sub-bituminous coal. The mechanism of HTT is also investigated by the Van Krevelen diagram and the FTIR analysis. Considering the energy yield and ash content, HTT at 180°C is found to be most favorable for large-scale production of solid fuel from EFB.

2.1 Background

As described in Chapter 1, some inherent properties imposed by raw EFB become challenges in its combustion, including high moisture, low energy density, hygroscopic nature, low heating value and high alkali content, limiting its usage as energy resources. Raw EFB was known to have low bulk density with high moisture content, making it difficult to be burnt or gasified with high efficiency and low emissions [1]. Moisture in biomass generally decreases its heating value [2]. The poor grindability of EFB can cause serious problems especially when the biomass is used in the pulverized system such as co-firing with coal [3, 4]. Moreover, very high load of untreated biomass is required to generate an equivalent amount of energy from coal due to its relatively low carbon content [5]. The ash content in EFB, particularly the alkali content and chlorine content, also poses an issue in the combustion furnace fouling and corrosion.

Since the objective is to produce durable pellets from EFB, the hydrothermal treatment (HTT) is employed in order to upgrade this biomass. A series of experimental lab-scale HTT was conducted at various temperatures and fixed holding time. It is expected that the product after HTT has better fuel qualities for solid fuel; for example the carbon content should be improved, thus energy content also improved. The product also has to be more hydrophobic, simply to make the pellet more resistance to the surrounding humidity for longer storage. The broken down of the lignocellulosic structure and the increase in the lignin content also expected for better pelletization. Furthermore, the mechanism of the effect of HTT on EFB has been investigated as well.

2.2 Material and method

2.2.1 Biomass material

The EFB samples was harvested in 2010 and collected from private palm oil mill company, Waris Selesa Sdn. Bhd., in Sabah, Malaysia. The samples were received in milled and dried condition from the company, with a uniform particle size ranging from 10 - 20 mm. The samples were stored in sealed plastic bags at the room temperature until use for experiments.

2.2.2 HTT

The HTT experiments were conducted using a commercially available batch type autoclave reactor (MMJ-500, Japan) with the reaction vessel volume of 500 ml. The facility consists of a reactor equipped with an automatic stirrer, a controllable electrical heater and a condenser. The detailed configuration of the facility is illustrated in Figure 2-1. In this experiment, 10 grams of EFB and distilled water in 1:10 biomass-water ratio was supplied to the reactor. Argon gas was used for purging operations in order to create oxygen-free environment inside the reactor. The reactor temperature was set at 100, 150, 180, 220°C, respectively, with the holding time of 30 minutes. After completed, the product was discharged from the reactor. The solid part was separated from the liquid by using the vacuum filtration, then oven dried at 105°C for 24 h, and stored in a sealed bag before further analysis. The liquid part was filled in the bottle and kept in a refrigerator. All HTT at four temperatures were conducted with the repetition at least three times to ensure the reproducibility and the consistency.

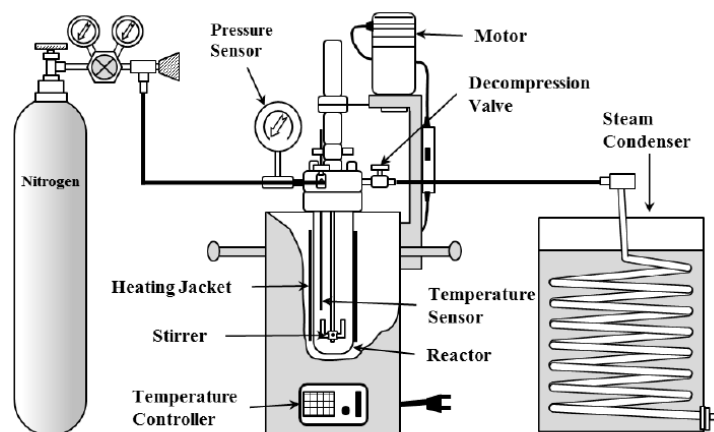


Figure 2-1. Lab scale hydrothermal apparatus (adapted from [6])

2.2.3 Analytical method

2.2.3.1 Ultimate analysis and HHV

The determination of the CHNS and Cl of EFB samples was performed using Vario Micro Cube Elemental Analyzer (Elementar, Germany), where oxygen was determined by difference as dry basis. The ultimate correlation by Channiwala and Parikh (2012) was used to estimate the HHV of the samples. Kieseler (2013) pointed that this correlation gives the most accurate result compared to the proximate correlation and the Dulong-formula ultimate correlation for hydrothermal treatment chars [7]. The correlation is given below:

$$\text{HHV} = 0.3491 \text{ C} + 1.1783 \text{ H} + 0.1005 \text{ S} - 0.1034 \text{ O} - 0.0151 \text{ N} - 0.0211 \text{ Ash} \quad (1)$$

2.2.3.2 Potassium content

The potassium element was analyzed by atomic absorption spectrometry (AAS) method using Z-5010 Polarized Zeeman Atomic Absorption Spectrophotometer (Hitachi, Japan). Preliminary treatment is required to decompose the biomass matrix and dissolve the inorganic elements into solution, allowing them to be introduced into the determination step. The biomass samples were digested using hot-plate digestion method. For the analysis, 0.5 g of the dry solid sample or 2 ml of the liquid sample was added with 3 ml HNO₃ 1.38 g/ml and 5 ml HClO₄ 60%. After the acid pretreatment, the solution was filtered and diluted to a proper volume for potassium content determination by AAS.

2.2.3.3 X-Ray Fluorescence Analysis

The ash compositions of untreated and treated EFB material were analyzed using the X-ray fluorescence (XRF) technique. For the XRF analysis, the sample was well ground into powder (i.e., particle size 250 μm) and around 2 g of EFB sample was used to determine the ash composition by S2 Ranger energy dispersive X-ray fluorescence spectrometer (Bruker AXS, Germany).

2.2.3.4 Thermo-gravimetric Analysis

The thermogravimetric analysis (TGA) was carried out by using a non-isothermal TGA analyzer (Shimadzu D-50 simultaneous TGA/DTA analyzer). Thermal decompositions under oxidative atmosphere were conducted by loading a sample of approximately 10 mg into a crucible. Then the samples were heated by a constant heating rate of 10 °C/min to minimize the heat transfer limitation [8, 9]. Air was used at a constant flow rate of 150 ml/min and the samples were heated from the ambient temperature to 900 °C. At least, three runs were completed for each sample to confirm the reproducibility. The mass loss (TG) and derivative curves (DTG) were continuously collected and represented as a function of time and temperature.

2.2.3.5 Scanning Electron Microscopy

Both raw and HT-EFB samples were mounted onto the surface of standard SEM stub using carbon tape. The samples were then placed into ion sputter coater MSP-1S (Shinkuu, Japan) where Pt-Pd was deposited on the surface of sample to provide a conductive coating. Scanning electron microscopy (SEM) was performed by the JSM-6610LA scanning electron microscope (JEOL Co., Ltd. Japan). A voltage of 10 kV with magnification of 430 times was used for the images collection.

2.2.3.6 Fourier transform infrared spectrometry (FTIR)

The Fourier transform infrared spectrometry (FTIR) was done by the JIR-SPX200 FT-IR spectrometer (JEOL Co., Ltd. Japan) to investigate the mechanism of HTT. The procedure name is "KBr pellet method", which is traditional method for transmission measurement. The fine sample is grinded and mixed with KBr, then pelletized. Then, it was scanned from 400 to 4000 cm^{-1} with the resolution of 4 cm^{-1} .

2.2.3.7 Liquid HTT residue analysis

Trace elements including heavy metals in the sample are analyzed using ICPE-9000 (Inductively Coupled Plasma Emission Spectrometer) (Shimadzu, Japan). The total C in liquid residue was determined using Total Organic Carbon Analyzer TOC-5000 (Shimadzu, Japan) while the total N was determined using Nitrogen Measuring Unit NM-1 attached to TOC-VE (Shimadzu, Japan). The pH and EC values were analyzed for the liquid sample using the pH and EC meters while those for the raw EFB was analyzed in a 1:10 raw EFB/distilled water solution following a 15-min mixing.

To evaluate the phytotoxicity of the liquid, a germination test was performed. Twenty seeds of komatsuna (*Brassica rapa* var. *perviridis*) were placed in a petri dish containing special filter paper (Tanepita, FHK, Japan), added with 3 ml distilled water as control, or the liquid HTT samples. The liquid HTT samples were diluted to different solutions. The petri dishes were then incubated at 25°C for 96 hours in the dark room. Three replicates were set out for each treatment, including distilled water that was used as a control.

After incubated, germinated seeds were counted, and the root and the shoot length were measured. The GI was then calculated using the Germination Index formula [10] as follows:

$$\text{Germination index (GI)} = \frac{S_i \times \text{MRL}_i}{S_c \times \text{MRL}_c} \times 100$$

Where,

S_i = average number of seed germinated in the sample

S_c = average number of seed germinated in the control

MRL_i = average of the root length in the sample
 MRL_c = average of the root length in the control

Data were analyzed statistically using ANOVA provided by Data Analysis ToolPack of the Excel and means were compared by Fisher's Least Significant Difference (LSD) test at 5% probability level to determine the significant difference among the various treatment [11].

2.2.4 Process analysis

The process analysis of lab scale solid fuel production from EFB was conducted to calculate the mass and energy balances, so that the system performance and estimated energy consumption and recovery can be obtained. Some assumptions were also made for these calculations.

2.2.4.1 Mass balance

The mass balance equations measured two main material flows of water and solids. The amount of the products was determined between each experiment within the control volume as follows:

- Input and output of the small-scale autoclave facility for HTT,
- Input and output of the vacuum filtration,
- Input and output of the drying.

The mass balance equation can be assumed as the following equations:

$$m_{EFB} + m_{added\ water} = m_{HTTEFB} + m_{off-gas} \quad (2-1)$$

Where

- m_{EFB} = dried EFB input mass
- $m_{added\ water}$ = mass of the additional water supplied to the autoclave
- m_{HTTEFB} = products mass after the treatment including the condensed steam
- $m_{off-gas}$ = blow-off gas output of the condenser (by the difference)

$$m_{HTTEFB} = m_{filtrated\ solid} + m_{filtrate} \quad (2-2)$$

Where,

- m_{HTTEFB} = mass of treated EFB being filtrated
- $m_{filtrated\ solid}$ = mass of the filtrated solid after vacuum filtration
- $m_{filtrate}$ = mass of the filtrated liquid after vacuum filtration

$$m_{filtrated\ solid} = m_{dried\ solid} + m_{evap\ moisture} \quad (2-3)$$

Where,

- $m_{filtrated\ solid}$ = the filtrated solid that being dried
 $m_{dried\ solid}$ = mass of the dried solid after drying, assumed as totally dried
 $m_{evap-moisture}$ = evaporated moisture during drying.

2.2.4.2 Energy balance

Since the main objective of this work is to produce solid fuel products, expectedly with greater heating values and to recover energy from EFB biomass, there is a special interest to discuss about the energy consumption and the energy recovery of the proposed lab-scale HTT process. Here, an ‘‘Energy Output/Input Ratio’’ is adapted to estimate the net energy efficiency [12]. The ratio was defined as the ratio of the energy content of the product to the energy input. The equation is as follows:

$$Energy\ \frac{output}{input}\ ratio = \frac{HHV\ of\ product\ \times\ dried\ mass}{Energy\ input} \quad (2-4)$$

Where,

- HHV (dry basis) = the higher heating value of HTT-EFB
Dried mass = dried HTT-EFB after the drying, and
Energy input = calculated by equation (2-5)

$$Energy\ input = [m_{EFB} \cdot C_p \cdot (T_{HT} - T_{25})] + [m_{water} \cdot (h_{g,T} - h_{l,T25})] \quad (2-5)$$

Where,

- m_{EFB} = dried Raw-EFB mass
 C_p = the specific heat of Raw-EFB
 T_{HT} = the specific temperature for each HTT experiment
 T_{25} = the room temperature, assumed to be 25°C
 $h_{g,T}$ = the enthalpy of the saturated vapor at the specific temperature
 $h_{l,T25}$ = the enthalpy of the saturated liquid at 25°C
 m_{water} = the water added

For the simplification of calculation, some assumptions have been made as follows:

- The water was heated from 25 °C to the saturated vapor water state in each specific temperature.
- The energy consumption of the electrical stirrer and other electrical utilities were neglected.
- The energy utilized in the vacuum filtration has also been neglected.

- The energy used for water evaporation was estimated by multiplying the amount of moisture evaporated in the drying with a latent heat for evaporation of water (2.26 MJ/kg).

The specific heat of raw EFB was assumed to be 1.48 kJ/kg·K [13]

2.3 Result and Discussions

2.3.1 Mass yield and energy value of hydrochars

HTT of EFB was performed in hot compressed water at temperatures of 100, 150, 180, and 220°C for 30 min. The mass (solid) yield data were collected and the HHV, energy densification ratio, and energy yield of the hydrochars were calculated. The results were summarized in Table 2-1. The produced hydrochars are denoted as HTT with the number showing the temperature under which the hydrochars were produced.

The calculation for the mass yield, energy densification ratio, and energy yield were based on literature [14] and defined as follows:

$$\text{Mass yield} = \frac{\text{dried mass of hydrochars}}{\text{dried mass of raw EFB}} \times 100\% \quad (2-6)$$

$$\text{Energy densification ratio} = \frac{\text{HHV of dried hydrochars}}{\text{HHV of raw EFB}} \quad (2-7)$$

$$\text{Energy yield} = \text{Mass yield} \times \text{Energy densification ratio} \quad (2-8)$$

As shown in Table 2-1, HTT temperature had a significant effect on the mass yield, the energy densification ratio and the energy yield of the produced hydrochars. Hydrochar yields showed a decreasing trend with the increasing temperature, as a higher solid recovery was found in the lower temperature. The mass yield of 91.4% was observed at the temperature of 100°C, and then decreased to approximately 80.4%, 69.3%, and 55.7% at the temperatures of 150, 180 and 220°C, respectively. Liu et al. (2013) reported a solid yield of hydrothermally carbonized coconut fiber and eucalyptus leaves are 70% and 65% at the temperature of 200°C, respectively [15].

In accordance to the mass yield, increasing the temperature led to a decrease in the energy yield, while the energy densification ratio increased. The HHV of hydrochars increased positively with the temperature. HTT-220 hydrochar has a heating value which almost equals to a low-grade sub-bituminous coal (approximately 20 MJ/kg [16]). Thus, it may be possible to use the HTT products as a solid co-firing fuel with coal. The likely explanation for the elevated HHV is that HHV highly correlated with the elemental composition of the hydrochars. The changes in the chemical composition of EFB during HTT will directly affects the energy contained in the biomass. The chemical changes in EFB during HTT will be discussed in detail in the next sub-chapter.

Table 2-1. HHV, mass, energy yields of the raw EFB and the corresponding hydrochars

Properties	Raw	HTT-100	HTT-150	HTT-180	HTT-220
HHV, dry (MJ/kg)	16.7	16.8	17.5	18.0	19.6
Mass yield (%)		91.4	80.4	69.3	55.7
Energy densification ratio		1.01	1.05	1.08	1.17
Energy yield (%)		92	84	75	65

The calculated energy densification ratio increases with the increase of the reaction temperature, from 1.01 at 100°C to 1.17 at 220°C. As shown in Table 2-1, generally a high energy yield was obtained at the low temperature of HTT (average of 88% at temperature lower than 180°C), while at the high temperature of 220°C the lowest energy yield was obtained (65%). During the HTT, the decomposition of lignocellulose is more severe at a higher temperature, leading to the higher mass loss at 220°C which is dominated by the decomposition of the hemicellulose component.

2.3.2 Physicochemical characteristics of hydrochars

The physicochemical characteristics of the hydrochars were evaluated via ultimate analysis, which is shown in Table 2-2. The ultimate analysis of raw EFB is also presented as a comparison between the elemental values of hydrochar before and after the pretreatment.

Table 2-2. Chemical characteristics and properties of the raw EFB, and the hydrochars

Element	Weight Percentage (wt%), dry				
	Raw	HTT-100	HTT-150	HTT-180	HTT-220
Ash	4.9	4.6	3.4	2.2	4.1
C	43.56	44.07	45.25	46.43	49.98
H	5.34	5.24	5.51	5.57	5.38
N	0.56	0.79	0.59	0.4	0.77
S	0.11	0.08	0.09	0.03	0.09
Cl	0.67	0.23	0.26	0.18	0.5
O (diff)	44.86	44.99	44.9	45.19	39.18
K (%DM)	3.24	1.46	1.48	0.84	0.9

The elemental compositions of hydrochars were evidently altered by HTT, particularly at the HTT temperature of 220°C. The HTT decomposes the EFB biomass material and yields products with higher carbon content. The HTT temperature affects the carbon fraction which steadily increases with the increase of the HTT temperature. HTT-220 hydrochar shows the maximum increase of the carbon content, with an increase of 14.7%, compared to raw EFB. The maximum decrease of oxygen was also observed for HTT-220, as a result of the carbonization process, representing the removal of this element during HTT process.

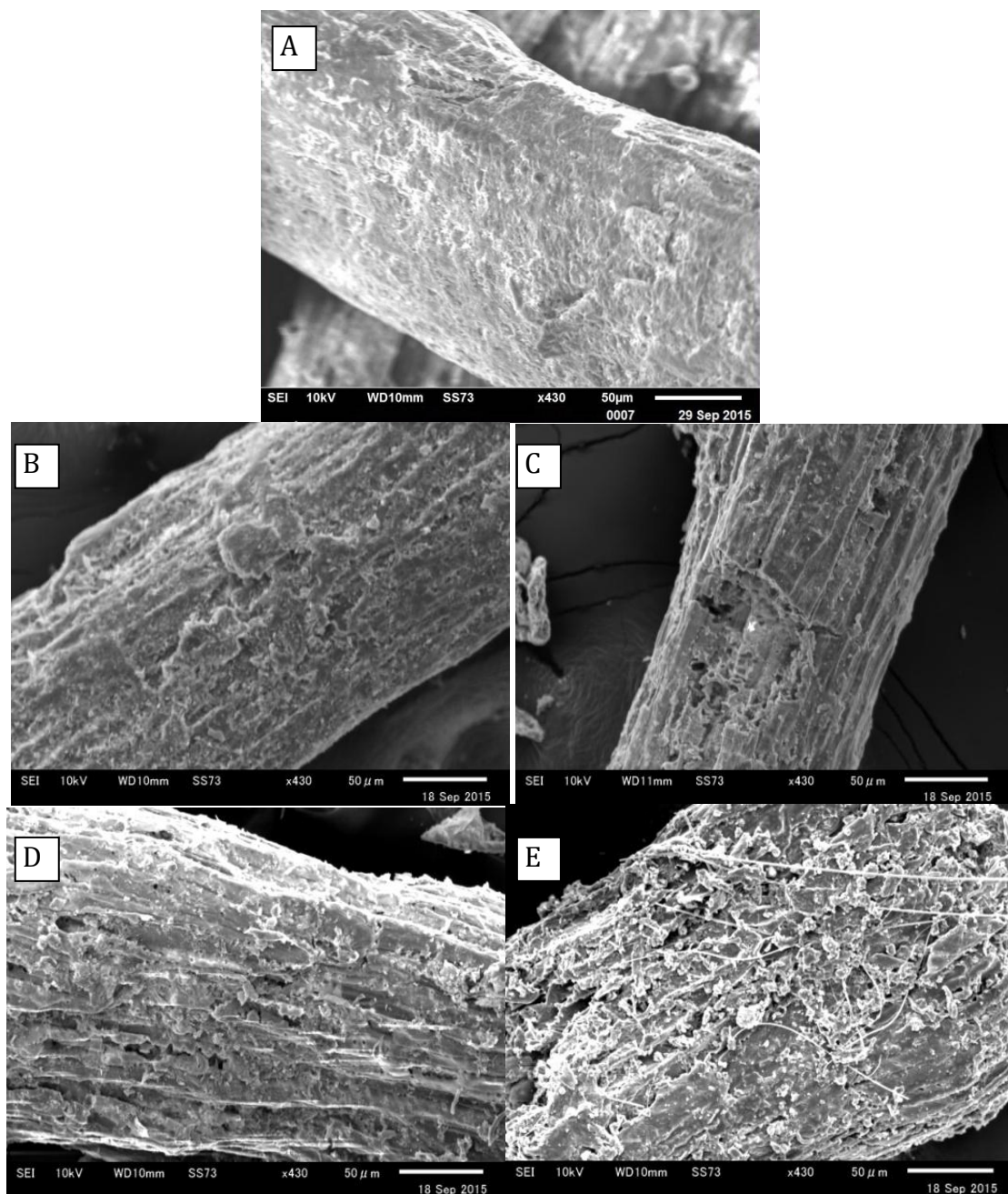


Figure 2-2. The SEM images of EFB hydrochars (A= raw EFB, B=HTT-100, C=HTT-150, D=HTT-180, E=HTT 220).

The decomposition severity also can be seen from the close observation of hydrochars by means of the electron microscopy techniques (SEM). The clear comparison on the morphology structure of the raw EFB and its corresponding hydrochars can be seen in the SEM images depicted in Figure 2-2. The SEM images revealed morphology changes of the raw EFB after HTT, and the morphology difference among the hydrochars obtained at different temperatures. The SEM image of raw EFB (Figure 2-2(A)) shows the lignocellulosic cellular structure that is not yet damaged by the HTT process. Hydrochars at low HTT temperatures (100 and 150°C) show no significant

transformations, only a light rupture on the surface of the biomass was seen, indicating that a low HTT temperature (under 150°C) is not enough to decompose the fibrous structure of EFB. However, porous structure and some breakdown of the lignocellulosic materials were observed for the hydrochars obtained from HTT at higher temperatures. Moreover, numerous globules and some fibers were detected on the surface of HTT-220 hydrochar. The globules are possibly formed by partial degradation of cellulosic component and subsequent precipitation followed by the growth as sphere [17]. The fibers are thought to be lignin that is not undergoing degradation at 220°C, due to its thermal stability.

The obtained hydrochars contained a lower amount of ash compared to the raw EFB, ranging from 2.2 to 4.6 wt% (Table 2-2). The ash content was significantly reduced after HTT, progressively with the increase of the temperature. Inorganic material in the form of either loose dirt from harvesting or loosely bonded in a cross-linked matrix is removed during the HTT process leading to the decrease of the ash content. There is also some expectation that additional acidity produced in HTT may solubilize and remove inorganics [18]. The inorganic solubilization from EFB was increasing with the increase of the severity of the HTT conditions. Nonetheless, HTT-220 hydrochar exhibited a higher ash content compared to HTT-180 hydrochar. Under a higher HTT temperature, EFB becomes more porous as all the hemicelluloses and extractives will be reacted and much of the cellulose will be reacted as well [19]. Porous structure might absorb some inorganics, which might explain the increase of the ash content of HTT-220 hydrochar, as compared to HTT-180 hydrochar. The bigger pore size observed in the microscopy observation also supports this reason. The use of the low-ash hydrochars as fuel will be advantageous because it will reduce the potential of solid deposition on combustor surfaces that commonly found for combustion of high-ash fuel [20].

The Cl content decreased with the increasing HTT temperature, with the maximum decrease was seen for HTT at 180°C (see Table 2-2). The high chlorine and alkali contents of some biomass actually raise concerns regarding corrosion. The chlorine concentration should be minimized in all cases. Therefore, lowered Cl content after HTT-180°C is benefit in reducing the problems in the combustor, particularly the corrosion concern.

However, at higher T (220°C), the Cl content was seen increasing. Many researches were also reported that the behavior of the inorganics during hydrothermal carbonization is largely unknown and there is also little evidence on how the ash content is dependent on the process parameters [15, 21]. The reason why chlorine increased at HTT 220°C after the optimum chlorine decrease at the temperature of 180°C is because the chlorine content (as well as other inorganic content) was highly related to the ash content in the samples. As the ash content in the samples increased (increased in the HTT-220 hydrochars), the percentage of the chlorine also increased.

There are 2 hypotheses to explain this phenomenon. Firstly, under higher temperature (220°C) the degradation of the hemicelluloses and cellulose is faster than the solubilization of the ash (inorganic constituents), thus resulting in the higher ash content in the produced hydrochar. This increase in the ash content observed with the treatment severity was due to the loss of solubilized biomass. In other words, the measured ash was due to enrichment in the sample due to loss of organic content [22].

Secondly, at a high temperature (220°C), all the hemicelluloses and extractives have been reacted and some part of cellulose has reacted as well, leaving behind a porous solid which is also shown in the SEM images (Figure 2-4). As explained previously, the porous structure might absorb some inorganics, which might explain the increase in the ash content and inorganic contents (K, Cl, etc) [19]. This hypothesis was consistent with previous reports [15, 21] which had reported that the ash might become less soluble and precipitated from solution at higher temperatures and pressures. The precipitated ash might be left in the porous structure of the hydrochar. The report [21] suggested that carbonization conditions should be optimized to obtain a hydrochar with the desired ash content. The presence of Cl content in the hydrochars by mapping using SEM-EDX (Energy dispersive X-ray) analysis was also conducted and shown in Figure 2-3.

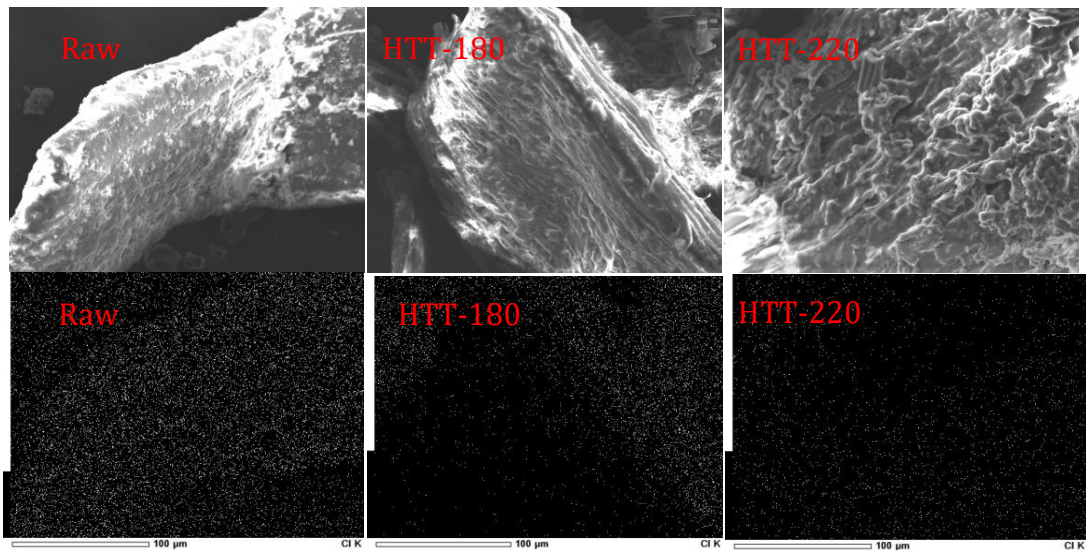


Figure 2-3. Mapping of the chlorine content on the hydrochar surface by SEM-EDX

Table 2-3. Elemental metal analysis of hydrochar by SEM-EDX

Sample	Na (%)	K (%)	Mg (%)	Ca (%)	Cl (%)	Si (%)
Raw	0.7	56.1	2.7	10.4	8.1	22.0
HTT-180	N/A	48.7	5.7	25.4	3.3	16.9
HTT-220	4.2	45.0	9.3	13.4	8.5	20.0

EDX analysis has shown that the white dots seen on the surface of the raw-EFB particles have high concentration of Cl. On the surface of HTT-180 hydrochar, the white dots were seen reduced, and more dots had appeared on the surface of the HTT-

220 hydrochar. The characterization of the hydrochar samples using SEM-EDX has shown that substantial removal of Cl is taking place after HTT at 180°C. Nonetheless, some Cl was stayed on the surface and in pores of the HTT-220 hydrochar probably due to re-absorption or precipitation of the element. The elemental analysis of the hydrochars by SEM-EDX also showed the increase percentage of Cl in the surface particle of HTT-220 hydrochar (see Table 2-3). However, SEM-EDX provides only semi-quantitative results and thus they cannot be used for an accurate estimation.

The results showed here implied that the fuel qualities of the hydrochars are improved compared to its parent biomass, having decreased oxygen and ash contents, and increased carbon content and HHV. The resulting hydrochar has the potential to be a satisfactory solid fuel for either direct combustion or co-combustion with coal. A higher reaction temperature produced relatively higher HHV especially at 220°C, but considering the energy yield and the ash content of the product, HTT at 180°C seems more favorable for the large-scale production of solid fuel from EFB. Moreover, the HTT reaction at a lower temperature and lower pressure results in less energy requirement and lower capital/operating costs.

2.3.3 Mass balance and energy balance

2.3.3.1 Mass balance

Figure 2-4 shows the input and output streams in the experimental lab-scale HTT process. The input streams includes the EFB and distilled water in 1 : 10 biomass to water ratio. The final dried solid product was obtained upon the drying of wet filtrated solid. In this study, the quantity of blow off gas is determined by balance and not measured directly.

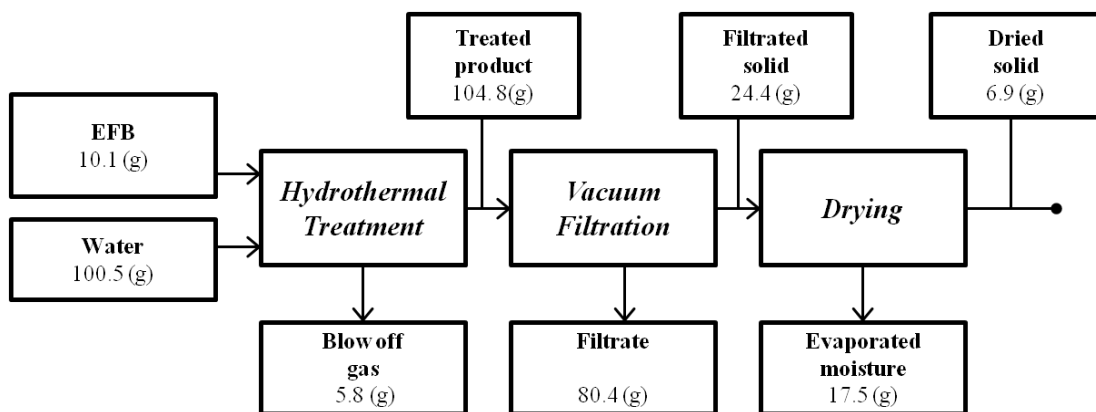


Figure 2-4. Mass balance for HTT of EFB at the temperature of 180°C

Approximately, 10 g of dried EFB was used in each experiment. Since the recovery of the treated product was conducted after the reactor temperature cooled down to under

the vaporization temperature of water, the product after HTT recovered is around 104.8 g which is equal to 93.8% of the total mass input. The final dried solid is around 6.9 g, which is equal to 6.3% of the total mass input to the system.

Table 2-4 Mass balance in the HTT process of EFB

Condition (°C, 30 min)	Hydrothermal treatment (%)			Filtration (%)		Drying (%)	
	EFB and water input	Treated product	Blow off gas	Filtrated solid	Filtrate	Dried solid	Evaporated moisture
100	100	91.3	8.7	25.8	65.5	8.3	17.5
150	100	91.5	8.5	24.8	66.6	7.3	17.5
180	100	93.8	6.2	21.5	72.3	6.3	15.2
220	100	90.9	9.1	14.7	76.2	5.1	9.6

All the experiment mass balance results are shown in Table 2-4. To simplify the calculation, the mass of system input was taken as the datum (100%). Dewatering by vacuum filtration resulted in quite large amount of filtrate at around 65.5%; and this liquid amount was increasing with the reaction temperature increased. Inversely, the moisture that needs to be removed by drying is decreased with the increasing the reaction temperature. This shows that the product obtained at a higher temperature has a better dewatering and drying performance. However the final dried product was seen to be decreased, from 8.3% at 100°C to 5.1% at 220°C. This is in consistent with the decreased mass yield at a higher HTT temperature discussed in the previous sub-chapter. The higher treatment temperature means more severe condition was applied; thus, the raw EFB was decomposed severely leading to a lower dried recovered mass.

2.3.3.2 Energy balance

The energy balance calculation result of the lab-scale HTT is summarized in Table 2-5 by taking the percentage of the total energy input (100%) as the datum. Some assumption has been taken for this calculation. From the assumptions, the energy input may be approximated by the energy required to heat the reaction input, in this case EFB and added water, from room temperature (T_{25}) to the specified reaction temperature (T_T). The recovered energy (output energy) from the final product was the multiplication of the HHV of HTT-EFB and its dried mass.

As shown in Table 2-5, all the calculated energy output/input ratios were <1.0, suggesting that the present HTT operations in the batch reactor were energy inefficient. The explanation for this is that the water to biomass ratio (1:10) used in this experiment is too high. Thus, energy input was mostly used for heating up the water. For all of the experiments, the EFB utilized is in dried form, then we needed to add water in ratio 1:10 (biomass to water) to make sure the submerged condition of the sample inside the reactor due to bulky nature of EFB. Taking 8.1% of the total energy input for drying, the 220°C HTT demonstrated the best drying performances. However, the energy required for HTT was the highest leading to the lowest energy output/input ratio. The

highest energy output/input ratio was obtained under the 100°C treatment condition while the required energy for drying was the highest; showing that the larger moisture content was left after the filtration process, which means low dewaterability compared to other conditions. Its energy used in HTT was 85.6% of the total energy input and the required energy for the filtration and drying was 14.4% of the total energy input. Admittedly, due to the above assumptions, the obtained energy output/input ratio can only be an approximation, which may however be used for qualitative discussion of the net energy efficiency for the investigated process.

Table 2-5. Estimated energy produced and utilized

Condition (°C, 30 min)	Energy output (%)	Energy input (%)			Energy Output/Input ratio
		HTT	Filtration & Drying	Total	
100	50.7	85.6	14.4	100.0	0.51
150	45.4	85.9	14.1	100.0	0.45
180	40.6	87.7	12.3	100.0	0.41
220	36.9	91.9	8.1	100.0	0.37

It was realized that in the real application, biomass to water ratio 1:10 is not applicable because too high energy will be utilized for heating up the water to the target temperature. As explained before, the ratio of 1:10 used in the lab scale autoclave was needed to make sure that enough water was available to submerge the EFB samples to ensure complete sample mixing during HTT. In the large scale, big mixing blade is utilized to mix the sample and the steam will be supplied accordingly until reaching the target temperature we set. To determine the steam supply (or water consumption) in the large scale, it can be calculated based on this equation (adapted from Prawisudha (2013)) [23] :

$$\left\{ \begin{array}{l} \text{Energy} \\ \text{for steam} \\ \text{injection} \\ \text{phase} \end{array} \right\} = \left\{ \begin{array}{l} \text{Energy} \\ \text{from} \\ \text{steam} \\ \text{@injection} \end{array} \right\} + \left\{ \begin{array}{l} \text{Energy} \\ \text{from} \\ \text{motor} \\ \text{@inj.} \end{array} \right\} + \left\{ \begin{array}{l} \text{Energy} \\ \text{from} \\ \text{utility} \\ \text{@inj.} \end{array} \right\}$$

$$= \left\{ \begin{array}{l} \text{Energy} \\ \text{to heat} \\ \text{reactor} \end{array} \right\} + \left\{ \begin{array}{l} \text{Energy} \\ \text{to heat} \\ \text{EFB} \end{array} \right\} + \left\{ \begin{array}{l} \text{Energy} \\ \text{to heat} \\ \text{water} \end{array} \right\}$$

In this calculation, assumptions were made as follows:

1. The process was performed in saturated liquid phase.
2. The specific heat of Raw EFB was assumed to be 1.48 kJ/kg.K [13].
3. The hydrothermal reactor model was derived from a technical drawing of the plant utilized in Prawisudha (2013) [23] and the dimensions was shown in Table 2-6.

4. The energy from motor and energy from utility during injection were neglected.

Table 2-6. Tank Dimensions and Operational Data (adapted from [23]).

Tank Operational Data			
Tank volume	V	m ³	3
L/D	X	-	2
Tank pressure	P	MPa	3
Safety Factor	SF	-	1.7
Material			Steel, structural
Yield strength	σ	MPa	345
Density	ρ	kg/m ³	7850
Specific heat	cp	kJ/kg.K	0.456
Tank Dimension			
Tank diameter	D	M	1.24
Tank length	L	M	2.48
Tank thickness	t	mm	18.3
Tank Plate Properties			
Plate volume	Vp	m ³	0.2131
Plate mass	Mp	kg	1673.1
Heat capacity	Cp	kJ/K	762.9

Therefore, to calculate the water consumption at the injection phase, the below equation was adopted from Prawisudha (2013) [23] as follows:

$$m_{\text{water},i} (h_{\text{steam}(T,p)} - h_{\text{water}(T_0)}) = [m_{\text{reactor}} \cdot c_{p,\text{reactor}}(T - T_0)] + [m_{\text{EFB}} \cdot c_{p,\text{EFB}}(T - T_0)] + [X \cdot m_{\text{EFB}}(h_{\text{sat}}(T) - h_{\text{water}(T_0)})]$$

Where

$m_{\text{water},i}$	= accumulative water consumption at the injection phase (kg)
$h_{\text{steam}(T,p)}$	= enthalpy of steam at the operational T and P (kJ/kg)
$h_{\text{water}(T_0)}$	= enthalpy of water at the initial temperature $T_0 = 25^\circ\text{C}$ (kJ/kg)
m_{reactor}	= reactor mass as a single metal body (kg)
$c_{p,\text{reactor}}$	= reactor specific heat (kJ/kg.K)
m_{EFB}	= dry EFB mass (kg)
$c_{p,\text{EFB}}$	= dry EFB specific heat (kJ/kg.K)
X	= moisture content, wet base (kg/kg)
$h_{\text{sat}}(T)$	= enthalpy of water at the saturated liquid temperature T (kJ/kg)

From the calculated result, to heat up 1 ton raw EFB feedstock with 60% moisture content to the operation temperature of 180°C and pressure 1 MPa in the commercial scale reactor, the water consumption (steam supply) needed is 678.6 kg. As a result, the biomass (wet) to water ratio becomes approximately 1: 0.68. It can be noted that if the energy from motor and utility were not neglected, the water consumption might be lower than the result in this calculation.

From previous investigation on commercial scale HTT of municipal solid waste (MSW), Prawisudha [24] stated that around 700 kg water is consumed for 599 kg input raw MSW; given an approximately 1:1 biomass to water ratio. Other investigation by Areprasert on pilot-scale HTT of paper sludge [25] showed for input paper sludge (moisture content 76%) as much as 351 kg, it will utilized 138 kg of steam; giving a ratio of 1:0.5. Therefore, to give a picture of energy balance for HTT EFB in bigger scale, the energy balance will be re-calculated assuming that the biomass to water ratio is 1:0.68 based on the above calculation and presented in Table 2-7.

Table 2-7 Re-calculated energy balance assuming biomass to water ratio 1:0.68

Condition (°C, 30 min)	Energy output (%)	Energy input (%)			Energy Output/Input ratio
		HTT	Filtration & Drying	Total	
100	709.8	86.3	13.7	100	7.10
150	616.7	87.0	13.0	100	6.17
180	541.0	88.8	11.2	100	5.41
220	478.3	92.9	7.1	100	4.78

From Table 2-7, we can see that the energy input percentage for HTT phase and filtration and drying phase is slightly different with the previous calculation, but still comparable. However, a significant difference can be noticed for energy output/input ratio that now >1.0; implied that now the system is more efficient. Therefore, it can be understood that the biggest energy consumption will be mainly the energy need for heating up water (and moisture) or for generating steam.

2.3.4 Combustion characteristics

The combustion characteristics of raw EFB biomass and hydrochars were depicted in the thermal gravimetric (TG) and differential thermal gravimetric (DTG) profiles as a function of the processing temperature in Figure 2-5. The combustion characteristic was investigated via combustion of HTT-180 and HTT-220 samples, along with the raw EFB sample for comparison.

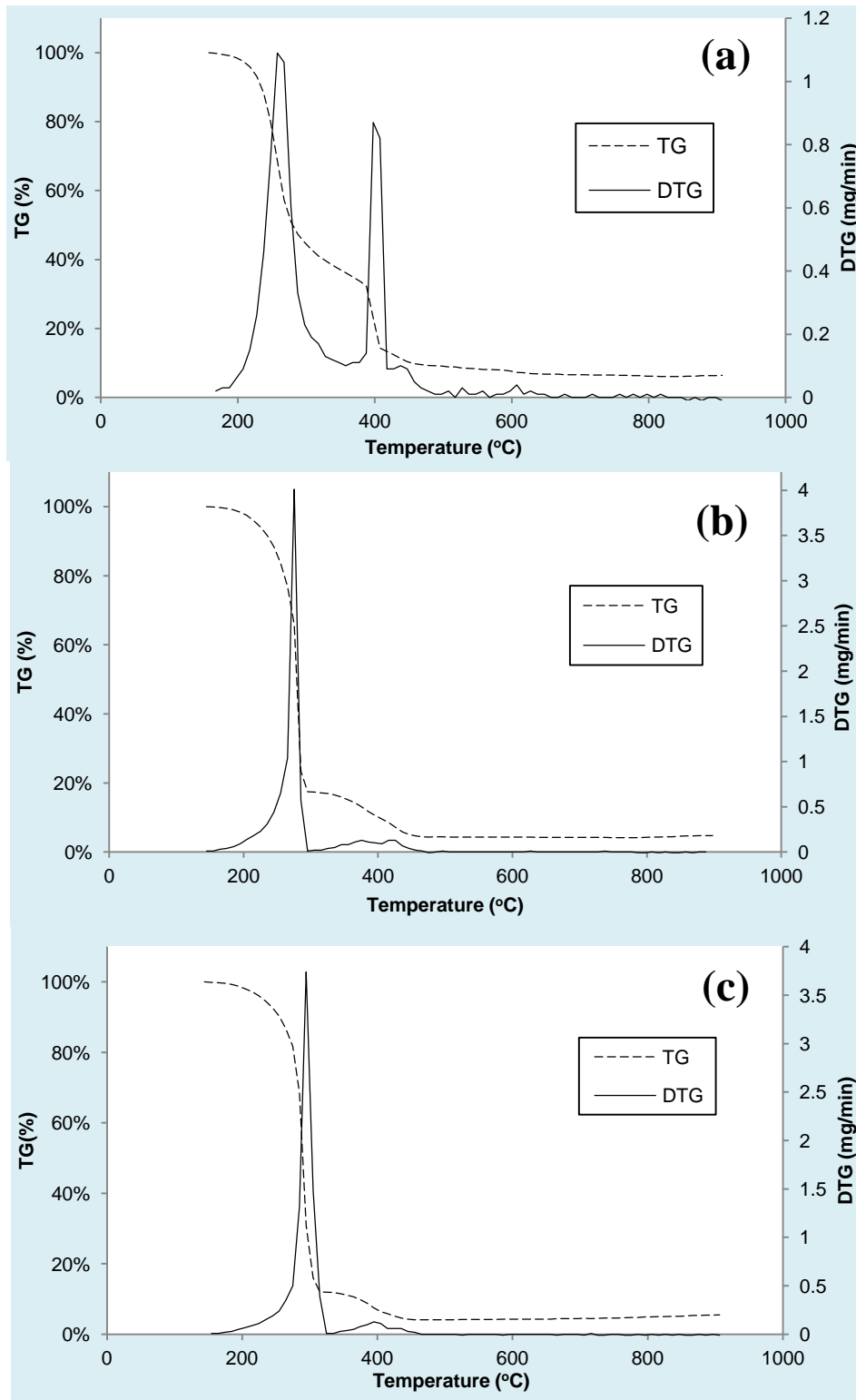


Figure 2-5. TG and DTG curves of raw EFB and its corresponding hydrochars in oxidative atmosphere (a=raw EFB, b=HTT-180, c=HTT-220).

Table 2-8 summarizes the characteristics temperatures and peak points of the combustion process. To note, the TG and DTG curves plots were started from the

temperature above 140°C where the water evaporation stage finished. Overall, from the DTG curves, it was clearly seen that there are two peaks present in the combustion of raw EFB, in contrast with the combustion of corresponding hydrochars that have only one obvious peak.

From Figure 2-5(a), the raw EFB combustion appears in two stages; the first stage is between 235 and 337 °C, and the second stage is between 388 and 431 °C. The temperature region of 200-400 °C is typical for the decomposition of hemicelluloses and cellulose [26]. The defined peaks appeared in both stages of the raw EFB combustion are in agreement with the hemicelluloses and cellulose contents of the EFB. Increasing the temperature further from around 200°C resulted in the chemical bond breakdown and the release of light volatile compounds. The less marked decomposition at higher temperature above 450°C was indicative for the lower lignin content present in the raw EFB [27]. This observation can be explained by changes in the composition of EFB during HTT; the relative amount of lignin molecules was increased due to the significant decrease of the hemicellulose fraction. The rate of destruction of the polymeric structure of biomass typically depends on the reaction time, the temperature and the reaction medium. In the hydrothermal degradation of biomass, the reaction mechanism is initiated by hydrolysis, which exhibits lower activation energy of hemicelluloses and cellulose than most of the pyrolytic decomposition reactions. Therefore, the principle biomass components are less stable under hydrothermal conditions, which lead to lower decomposition temperatures. In contrast with most of the pyrolytic hemicelluloses decomposition that usually happen between 200 - 400°C, hemicelluloses decomposes between 180 – 200 °C under HTT condition. It is also favoring the rapid degradation and depolymerisation of these polymers into the water soluble products like oligomers and monomers [21, 28]. Since the hemicelluloses starts to decompose during HTT at 180°C, the initial combustion temperature for both hydrochars was increased (Table 2-8) compare to the raw EFB which corresponds to the loss of hemicelluloses after the HTT process.

Table 2-8 shows that the highest weight loss rate was appeared in the higher temperature for HTT-180 hydrochar (at 285°C) and HTT-220 hydrochar (at 295°C). This implies that the hydrochars have lower reactivity compared to raw EFB as the temperature at the maximum weight loss rate is negatively proportional to the reactivity [29]. In Figure 2-5(b) and 2-5(c), one sharp peak appears in the temperature range of 200-300 °C obviously, and a smaller peak is observable at the temperature above 400 °C. The first peak shows that the combustion occurred was quick and intensive with significantly high maximum weight loss rate of 4.01 mg/min and 3.74 mg/min for HTT-180 and HTT-220, respectively. Meanwhile, the smaller peak above 400°C is indicative for the combustion of lignin content. The raw EFB relatively has more hemicellulose content than the HTT treated EFB; hence, its primary combustion stage takes place at a lower temperature near the range of the hemicellulose combustion temperature. As explained previously, HTT decreased the hemicellulose content in EFB. More severe

condition of HTT will lead to the lower content of hemicellulose. Then the weight loss curve of the combustion process will be shifted to a higher temperature at which the decomposition is mainly dominated by the cellulose and lignin degradation.

Table 2-8. The combustion characteristic parameters for the raw EFB and its corresponding hydrochars

Sample	Initial combustion temperature (°C)	First stage		Second stage		Final combustion temperature (°C)	Residue (db,wt%)
		T _{max} (°C)	DTG _{max} (mg/min)	T _{max} (°C)	DTG _{max} (mg/min)		
Raw EFB	198	258	1.09	398	0.87	467	5.0
HTT-180	225	285	4.01			456	4.3
HTT-220	215	295	3.74			451	4.1

The combustion of hydrochars shifted to a higher temperature but a narrower range (from 198 – 467 °C for the raw EFB to 225 – 456 °C for HTT-180) compared to its corresponding raw material. These elevated combustion temperatures demonstrate that the hydrochars was combusted more homogenously, improved the combustion safety, and suggested that a higher thermal efficiency could be achieved from the combustion of hydrochars [2, 29, 30]. It was known that a low combustion temperature for biomass is related to high pollutant emissions [30], thus with the elevated combustion temperatures, the pollutant emissions might be reduced by the use of this EFB hydrochars. In brief, it was observed that HTT at a mild temperature caused the decomposition of hemicelluloses resulting in the change of the combustion behavior of EFB; such as elevated combustion temperature regions and smaller differences in the reactivity of the biomass components.

2.3.5 Mechanism of HTT

2.3.5.1 Van Kravlen Diagram

Under HTT process, the EFB biomass undergo a coalification-like process [20]. In order to examine the effect of HTT on the atomic composition and to analyze the chemical transformations that possibly take place during HTT, the atomic H/C and O/C ratios of biomass and the corresponding hydrochars were plotted in a Van Kravlen diagram. Van Kravlen diagrams allow for delineation of reaction pathways, where straight lines were drawn to represent the dehydration and decarboxylation pathways [31].

As discussed in the sub-chapter 2.3.2, HTT altered the chemical characteristics of the raw EFB. The raw EFB has high atomic H/C and O/C ratios. The H/C and O/C ratios were decreased with increasing the HTT temperature, even at the low temperature of 200°C, the ratios were far lower than that of raw EFB. The alterations was also resulted in the significant decrease of the O/C ratio at 220°C compared to other lower operating

temperatures, shifting the fuel value of the raw EFB from the biomass region at the top right of the Van Kravelen diagram to a near peat region as illustrated in Figure 2-6. This result shows that the hydrochar obtained by 220°C HTT was denser, since the degradation of hemicelluloses and all extractives at HTT above 200°C enhances densification [32]. In Figure 2-7, we can notice that there is no significant compositional change for hydrochars at the HTT temperature lower than 180°C due to the fact that the most easily reactive hemicelluloses and aqueous soluble do not start reacting until the temperature reaches 180°C [32, 33].

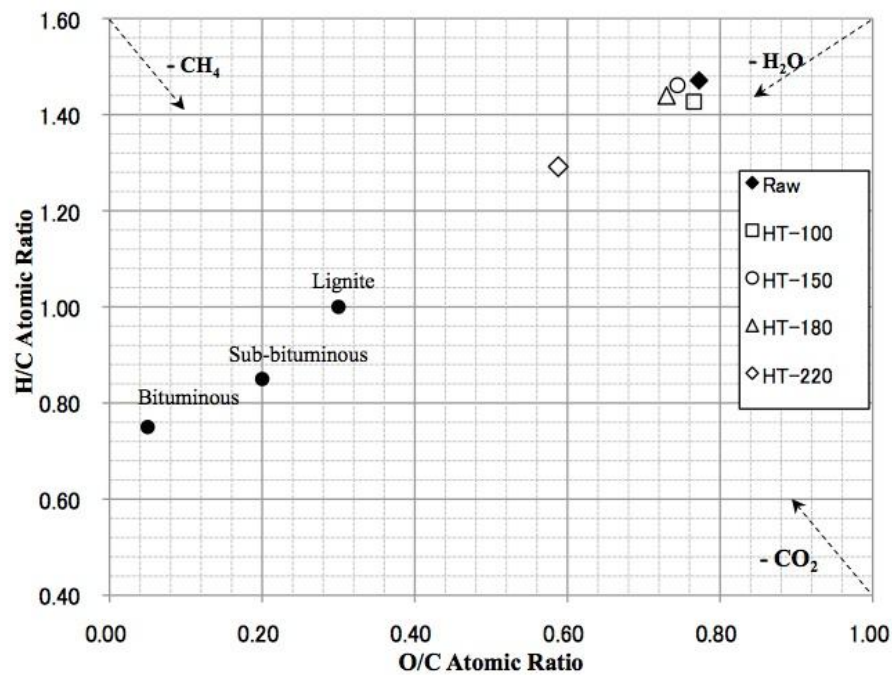


Figure 2-6. Van Kravelen diagram of raw EFB and its resulting hydrochar at various HTT temperatures

It can be noticed from the depicted diagram that the dehydration is the predominant reaction during HTT. The slope of the trajectories shown in Figure 2-6 suggests that the O content decreased in proportion to the H content, probably due to the dehydration. It is clear that the decrease in O and H content occurred mainly in the range of 180–220°C. Generally, a fuel with low H/C and O/C ratios is favorable because of the reduced energy loss, smoke and water vapor during the combustion process [15].

2.3.5.2 FTIR

When an infrared light source irradiates a sample, molecules in the sample can absorb certain wavelengths of light, so that absorption bands appear in FTIR spectra. In general, the infrared spectrum interval is divided into three areas: (1) near-infrared region, 12800–4000 cm^{-1} ; (2) mid-infrared region, 4000–400 cm^{-1} ; and (3) far-infrared region, 400–10 cm^{-1} [34]. Based on the combined analysis of the two types of vibration

frequency, the group frequency and the fingerprint frequency, the FTIR spectra of samples can be interpreted.

Therefore, further insight into the chemical composition of the material may be obtained by FTIR-ATR. In Figure 2-7, a comparison on the surface spectroscopy of the raw EFB and the corresponding hydrochars processed at 150°C and 180°C is illustrated. It should be noted that the peak around 2300 to 2400 cm^{-1} was attributed to uncontrollable CO_2 in the measurement environment. Determination of the main functional groups for a given wave number is based on previous reports [33, 35].

As indicated in Figure 2-7, the FTIR spectra are assigned into five regions representing the main identification peaks. It seems that there were some changes in the FTIR adsorption peaks due to HTT, although the changes were not tremendous in FTIR spectra of hydrochars.

According to identification peaks, the characteristic of the peak could be explained as follows[20, 33, 35, 36] :

- (1) Wide band at 3700 – 3000 cm^{-1} is attributed to the O-H stretching vibrations in the hydroxyl and carboxyl groups [36]. In relation to the raw-EFB, the intensity of the peaks decreased with the increasing the HTT temperature. This band detects the presence of water, indicating that with the elevated temperature, the water molecules within solids were gradually expelled [20]. In other words, the dehydration process was occurred during HTT. This also indicates that the hydrochars is more hydrophobic compared to the raw EFB.
- (2) A small double peak at 3000 – 2800 cm^{-1} shows the vibrations of aliphatic C-H compounds [27], suggesting the presence of aliphatic structures [36]. The weakened peaks as the temperature elevated indicating that several long aliphatic chains were broken down [20].
- (3) The peak at 1700 – 1740 cm^{-1} is attributed to the carbonyl (C=O) stretching vibrations. This carbonyl can be assigned to C=O of ketone or unconjugated xylan, which identify the hemicelluloses components [33]. This identified peak becomes weak with increasing the reaction temperature, since hemicelluloses start hydrolyzing at the HTT temperature above 180°C [37] . The peak at around 1630 cm^{-1} and at 1515 cm^{-1} were unchanged during HTT, which correspond to C=C stretching vibrations present in lignin [27] and aromatic skeletal vibrations derived from lignin [20], respectively. The presence of these peaks marked the inert behavior of lignin during HTT under a mild temperature.
- (4) Several peaks at this region were indicating the characteristics of cellulose that steadily present in HTT under a mild temperature considering the fact that the cellulose hydrolysis starts above 220°C [35]. The peak at around 1270 cm^{-1} , 1130 cm^{-1} , and 1050 cm^{-1} were appeared in the raw EFB, mostly indicating cellulose and lignin, and they became more intense in case of the HTT-EFB. In particular, peak at 1050 cm^{-1} was attributed to glycosidic bonds, indicating the presence of cellulose,

becomes stronger with HTT severity, probably due to cellulose concentration increasing [38].

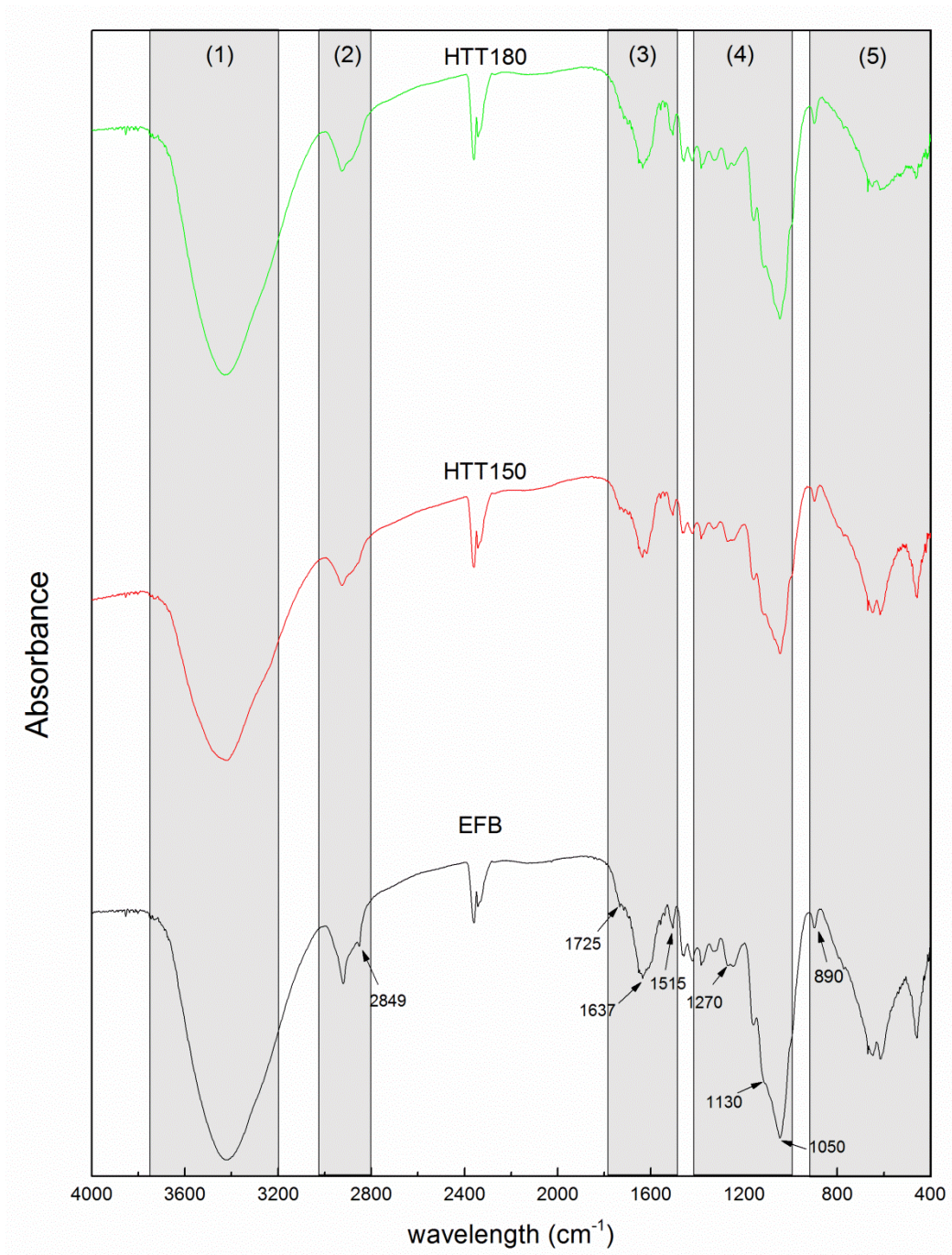


Figure 2-7. FTIR spectra of raw EFB and its derived hydrochar.

- (5) The peaks at $900 - 700 \text{ cm}^{-1}$ and $700 - 400 \text{ cm}^{-1}$ were attributed to the C-H bend in cellulose and hemicelluloses [38], respectively. As seen in Figure 2-7, the later peak was disappeared at the temperature of 180°C , indicating the hemicelluloses degradation. The 890 cm^{-1} peak revealed the anomeric C-groups, the C1-H deformation of cellulose that remained unchanged during HTT of 180°C [33].

From the FTIR analysis, it can be seen that raw-EFB comprise of cellulose, hemicellulose and lignin. Therefore, strong presences of single bonds components, such as O-H, C-H and C-O bonds, were expected. However, some decrease of peaks (in relation of Raw-EFB) suggested that the dehydration and the hydrolysis of hemicelluloses processes occurred during HTT of EFB. This is consistent with the previous analysis of O/C-H/C atomic ratio evolution based on Van Kravelen diagram.

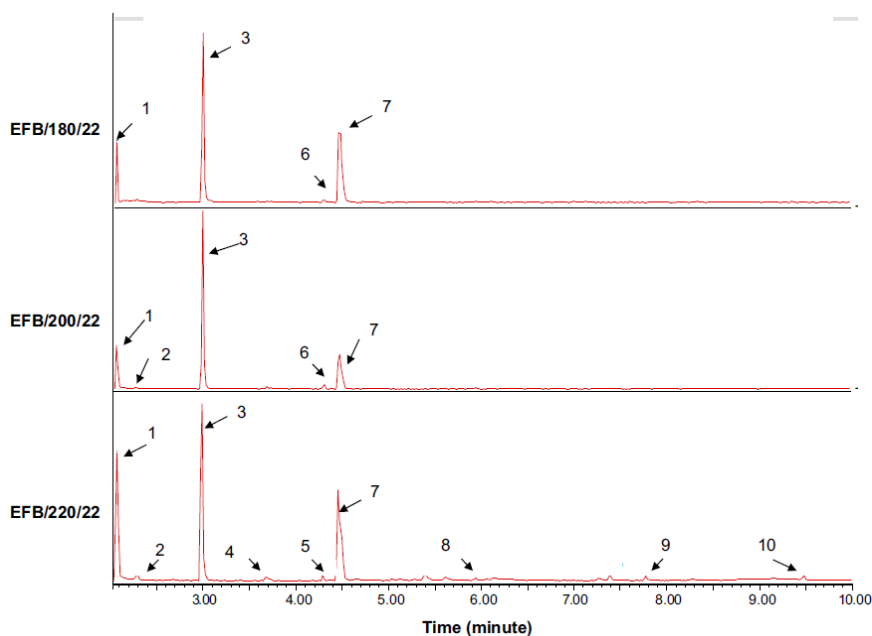


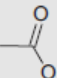
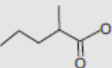
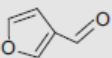

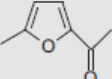
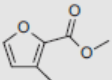
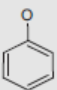
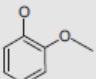

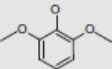
Figure 2-8. GC/MS chromatogram of the EFB liquid products of HTC process (EFB/Temperature/22) (adapted from [39])

More clarification on the reactions that might occur during HTT can be obtained by measuring the organic composition of the liquid HTT. However, the analysis on the organic composition of the liquid HTT has not been conducted due to the limitation in the equipment we have to analyze the organic component of such liquid product. However, the analysis of liquid HTT from EFB with holding time 22 h has been conducted by other researcher [39]. Figure 2-8 and Table 2-9 showed the GC/MS chromatogram and the organic component detection of EFB liquid product from the study, respectively.

From the analysis, it was found that the hydrolyzed products were not detected in the liquid sample. This is attributed to the products of hydrolysis being further converted through dehydration, and possibly depolymerization. The hydrolysis process occurs efficiently in the relatively short time (~2h) [39]. Hydrolytic reactions are the major solid surface reactions, where water reacts with cellulose or hemicellulose and breaks ester and ether bonds (mainly β -(1-4) glycosidic bonds), resulting in a wide range of products including soluble oligomers like (oligo-) saccharides, and 5-HMF from

cellulose, and furfuraldehyde (furfurals) from hemicelluloses. With increased reaction time, these oligomers further hydrolyze into simple mono- or disaccharides (e.g., glucose, fructose, xylose). On the other hand, 5 HMF further hydrolyzes into levulinic and formic acid [40]. The reaction pathway is illustrated in the Figure 2-9.

Table 2-9. Products detected in liquid extract after the HTC process at 180, 200 dan 220 °C for t = 22 h (adapted from [39])

ID no	Compound	Structure	Formula	Mw	Retention time (minute)	Area (%) ^a
1	Acetic acid		C ₂ H ₄ O ₂	60	2.06	24.15(±0.31)
2	Pentanoic acid, 2-methyl-		C ₆ H ₁₂ O ₂	116	2.39	2.03(±0.04)
3	3-furaldehyde		C ₅ H ₄ O ₂	96	2.97	39.63(±0.12)
4	4,4-dimethyl-2-cyclopentene		C ₇ H ₁₂	96	3.69	2.63(±0.01)
5	Furfural, 5-methyl		C ₆ H ₆ O ₂	110	4.29	3.11(±0.04)
6	2-furancarboxylic acid, 3-methyl-, methyl ester		C ₇ H ₈ O ₃	140	4.31	2.39(±0.10)
7	Phenol		C ₆ H ₆ O	94	4.46	17.21(±0.07)
8	Phenol, 2-methoxy-		C ₇ H ₈ O ₂	124	5.94	2.63(±0.06)
9	Furfural, 5-hydroxymethyl		C ₆ H ₆ O ₃	126	7.78	3.08(±0.03)
10	Phenol, 2,6-dimethoxy-		C ₈ H ₁₀ O ₃	154	9.48	3.13(±0.09)

^a Percentage area (Area %) is taken from the area under the chromatogram.

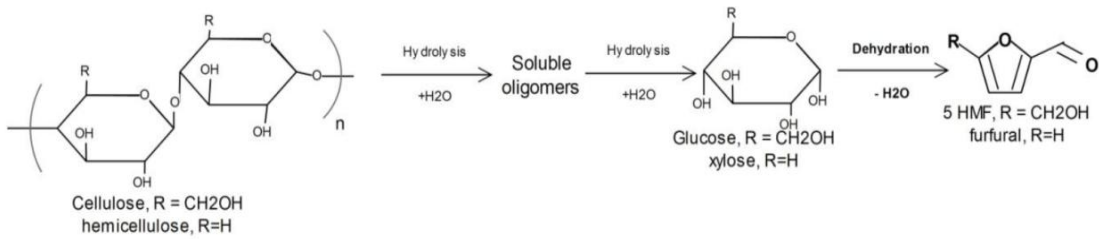


Figure 2-9. Pathways of cellulose and hemicellulose degradation under hydrothermal conditioning (adapted from [38])

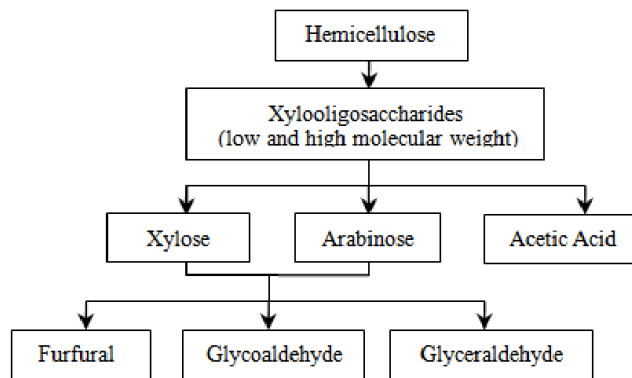


Figure 2-10. Main reaction pathway of hemicelluloses hydrolysis (adapted from [41])

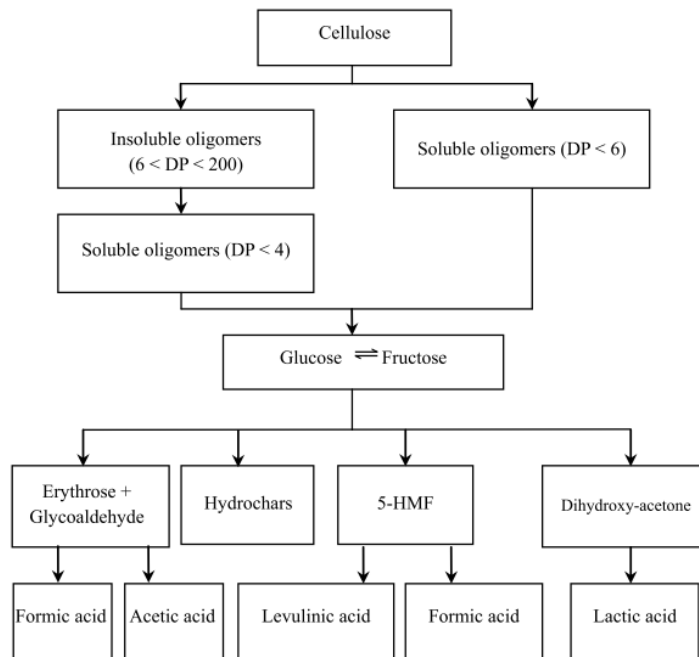


Figure 2-11. Main reaction pathways of cellulose hydrolysis (adapted from [41])

Since the experiment in this reference was conducted in a longer residence time (22 h), the unstable oligomers and sugar monomers further underwent dehydration process (which yielded water) that forms furfural such as 3-furaldehyde and 5-methyl furfural

(5-HMF) which also detected in the liquid sample as shown in the Table 2-9. Then, the unstable hydrolyzed products can be isomerized which have the possibility to further decompose into organic acids such as acetic and formic acid as explained in the pathways shown in Figures 2-10 and 2-11. More volatiles substance, such as aromatic and phenolic compounds, can be identified as the temperature increased. These substances will continue to react and decompose further into acid such as pentanoic and furancarboxylic acid and phenolic compounds, such as phenol.

Therefore, we can understand that the component from the liquid product can give more description in explaining the reactions occurring during HTT. From the liquid analysis results, it also showed that it was the hydrolysis and dehydration reactions that were mainly occurring in these subcritical water conditions during HTT.

2.3.6 Treatment of the liquid HTT residue

From the water consumption calculation result in the large scale HTT reactor, it can be seen that the biomass water ratio (1: 0.68) is far lower than the ratio in the lab-scale HTT reactor (1: 10). Consequently, it is expected that in the large scale, there is no significant liquid product produced after HTT process. Therefore, the consideration on how to treat the liquid from HTT process actually can be neglected. However, if it appears that there is liquid product produced, and the treatment of the produced liquid is inevitable, the way on how to treat the produced liquid is needed to be investigated.

The investigation on the possibility to discharge it back to the environment (or plantation) has been conducted. Similar to the liquid from washing process, the properties of the liquid product like the macro- and micro-nutrients content analysis, the pH and EC analysis, and the phytotoxicity test were also performed.

Macronutrients

The macronutrients content in the liquid HTT products were analyzed, and presented in Figure 2-12. The solubilization ratio, defined as the ratio of the element content in the initial EFB sample minus the content in the treated sample divided by the initial element content, was calculated to know the HTT effect on the solubilization of the macronutrients from EFB to the water medium. The solubilization ratios of the primary macronutrients N, P, K are depicted in Figure 2-13. It can be seen from Figure 2-13 that the HTT reaction temperature has a noticeable impact on the N, P, and K solubilization, as it linearly increased with the reaction temperature increase, especially for K. The maximum solubilization ratios for N, P and K are 37.2, 9.8, and 64.8%, respectively. Nevertheless, the macronutrients concentration shown in Figure 2-12 is comparatively not so high compared with those of commercial liquid fertilizers.

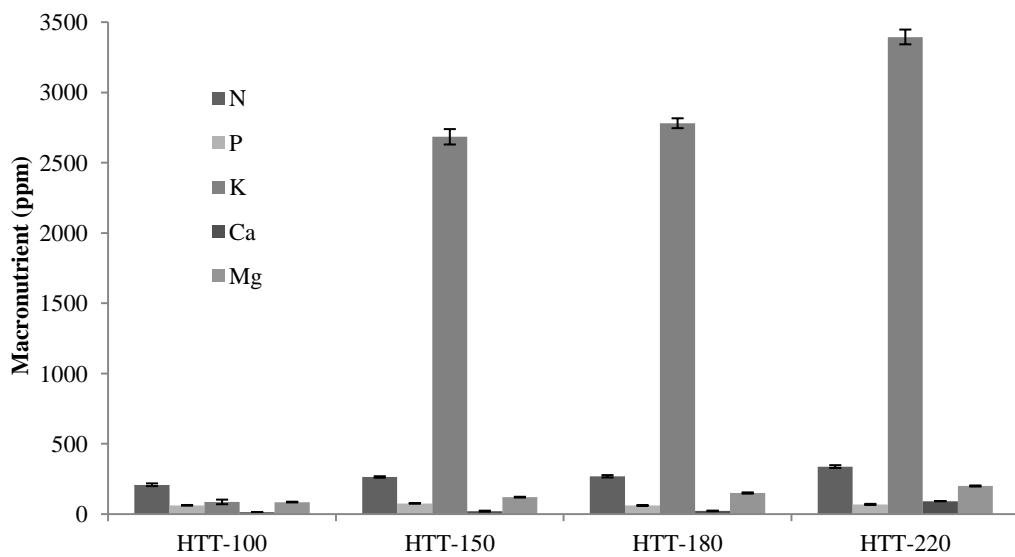


Figure 2-12. Macronutrient in liquid product

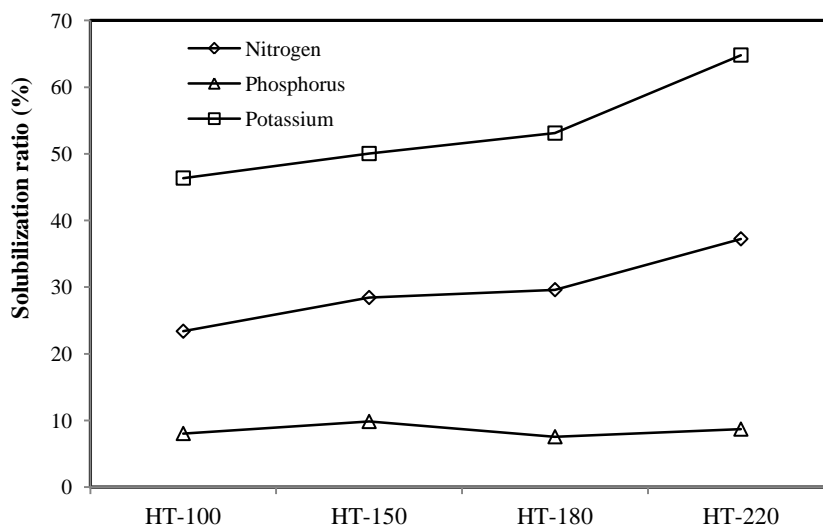


Figure 2-13. N, P, K solubilization ratios

Micronutrients

These micronutrients elements are presented in Table 2-10. From the qualitative analysis, the heavy metal elements like Pb, Cd and Cr were in low detection or even not detected (ND). Thus, all of HTT products are free from harmful risk of heavy metals. The same trend as macronutrient release during HTT was observed, where more elements were dissolved as the HTT temperature increases.

pH and EC

The increase in the acidity in the liquid product was observed after HTT, as seen in Table 2-10. Considering that the distilled water was originally neutral, the acidic condition was occurred due to the formation of organic acids that typically took place during the HTT process [21]. During HTT, the degradation of hemicelluloses, cellulose and extractives produced concentrated sugars and organic acids which then dissolved into water. The produced organic acids decreased the pH of the liquid phase. From Table 2-10, it can be seen that HTT-220 liquid product had pH as low as 4.1. More severe decomposition occurred at the higher reaction temperature will result in more formation of organic acids. The optimum pH value for plants to take up nutrients that applied to the root zone and foliage is ranging from 5.5- 8.5 [10].

Table 2-10. Micronutrient and heavy metal in liquid residue.

Sample		pH	EC (dSm-1)	Micronutrient and Heavy Metal (ppm)								
				Ba	Fe	Mn	Zn	B	Cr	Cu	Pb	Cd
HTT-100	average	6.6	5.4	0.43	8.36	2.06	3.29	ND	ND	ND	ND	ND
	SD	0.0	0.0	0.02	0.18	0.01	0.05					
HTT-150	average	5.9	6.2	0.63	14.77	2.55	3.98	ND	ND	ND	ND	ND
	SD	0.0	0.0	0.04	0.47	0.04	0.11					
HTT-180	average	5.0	7.0	0.56	19.37	3.32	3.48	ND	ND	ND	ND	ND
	SD	0.0	0.0	0.01	0.17	0.03	0.07					
HTT-220	average	4.1	9.0	0.72	64.74	5.67	9.22	ND	ND	ND	ND	ND
	SD	0.0	0.0	0.01	0.61	0.04	0.14					

From Table 2-10, it can be noticed that the EC values increased with the increase of the HTT temperature. The EC value of 1.5 dS/m is considered as the upper limit value for growing media and is tolerable for plants with medium sensitivity [10]. High concentration of soluble organics can depress growth because the ions contributing to high EC could compete with fertilizer nutrients for plant uptake. The EC values of liquid HTT products are quite high, which exceed the stated limit. Since very low pH and high EC in the HTT liquid may harm to the plant growth, the dilution of the liquid will be an important factor for the application of the fertilizer.

C/N ratio

The C/N ratio plays an important role in release of the nutrients to the soil. As the HTT temperature increased, more carbon compounds in the liquid phase could be seen resulting in the higher C/N ratio (Figure 2-14). Even for HTT at the lowest temperature, the C/N ratio was around 20 which indicated that the decomposition of organically bound nutrients to an inorganic form occurred at a slower pace.

A higher reaction temperature is able to transfer more nutrients from the solid to the liquid phase, but considering the values of pH, EC, and the C/N ratio, HTT at a lower temperature, 100-150°C, produced liquid product which was safer for the plant growth.

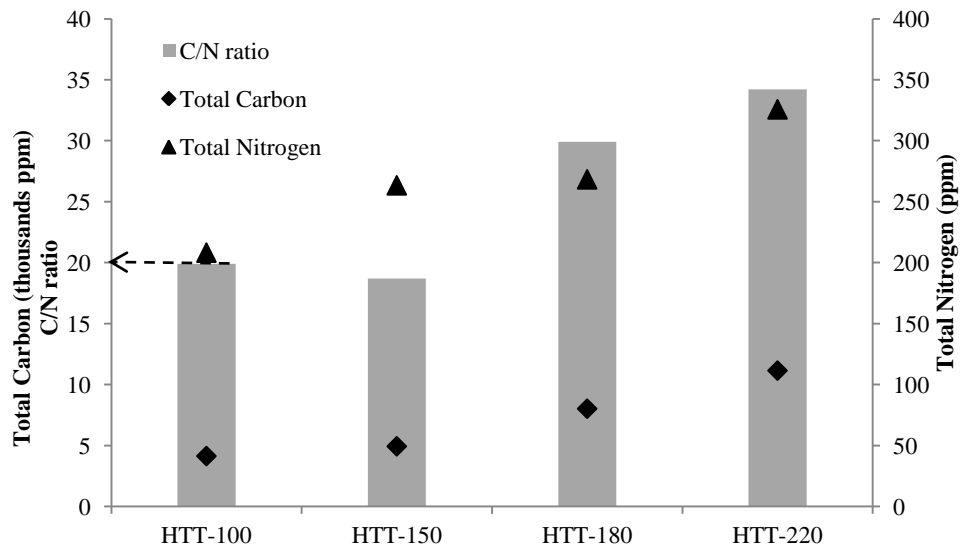


Figure 2-14. C/N ratios of HTT liquids at different temperatures

Phytotoxicity test

The detail of the effect of the liquid produced from HTT at 180°C on the Komatsuna seed is shown in Table 2-11. It was found that no germination occurred using the liquid HTT-220 with a high TC concentration. One possible reason is due to the formation of potentially toxic substances like phenols, furfurals and their derivatives under the treatment temperature high enough for lignin and sugar degradation. At a higher temperature, more organic acids, soluble salts and excessive ions were dissolved which then could cause fertilizer burn and seed damage. Dilution to lower concentration has a tendency to increase the GI which implies the decreasing of the harmful effect of liquid HTT. Table 2-11 shows that liquid HTT-180 at TC 300 ppm gives the highest GI and is significantly different with the other product (58.5%). However, the value is still lower than the GI limit to be considered as phytotoxic free. It is found that for compost as a reference, GI of $\geq 80\%$ is considered to be phytotoxic free [42]. Therefore, the dilution factor is one of important keys in the safe application of this liquid to the environment (plantation).

From the liquid product evaluation above, it can be concluded that similar to the washing leachate, the dilution factor is one of important keys for discharging this liquid HTT to the environment (plantation) safely. According to the heavy metal content result, the liquid products were free from harmful risk of heavy metals. Therefore, by optimizing the proper dilution factor, the liquids were safe to be discharged to the environment. The dilution factor needed might be around 40~100 times dilution.

Table 2-11. Effect of the HTT liquid product from EFB on the germination of Komatsuna seedlings.

Total Carbon (TC)	Germination Index (GI)			
	HTT-100	HTT-150	HTT-180	HTT-220
1500 ppm (5x dilution)**	26.6 ± 3.6abc*	17.9 ± 7.9abd	1.4 ± 0.3ab	0.0 ± 0.0ab
800 ppm (10x dilution)	31.2 ± 5.2ace	50.7 ± 7.9ce	13.7 ± 1.2ab	0.0 ± 0.0ab
300 ppm (30x dilution)	35.1 ± 1.7cde	36.0 ± 2.8cde	58.5 ± 11.5e	11.4 ± 4.1abd

*The results are the means of three replicates ± standard error. Value followed by the same letter(s) do not differ significantly according to LSD test ($\alpha=0.05$).

**The dilution calculation is approximately for the TC concentration of HTT-180

Other than discharging the liquid product with a proper dilution factor to the environment, treating the liquids by the common waste water treatment is also possible. Funke and Ziegler (2010) pointed out that the wastewater from the hydrothermal carbonization can be processed with aerobic and anaerobic treatment to lower the TOC significantly [21]. However, the cost for the treatment is expected to be higher than discharging the diluted liquids to the environment.

2.4 Summary

In this chapter, the HTT experiment for EFB was performed in order to evaluate the characteristics of the solid product as a fuel and to upgrade the fuel qualities of the biomass. The EFB was treated under subcritical hydrothermal conditions, with the temperature conditions of 100, 150, 180 and 220 °C for 30 min. The summary of the findings is described as follows:

1. The hydrochar yield showed decreasing trend with the increasing the HTT temperature. Inversely, the HHV showed the increasing trend; with the highest heating value recorded was 19.7 MJ/kg which is almost equal to that of low-grade sub-bituminous coal. In accordance to the mass yield, increasing the temperature led to a decrease in the energy yield, while the energy densification ratio increased.
2. In the view of physicochemical characteristics, the HTT-EFB has higher fuel property; higher carbon content, lower oxygen, and lower ash content.
3. From the energy consumption calculation, the water to biomass ratio of 1:10 leading to an inefficient energy recovery. The biggest energy consumption was coming from the energy need for heating up water (and moisture). In the larger scale, the steam input should be lower to ensure the feasibility of the HTT process. The high HTT temperature also enhanced the consumption energy that could not appropriate for bigger scale.
4. By considering the energy requirement and the improvement in the fuel property; such as the energy yield and the ash content, HTT at 180°C seems to be more preferred for the large-scale production of solid fuel from EFB.
5. The Van Kravelen diagram and FTIR analysis suggested that the main reaction pathways that might occur during the HTT process at a mild temperature were the dehydration and the hydrolysis of the hemicelluloses contained in raw-*EFB*.

References

1. Lam, P.S., Lam, P.Y., Sokhansanj, S., Lim, C.J., Bi, X.T., Stephen, J.D., Pribowo, A., Mabee, W.E.: Steam explosion of oil palm residues for the production of durable pellets. *Appl. Energy*. 141, 160–166 (2015).
2. Demirbas, A.: Combustion characteristics of different biomass fuels. *Prog. Energy Combust. Sci.* 30, 219–230 (2004).
3. Arias, B., Pevida, C., Feroso, J., Plaza, M.G., Rubiera, F., Pis, J.J.: Influence of torrefaction on the grindability and reactivity of woody biomass. *Fuel Process. Technol.* 89, 169–175 (2008).
4. van der Stelt, M.J.C., Gerhauser, H., Kiel, J.H.A., Ptasiński, K.J.: Biomass upgrading by torrefaction for the production of biofuels: A review. *Biomass and Bioenergy*. 35, 3748–3762 (2011).
5. Chew, J.J., Doshi, V.: Recent advances in biomass pretreatment – Torrefaction fundamentals and technology. *Renew. Sustain. Energy Rev.* 15, 4212–4222 (2011).
6. Nakhshiniev, B., Gonzales, H.B., Yoshikawa, K.: Hydrothermal Treatment of Date Palm Lignocellulose Residue for Organic Fertilizer Conversion: Effect on Cell Wall and Aerobic Degradation Rate. *Compost Sci. Util.* 20, 245–253 (2012).
7. Kieseler, S., Neubauer, Y., Zobel, N.: Ultimate and Proximate Correlations for Estimating the Higher Heating Value of Hydrothermal Solids. *Energy & Fuels*. 27, 908–918 (2013).
8. Gil, M. V, Casal, D., Pevida, C., Pis, J.J., Rubiera, F.: Thermal behaviour and kinetics of coal/biomass blends during co-combustion. *Bioresour. Technol.* 101, 5601–8 (2010).
9. Muthuraman, M., Namioka, T., Yoshikawa, K.: A comparative study on co-combustion performance of municipal solid waste and Indonesian coal with high ash Indian coal: A thermogravimetric analysis. *Fuel Process. Technol.* 91, 550–558 (2010).
10. Silva, M.E.F., Lemos, L.T., Bastos, M.M.S.M., Nunes, O.C., Cunha-Queda, A.C.: Recovery of humic-like substances from low quality composts. *Bioresour. Technol.* 128, 624–32 (2013).
11. Fang, M., Wong, J.W.: Effects of lime amendment on availability of heavy metals and maturation in sewage sludge composting. *Environ. Pollut.* 106, 83–89 (1999).
12. Xu, C., Lancaster, J.: Conversion of secondary pulp/paper sludge powder to liquid oil products for energy recovery by direct liquefaction in hot-compressed water. *Water Res.* 42, 1571–1582 (2008).
13. Nyakuma, B.B., Johari, A., Ahmad, A., Abdullah, T.A.T.: Comparative Analysis of the Calorific Fuel Properties of Empty Fruit Bunch Fiber and Briquette. *Energy Procedia*. 52, 466–473 (2014).
14. Reza, M.T., Yan, W., Uddin, M.H., Lynam, J.G., Hoekman, S.K., Coronella, C.J., Vásquez, V.R.: Reaction kinetics of hydrothermal carbonization of loblolly pine. *Bioresour. Technol.* 139, 161–9 (2013).
15. Liu, Z., Quek, A., Kent Hoekman, S., Balasubramanian, R.: Production of solid biochar fuel from waste biomass by hydrothermal carbonization. *Fuel*. 103, 943–949 (2013).

16. Annual Book of ASTM Standards. Part 26. Gaseous Fuels; Coal and Coke; Atmospheric Analysis. American society for testing and materials, Philadelphia (1999).
17. Sevilla, M., Fuertes, A.B.: Chemical and structural properties of carbonaceous products obtained by hydrothermal carbonization of saccharides. *Chemistry*. 15, 4195–203 (2009).
18. Lynam, J.G., Coronella, C.J., Yan, W., Reza, M.T., Vasquez, V.R.: Acetic acid and lithium chloride effects on hydrothermal carbonization of lignocellulosic biomass. *Bioresour. Technol.* 102, 6192–6199 (2011).
19. Reza, M.T., Lynam, J.G., Uddin, M.H., Coronella, C.J.: Hydrothermal carbonization: Fate of inorganics. *Biomass and Bioenergy*. 49, 86–94 (2013).
20. Yuliansyah, A.T., Hirajima, T., Kumagai, S., Sasaki, K.: Production of Solid Biofuel from Agricultural Wastes of the Palm Oil Industry by Hydrothermal Treatment. *Waste and Biomass Valorization*. 1, 395–405 (2010).
21. Funke, A., Ziegler, F.: Hydrothermal carbonization of biomass: A summary and discussion of chemical mechanisms for process engineering. *Biofuels, Bioprod. Biorefining*. 4, 160–177 (2010).
22. Runge, T., Wipperfurth, P., Zhang, C.: Improving biomass combustion quality using a liquid hot water treatment. *Biofuels*. 4, 73–83 (2013).
23. Prawisudha, P. Thesis dissertation: CHLORINE-FREE SOLID FUEL PRODUCTION FROM MUNICIPAL SOLID WASTE BY HYDROTHERMAL TREATMENT FOR CO-COMBUSTION WITH COAL, (2011).
24. Prawisudha, P., Namioka, T., Yoshikawa, K.: Coal alternative fuel production from municipal solid wastes employing hydrothermal treatment. *Appl. Energy*. 90, 298–304 (2012).
25. Areprasert, C., Zhao, P., Ma, D., Shen, Y., Yoshikawa, K.: Alternative Solid Fuel Production from Paper Sludge Employing Hydrothermal Treatment. *Energy & Fuels*. 28, 1198–1206 (2014).
26. Mohammed, M. a a, Salmiaton, a, Wan Azlina, W. a K.G., Mohamad Amran, M.S.: Gasification of oil palm empty fruit bunches: a characterization and kinetic study. *Bioresour. Technol.* 110, 628–36 (2012).
27. Parshetti, G.K., Kent Hoekman, S., Balasubramanian, R.: Chemical, structural and combustion characteristics of carbonaceous products obtained by hydrothermal carbonization of palm empty fruit bunches. *Bioresour. Technol.* 135, 683–9 (2013).
28. Bobleter, O.: Hydrothermal degradation of polymers derived from plants. *Prog. Polym. Sci.* 19, 797–841 (1994).
29. Haykırı-ac, H.: Combustion characteristics of different biomass materials. *Energy Convers. Manag.* 44, 155–162 (2003).
30. Khan, A.A., de Jong, W., Jansens, P.J., Spliethoff, H.: Biomass combustion in fluidized bed boilers: Potential problems and remedies. *Fuel Process. Technol.* 90, 21–50 (2009).
31. Lu, X., Flora, J.R. V, Berge, N.D.: Influence of process water quality on hydrothermal carbonization of cellulose. *Bioresour. Technol.* 154, 229–39 (2014).
32. Yan, W., Acharjee, T.C., Coronella, C.J., Vasquez, V.R.: Thermal pretreatment of lignocellulosic biomass. *Environ. Prog. Sustain. Energy*. 28, 435–440 (2009).
33. Kobayashi, N., Okada, N., Hirakawa, A., Sato, T., Kobayashi, J., Hatano, S., Itaya, Y., Mori, S.: Characteristics of Solid Residues Obtained from Hot-

- Compressed-Water Treatment of Woody Biomass. *Ind. Eng. Chem. Res.* 48, 373–379 (2009).
34. Deng, L., Che, D.: Chemical, Electrochemical and Spectral Characterization of Water Leachates from Biomass. (2012).
 35. Sevilla, M., Fuertes, a. B.: The production of carbon materials by hydrothermal carbonization of cellulose. *Carbon N. Y.* 47, 2281–2289 (2009).
 36. Sevilla, M., Maciá-Agulló, J.A., Fuertes, A.B.: Hydrothermal carbonization of biomass as a route for the sequestration of CO₂: Chemical and structural properties of the carbonized products. *Biomass and Bioenergy.* 35, 3152–3159 (2011).
 37. Yan, W., Hastings, J.T., Acharjee, T.C., Coronella, C.J., Vásquez, V.R.: Mass and Energy Balances of Wet Torrefaction of Lignocellulosic Biomass †. *Energy & Fuels.* 24, 4738–4742 (2010).
 38. Reza, M.T.: *Upgrading Biomass by Hydrothermal and Chemical Conditioning.* University of Nevada, Reno (2013).
 39. Jamari, S.S., Howse, J.R.: The effect of the hydrothermal carbonization process on palm oil empty fruit bunch. *Biomass and Bioenergy.* 47, 82–90 (2012).
 40. Funke, A., Ziegler, F.: Heat of reaction measurements for hydrothermal carbonization of biomass. *Bioresour. Technol.* 102, 7595–8 (2011).
 41. Cardenas-toro, F.P., Alcazar-alay, S.C., Forster-carneiro, T., Meireles, M.A. a: Obtaining Oligo- and Monosaccharides from Agroindustrial and Agricultural Residues Using Hydrothermal Treatments. *Food Public Heal.* 4, 123–139 (2014).
 42. California Compost Quality Council: *Compost maturity index.*, California (2001).

Chapter 3. Low potassium fuel from EFB via hydrothermal treatment and water washing

Abstract: High potassium content in EFB leads to the high slagging and fouling tendency when it is combusted in furnace. The removal of the potassium content by combination of HTT and the water washing is described in chapter 3. After HTT, the treated product was subjected to water washing experiments that were conducted using a batch-washing system. The samples were mixed with the ratios of 1:5, 1:8, 1:10, 1:20 and 1:50 of distilled water at the washing temperature of 60°C for 15 minutes. The results indicated that the major removal of potassium was attributed to the HTT process, with 92% potassium removal can be obtained after HTT combined with the water washing process. The combination also lowered the ash content and the chlorine content of EFB down to averagely 0.9% and 0.19%, respectively. According to the results, it was found that 180°C was the optimum HTT temperature for the effective potassium removal. Combination of HTT and the water washing improved the slagging and fouling indices, exhibiting positive results in the term of the deposition tendency, thus clarified that the removal of potassium may lead to lower deposition tendency.

3.1 Background

There is still a problem when the EFB biomass is combusted; it still contains high alkali content, particularly potassium [1]. Considerable attention has been paid to the slagging and fouling problems when combusting EFB in boilers. During combustion, some compounds evolving from abundant alkali metals in EFB will go into the gas-phase condensate and deposit on low-temperature surfaces of heat exchange equipment, causing the abovementioned problems.

Potassium, a major alkali in biomass, is known to contribute to the easy formation of compounds with low melting point which leads to the formation of fireside deposits [2]. EFB appears to have relatively high amount of potassium of 3-4%-dry wt. Potassium is transformed during combustion and combines with other elements such as chlorine, sulfur and silica to form low melting point compounds [2]. The potassium content in particular is important to indicate potential ash deposition through vaporization and condensation. Potassium in biomass is apparently tied up as organically bound, occurs as dissolved salts inherent moisture, cations attached to carboxylic and other functional groups, complex ions, and chemisorb material [3].

In order to prevent slagging and fouling in boilers, elimination of troublesome component is necessary. Potassium occurs as either water soluble or ion exchangeable, thus easily removed by pretreatment using water. Previous investigations on removal of

troublesome elements from biomass prior to conversion by means of controlled washing or leaching process have been carried out [4, 5]. Removing elements after initial primary conversion (e.g. char wash) has been proposed as well [6]. Therefore, this chapter will focus on the removal of potassium from EFB hydrochars by means of combination of HTT and batch washing treatment. The removal efficiency of potassium has been examined for various HTT and washing conditions. Some indices to determine slagging and fouling tendencies were calculated, using elemental analysis of ash. The thermogravimetric analyses of washed and unwashed hydrochar were investigated to evaluate the thermal behavior of the fuel after washing.

3.2 Material and methods

3.2.1 Biomass material

The EFB samples were harvested in 2010 and collected from private palm oil mill company, Waris Selesa Sdn. Bhd., in Sabah, Malaysia. The samples were received in milled and dried condition from the company, with a uniform particle size ranging from 10 - 20 mm. The samples were stored in sealed plastic bags at the room temperature until use for experiments.

3.2.2 HTT experiments

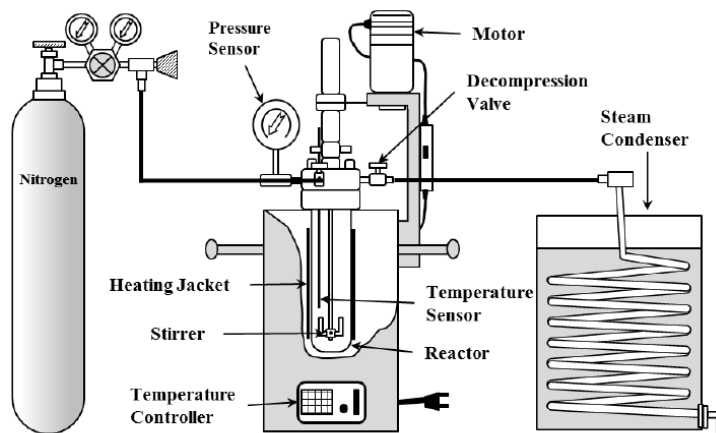


Figure 3-1. Lab scale hydrothermal apparatus (adapted from [7])

The HTT experiments were conducted using a commercially available batch type autoclave reactor (MMJ-500, Japan) with the reaction vessel volume of 500 ml. The detail procedure was described in Chapter 2. The reactor temperature was set at 100, 150, 180, 220°C, respectively, with the holding time of 30 minutes. After completed, the product was discharged from the reactor. The solid part was separated from the liquid by using the vacuum filtration, then oven dried at 105°C for 24 h, and stored in a sealed bag before further analysis. The liquid part was filled in the bottle and kept in a refrigerator, and defined as liquid HTT.

3.2.3 Washing experiments

The washing process was studied applying several process parameters. Different hydrochars and solid-liquid ratios were applied. The washing processes were conducted by heating a certain ratio of distilled water to 60 °C and adding 3 g of the sample. The sample and water were mixed with a magnetic stirrer rotating at 600 rpm. Five samples; raw EFB, hydrochar produced at 100 °C (HTT- 100), HTT-150, HTT-180, and HTT-220 were used in the washing experiment. The biomass to distilled water ratio during the washing was 1:5, 1:8, 1:10, 1:20 and 1:50. The investigated leaching duration was 15 min. After the washing process, the mixture was separated using a vacuum filter. The solid was oven dried at 105 °C for 24 h, and stored in a sealed bag. HTW denotes for the hydrothermally treated and washed sample. The solid sample and liquid sample obtained after washing are designated as solid washing and liquid washing, respectively.

3.2.4 Analytical methods

3.2.4.1 AAS

The potassium element was analyzed by the atomic absorption spectrometry (AAS) method using Z-5010 Polarized Zeeman Atomic Absorption Spectrophotometer (Hitachi, Japan). Preliminary treatment is required to decompose the biomass matrix and dissolve the inorganic elements into solution, allowing them to be introduced into the determination step. The biomass samples were digested using hot-plate digestion method. For the analysis, 0.5 g of the dry solid sample or 2 ml of the liquid sample was added with 3 ml HNO₃ 1.38 g/ml and 5 ml HClO₄ 60%. After acid pretreatment, the solution was filtered and diluted to a proper volume for potassium content determination by AAS.

3.2.4.2 Ultimate and HHV analysis

The determination of the CHNS and Cl of EFB samples was performed using Vario Micro Cube Elemental Analyzer (Elementar, Germany), where oxygen was determined by difference as dry basis. The ultimate correlation by Channiwala and Parikh (2012) was used to estimate the HHV of the samples. Kieseler's study showed that this correlation gives the most accurate result compare to proximate correlation and Dulong-formula ultimate correlation for hydrochars [8].

3.2.4.3 XRF

The ash compositions of untreated and treated EFB material were analyzed using the X-ray fluorescence (XRF) technique. For the XRF analysis, the sample was well ground into powder (i.e., particle size 250 µm) and around 2 g of EFB sample was used to

determine the ash composition by S2 Ranger energy dispersive X-ray fluorescence spectrometer (Bruker AXS, Germany).

3.2.4.4 TGA

The thermogravimetric analysis (TGA) was carried out by using a non-isothermal TGA analyzer (Shimadzu D-50 simultaneous TGA/DTA analyzer). Thermal decompositions under the oxidative atmosphere were conducted by loading a sample of approximately 10 mg into a crucible. Then the samples were heated by a constant heating rate of 10 °C/min to minimize the heat transfer limitation [9, 10]. Air was used at a constant flow rate of 150 ml/min and the samples were heated from the ambient temperature to 900 °C. At least, three runs were completed for each sample to confirm the reproducibility. The mass loss (TG) and the derivative curves (DTG) were continuously collected and represented as a function of time and temperature.

3.2.4.5 Fourier transform infrared spectrometry (FTIR)

The Fourier transform infrared spectrometry (FTIR) was done by the JIR-SPX200 FT-IR spectrometer (JEOL Co., Ltd. Japan) to investigate chemical changes during washing treatment. The procedure name is "KBr pellet method", which is traditional method for transmission measurement. The fine sample is grinded and mixed with KBr, then pelletized. Then, it was scanned from 400 to 4000 cm^{-1} with the resolution of 4 cm^{-1} .

3.2.5 Data Analysis

3.2.5.1 Removal efficiency of potassium

In this study, the removal efficiency of potassium element was quantified on the basis of mass balance in the system, which is defined as:

$$X_p = \left(1 - \frac{m_f \times C_f}{m_i \times C_i}\right) \times 100 \quad (3-1)$$

Where

X_p = the removal efficiency of potassium (%)

m_f = the final mass of the washed sample (g)

m_i = the initial mass of the sample (g),

C_f = the concentration of potassium element in the washed sample (mg/kg)

C_i = the concentration of potassium content in the original sample (mg/kg)

3.2.5.2 Slagging and fouling indices

Some indices for slagging and fouling have been widely used as a measure of deposition tendency of a fuel ash. The tendency of ash from raw, HT treated, and washed EFB was defined using these indices listed in Table 3-1.

Table 3-1. Slagging, fouling, alkali, and ratio-slag indices, Cl content, definition and their limits [11]

Index	Expression	Limit			
		Low	Medium	High	Extremely High
Slagging Index (SI)	$SI = (B/A) \times S^d$ $S^d = \% \text{ of S in dry fuel}$	0.6	0.6-2.0	2.0-2.6	> 2.6
Alkali Index (AI)	$AI = (Na_2O + K_2O)$ in kg/GJ		0.17-0.34	≥ 0.34	
Fouling Index (FI)	$FI = (B/A) \times (Na_2O + K_2O)$	≤ 0.6	0.6-40	≥ 40	
Chlorine Content (Cl)	Cl as received (%)	< 0.2	0.2-0.3	0.3-0.5	>0.5

A (Acid)= $SiO_2 + Al_2O_3 + TiO_2$

B (Base)= $Fe_2O_3 + CaO + MgO + Na_2O + K_2O + SO_3 + P_2O_5$

3.3 Results and discussion

3.3.1 Fuel properties of washed hydrochar

In order to compare the fuel properties between unwashed hydrochars and washed hydrochars, the elemental composition as well as the calorific value are listed in Table 3-2. The properties of raw EFB and the washed raw-EFB were also listed.

Table 3-2. Ultimate analysis and HHV of the raw-EFB and resulting hydrochar at various HTT and washing conditions*

Element	Weight Percentage (wt%), dry									
	Raw		HTT-100		HTT-150		HTT-180		HTT-220	
	Unwashed	Washed	Unwashed	Washed	Unwashed	Washed	Unwashed	Washed	Unwashed	Washed
Ash	4.9	2	4.6	3.1	3.4	2.7	2.2	0.9	4.1	2.7
C	43.6	45.0	44.1	44.8	45.2	45.0	46.4	46.8	50.0	50.7
H	5.3	5.8	5.2	5.4	5.5	5.5	5.6	5.9	5.4	5.5
N	0.6	0.4	0.8	0.8	0.6	0.6	0.4	0.3	0.8	0.7
S	0.11	0.07	0.08	0.09	0.09	0.04	0.03	0.04	0.09	0.06
O**	45.5	46.7	45.2	45.8	45.2	46.1	45.4	46.1	39.7	40.3
Cl	0.7	0.5	0.2	0.1	0.3	0.1	0.2	0.2	0.5	0.3
HHVdry (MJ/kg)	16.7	17.7	16.8	17.2	17.5	17.4	18.0	18.5	19.6	20.0

*) 1:10 ratio, temperature 60°C, duration 15 min

**) by difference

The obvious compositional alterations observed from the washed hydrochars were seen in the ash content and the chlorine content. Reduction in the ash content has been observed for all the hydrochars by washing. The HTT itself could leach out ash, and reduce the ash content of the samples, with a modest reduction compared to raw-EFB. Furthermore, from Table 3-2, the ash content of HTT-180 even dropped to less than 1% with the additional washing process. Ash content reduction was due to the reason that washing the samples extracted large amount of alkali metals, chlorine, in addition to variable amounts of other materials caused by contamination of EFB with solid or dirt [12, 5, 13]. The ash content of the hydrochar becomes important considering its end-use as fuel. For example in pellet production, the current commercial pellets in the market is obliged to have an ash content of less than 1%, while the “standard” pellets could have as much as 2% ash [14]. The lowest ash content obtained was from treating EFB at 180°C which is 2.2%; still higher than the limit for commercial pellets use. Therefore, in order to meet the requirement, it seems more effective to employ the washing step after HTT.

The chlorine content of raw-EFB is approximately 0.7%. The high chlorine content of EFB may cause corrosion problems in thermo-chemical conversion systems and contribute to acid gas formation [2, 4]. In Table 3-2, the reduction of chlorine of about 72% was observed after employing HTT and washing, leading to a better fuel property for combustion since it can lower the deposition tendency in boiler [2]. As chlorine is commonly found in the form the monovalent ion chloride (Cl⁻) which is loosely bound to exchange site and in low quantities as organic compounds [5, 15], it could be easily removed during HTT and washing process. Previous work has also suggested that by washing the ionic form of chlorine could be easily removed [13, 15].

Beside the changes in ash and chlorine content, other elemental elements like C, H, O, and N are seen only has a slight changes after washing. The carbon fraction seems to increase slightly for all the washed samples, probably as the consequence of the decrease in the ash content due to washing. The other possible reason might be due to a substantial amount of sugar would enter water during washing of biomass as pointed out by He et al. [16]. The significant reduction in the ash also caused the HHV of the samples increase modestly. After washing, the HHV increases with a percentage varied from 2.04% in the case of HTT-220 to 2.78% in HTT-180 sample. This also pointed out by Jenkins et al (1996) that stated the increase in HHV may be correlated to the decrease in the ash content of the washed straws [13].

3.3.2 Effect of HTT and washing on potassium content

A high concentration of potassium in biomass fuel tends to result in the easy formation of compounds with low melting points. Thus, the potassium content in particular is important to indicate potential ash fusion or ash deposition. Potassium content of the raw-EFB was found relatively high with approximately 32.4 g/kg of biomass or around

3.2 wt%. Potassium is usually present in biomass in the form of ionic K^+ and highly soluble in water [15], also forms weak complexes with organic acid ions [5]. Hence, potassium is easily leached from the biomass.

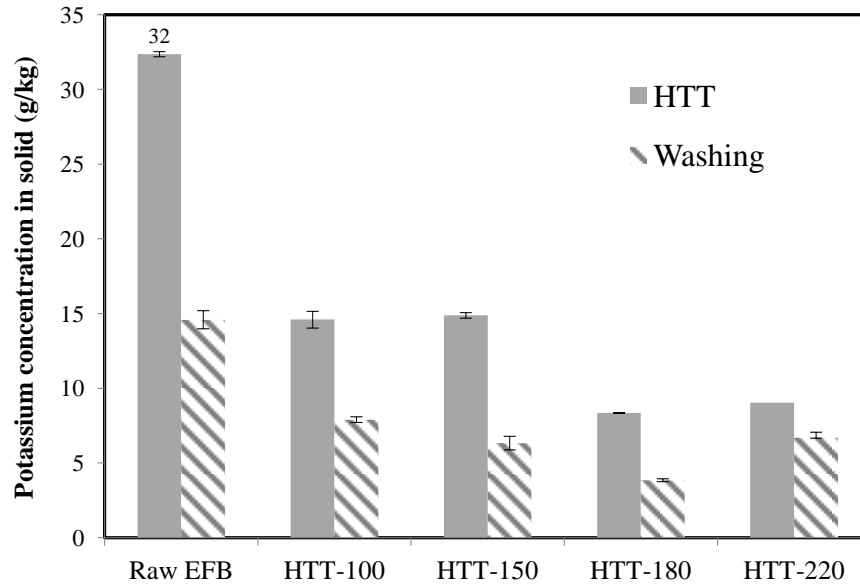


Figure 3-2. Potassium concentration of EFB after HTT and washing

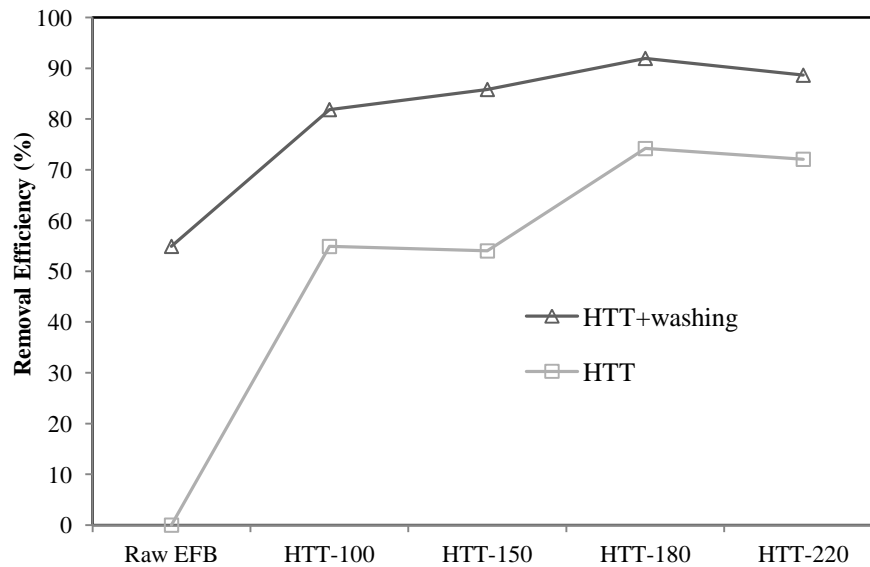


Figure 3-3. Potassium removal efficiency of EFB after HTT and washing

The quantification of potassium species for the raw-EFB and the resulting hydrochars before and after water washing are presented in Figure 3-2. It is evident that various extents of removal of potassium content can be achieved via water washing. By washing raw-EFB with 1:10 biomass-water ratio, up to 54.9% of potassium content in the raw-EFB can be removed (see Figure 3-3). However, when the biomass was treated with HTT process prior to washing process, the removal efficiency can be enhanced to

above 80%, even 92% in the case of HTT-180. Potassium was released mostly during HTT, with the removal efficiency increase with the increase of the HTT temperature. From Figure 3-3, it can be seen that HTT at 180°C optimally removed most potassium to the liquid fraction with the removal efficiency of 74.1%. In contrast, Reza et al (2013) reported that the hydrothermal carbonization at 200°C (5 min holding time) can be very effective in removing inorganics, such as Ca, S, P, Mg and K, from corn stover, miscanthus, switch grass and rice hull biomass [17]. The different biomass feedstock could explain these observations. For HTT-220, the efficiency of the washing stage is found lower than other cases, which might be due to the re-absorption by porous structure produced from HTT under the reaction at 220°C.

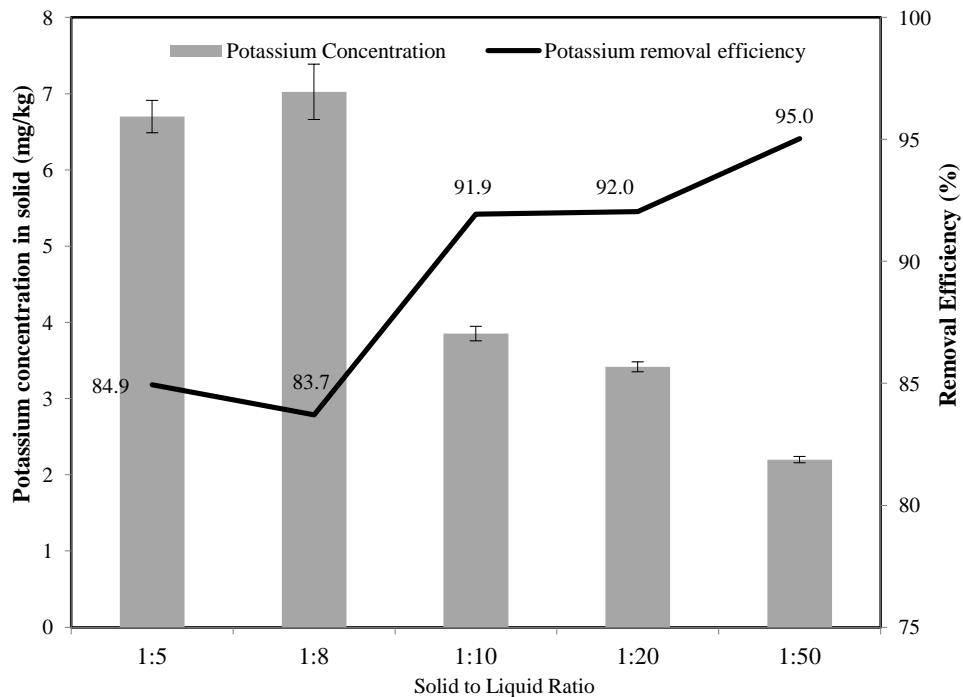


Figure 3-4. Potassium concentration and potassium removal efficiency of washed hydrochar at various biomass- to-water ratio.

Figure 3-4 shows the potassium concentration and the removal efficiency of HTT-180 sample washed with various biomass/water ratios ranging from 1:5 to 1:50. It can be observed that the washing process using solid-liquid ratio less than eight resulted in insignificant difference of the potassium release. By increasing the water ratio up to 1:50 in the washing stage, 95% of potassium in EFB can be removed. The more water volume used, the more potassium will diffuse to the liquid fractions, since the concentration will decrease in the solution. Therefore, it is essential to optimize the water to biomass ratio for washing as a pretreatment because the resulted product will require higher energy input to dry prior to combustion.

The stage-washing (more than 1 time-washing) for the untreated EFB biomass has also been considered in this study to increase the potassium removal efficiency higher than

the combination of pretreatments conducted in this study. However, the potassium removal efficiency obtained from this combination was found as the highest. Previous studies reported that 80 – 90% of the total potassium exists in the form of mobile (water soluble or ion exchangeable) species in biomass [2, 18]. Potassium exists as a univalent ion (K^+) that highly mobile and a large fraction (>80%) of potassium can be extracted from biomass by water washing. The rest portion of the potassium is bound to an organic matrix (carboxylic and other functional groups) because of the high amount of oxygen-containing functional groups in biomass [19]. Therefore, the 100% removal of potassium by only water washing is not possible and there was no research that showed complete removal of potassium. This is in good agreement with the mode of existence of potassium in biomass. Therefore, we will need other pretreatment that is able to break the potassium bound to an organic matrix to enhance the removal efficiency. The comparison between the advantage of washing treatment and combination of HTT and washing are summarized in the Table 3-3.

Table 3-3. Comparison between the advantage of washing treatment and combination of HTT and washing

Evaluation Item	Washing (2-3 times)	HTT + washing
Operation	Easy	Difficult
Cost	Low	High
Energy consumption	Low	High
Potassium removal efficiency	83 – 90% [5, 13] Maximum 90.4 % (washing at 30°C, 1:12.5, 3 h)	82 – 92% [This study] Maximum 92% (HTT 180°C, washing at 60°C, 1:10, 15 min)
Water requirement	High	Low
Improvement on fuel qualities	Not so significant - slightly increased C content - slightly increased HHV	Significant - increased C content - increased HHV - hydrophobic - high dewatering and drying performance - biomass structural change is benefit for pelletization

Since the end-of-use of the hydrochars is to make a pellet, this study showed that HTT was able to improve the fuel properties and the hydrophobicity of the biomass, and also expected to increase the strength and durability of pellets made from the hydrochars. Meanwhile, the combination of HTT and water washing was more effective in removing potassium content from the EFB biomass compare to treatment using only water-washing, as seen in Table 3-3. The HTT was able to decompose hemicelluloses, and disrupted the lignocellulosic matrix that can extract more potassium that attached to organic matrix. The maximum removal of potassium by only water washing is 90%

while the combination of HTT and washing treatment is able to enhance the removal higher than 90% (up to 95% if using water ratio 1:50). By combining these two pre-treatment processes prior to pelletization, the pre-treated pellets might resolve both the dust explosion during transportation (because the pellets will become stronger and more durable) and the slagging issues of the combustion furnace. This combination of the two pre-treatments might also give more advantage in improving the properties of the oil palm residue pellets.

3.3.3 Potassium balance

To investigate more about the potassium distribution after HTT and the washing process, the potassium balance were calculated based on the determined mass balance and the potassium concentration in each fraction. The total amount of potassium species originally available in biomass was taken as the datum (100%). The potassium distribution after the combined pretreatment of HTT and washing is presented in Figure 3-5.

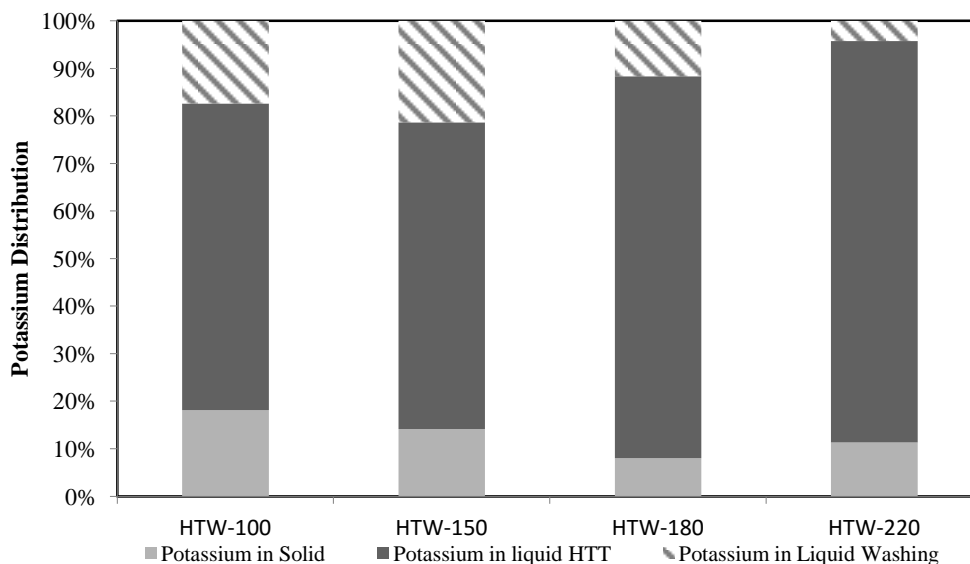


Figure 3-5. Potassium distribution in the product after HTT and washing

Considering the characteristic of potassium in biomass that is easily water-soluble, it can be seen that only less than 20% of potassium is retained in the solid product after HTT. As seen in Fig 6, the HTT liquid contains a considerable amount of potassium. Beside potassium, the other essential nutrient for plant growth such as phosphorus, sulfur, nitrogen might also solubilize to the liquid washing. Since the liquid washing, or commonly known as leachate, is then need to be treated in water treatment; thus, the probability of using leachate as fertilizer is further investigated in another chapter in this thesis.

After the HTT process, the autoclave is opened slightly to decrease the pressure inside and the steam produced are allowed to condense which is then stated as the condensed water. It is noteworthy that only slight amount of potassium was present in the condensed water after HTT. Consequently, the condensed water can be reutilized as make-up water for washing process to minimize the water consumption. Application of HTT integrated with washing process would be more feasible from a practical point of view.

However, the different condition in the large scale application is needed to be taken into consideration. The lower water/steam consumption in the large scale HTT reactor might affect the potassium removal for the HTT process. However, we hypothesized that even though the potassium removal efficiency in the HTT process is appeared to be lower, the combine removal efficiency of HTT and washing will be the same. The difference will be only in the proportion of the removal efficiency between the HTT process and the washing process. It was expected that the higher removal efficiency will be shifted to the washing process. This is because the lower water ratio in the large scale HTT reactor and with the aid of bigger mixing blade will still be able to decompose the EFB and damage the lignocellulosic component of the EFB, thus facilitating and improving the potassium solubilization in the subsequent washing process, giving similar total potassium removal with the lab-scale result. Nonetheless, it is still a hypothesis; we could not assure the exact result unless we could try the experiment in the large scale reactor and determine the optimized water ratio for the washing process. For the optimization in overall process system of the large scale solid fuel production, the deeper investigation using the large scale HTT and washing reactor is suggested to be conducted as well for further study.

3.3.4 Ash composition and slagging fouling tendency

In addition to the characteristics of the samples listed in Table 3-2, the composition of the ash is also important in predicting the behavior of a fuel in a combustion furnace. The role of alkali metals and silica in ash fusion and deposition in furnaces for biomass materials is well known [2, 20, 21]. For the purpose of this study, the inorganic elements content in the ashes were determined, in order to investigate their deposition tendency in the combustion furnace.

Table 3-4 presents the ash elemental percentage obtained by the XRF analysis. The elemental species in ash was generally found as an oxide [23]. It was observed that the alkali levels are quite high in raw-EFB; with potassium oxide appear as dominant species with the percentage of 49.1%, showing its nature tendency to cause slagging and fouling. Employing HTT and the washing processes were able to significantly change the relative composition in ash, where the alkali values were much reduced. A total decrease as high as 72% in K_2O was observed after the pretreatments. This result also proved that a high fraction of potassium was released to the aqueous side, and

remained only small fraction in the ash. However, some species such as SiO₂ and Al₂O₃ only have a slight change after both processes. Si is found to be very stable which is covalently bonded within biomass organic matrix [17].

The Na₂O was seen increased after HTT and washing in spite of it being an alkali that behaves like potassium. This is due to the ash element was presented as weight percentage of the all the elements in the ash, not in the biomass. However, when we calculated the Na₂O percentage presents in the biomass EFB as seen in Table 3-5, we can see that the percentage appeared to be much reduced after both pretreatments. This was because the ash was also reduced due to HTT and washing pretreatments. As stated before, Na is also an alkali element, and like potassium, also exists in the biomass as a water-soluble fraction, thus also easily removed by water. Therefore, Na content in the biomass was increased after HTT and washing. From Table 3-5, we also can see that most of the inorganic in the EFB biomass was decreased after HTT and washing.

Table 3-4. Ash composition of raw-EFB and pretreated EFB

Element (%wt of ash)	K ₂ O	SiO ₂	CaO	Fe ₂ O ₃	MgO	SO ₃	Na ₂ O	P ₂ O ₅	Al ₂ O ₃	TiO ₂	
Raw EFB	Unwashed	48.9	19.0	7.9	5.5	4.4	4.0	3.9	3.0	2.5	0.7
	Washed	50.9	32.1	N/A	1.9	7.4	7.4	N/A	N/A	N/A	N/A
HTT-180	Unwashed	27.0	28.6	10.7	6.6	5.9	4.9	6.1	2.5	6.8	0.7
	Washed 1:10	13.5	33.9	9.3	4.5	8.2	6.0	11.9	2.8	9.5	0.4
	Washed 1:50	10.9	38.4	9.3	3.1	8.7	7.4	12.9	N/A	8.4	0.5

Pronobis et al (2005) used different correlations to analyze the slagging/fouling tendency of coal ashes from the measured ash composition [22]. In general, the correlations define the form of basic-to-acid ratio (B/A) where basic group is compounds with low melting temperature (Fe₂O₃+CaO+MgO+Na₂O+K₂O) and the acid group is compounds with higher melting temperature (SiO₂+Al₂O₃+TiO₂). The B/A ratio was generally used for coal and biomass, and the modified B/A ratio was proposed by adding P₂O₅ to the basic group since P content enhances the development of low melting point phases in fly ash [11]. Therefore, the modified B/A ratio was used in this study.

The evaluation of slagging and fouling tendencies of the raw-EFB, HTT-180 and washed HTT-180 is presented in Figure 3-6. The calculated slagging and fouling indices were defined from the Table 3-1 in sub-chapter 3.2.5.2. Except for SI, all the indices clearly showed that raw-EFB exhibited high tendency of deposition. The high content of basic group compounds, in particular alkali, apparently is the main cause of the high tendency presented in the indices. The SI value for raw-EFB was 0.4 exhibiting a low deposition probability due to low sulfur content in the biomass. However, it was

observed from Figure 3-6 that the effects of HTT and the washing process are more pronounced for AI, FI, and CI indices, where they can considerably lower the tendency of fouling. After HTT at 180°C, the FI and CI values of EFB can be reduced to low probability regime showing the low deposition tendency. The additional washing process affects in the improvement of the AI value, shifts the initially high occurrence of slagging and fouling to probable occurrence. From the calculated slagging and fouling indices, it could be concluded that raw-EFB originally has high tendency of fouling and this risk was significantly eased after pretreatment using HTT and washing.

Table 3-5. Ash element in the untreated and treated EFB.

Element (%wt of EFB)	Raw EFB		HTT-180	
	Unwashed	Washed	Unwashed	Washed
K ₂ O	2.40	1.02	0.59	0.12
SiO ₂	0.93	0.64	0.63	0.31
CaO	0.39	N/A	0.24	0.08
Fe ₂ O ₃	0.27	0.04	0.15	0.04
MgO	0.22	0.15	0.13	0.07
SO ₃	0.20	0.15	0.11	0.05
Na ₂ O	0.19	N/A	0.13	0.11
P ₂ O ₅	0.15	N/A	0.06	0.03
Al ₂ O ₃	0.12	N/A	0.15	0.09
TiO ₂	0.03	N/A	0.02	0.00

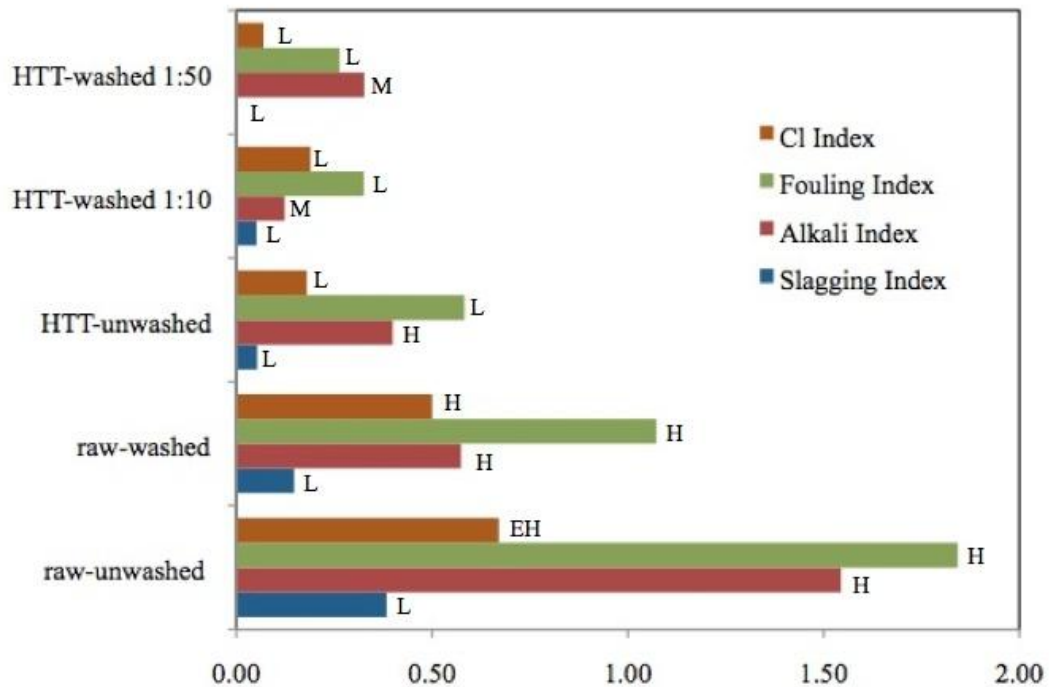


Figure 3-6. Slagging and fouling indices for raw-EFB and pretreated products (EH= extremely high, H = high, M = medium, L = low deposition)

3.3.5 Effect of washing on combustion characteristics

In Figure 3-7 and Figure 3-8, the thermogravimetry (TG) and derivative thermogravimetry (DTG) curves of the hydrochar produced from HTT at 180°C (HTT-180) and washed HTT-180 are presented, respectively. HTW-180 shown in Figure 3-7 and Figure 3-8 means the washed HTT-180 hydrochar. Since washing the sample with water could reduce the content of the problematic inorganic compounds related to ash fusibility, sample of washed hydrochar was analyzed under the oxidative atmosphere conditions to investigate its difference regarding the thermal behavior of the hydrochar after washing.

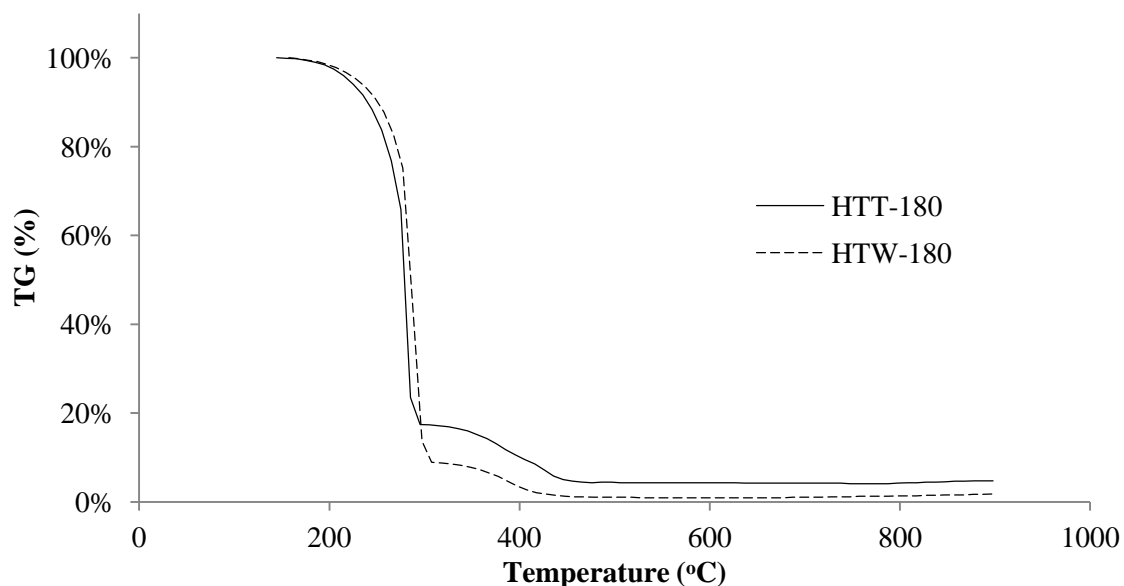


Figure 3-7. TGA profiles of unwashed and washed HTT-180 hydrochars

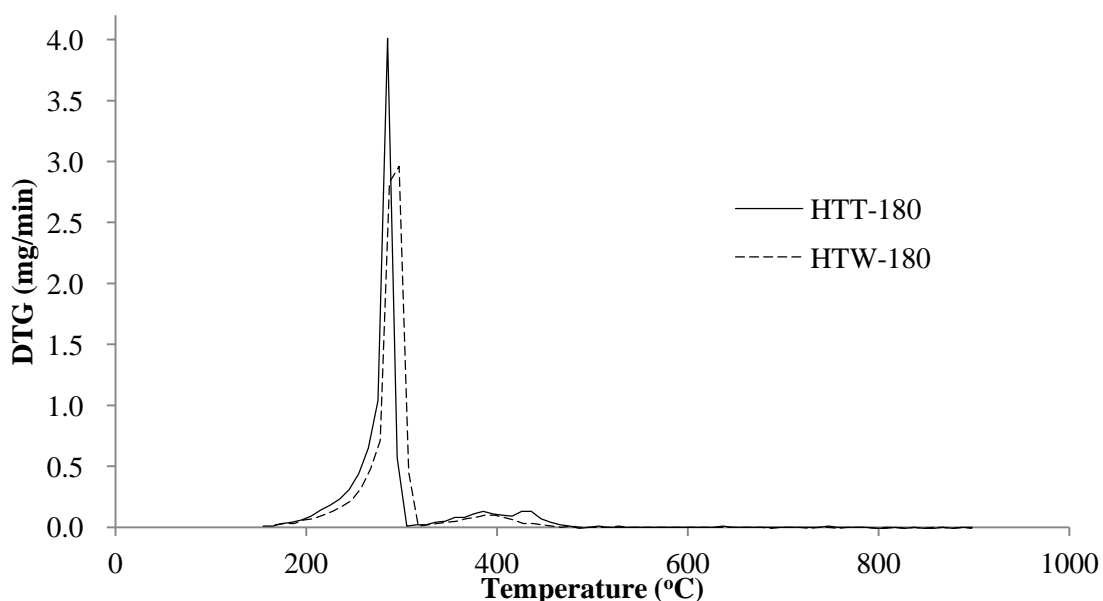


Figure 3-8. DTG profiles of unwashed and washed HTT-180 hydrochars
The TGA curve indicated the mass loss of the sample. TGA profiles in Figure 3-7 showed lower residues in the washed hydrochar compared to the unwashed hydrochar.

This may be due to the lower alkali and ash content in the washed hydrochar corresponding to removal by washing. Data in Table 3-6 also shows residue mass left after combustion both in unwashed and washed hydrochar. Table 3-6 shows the ignition temperature, the peak temperature and the maximum combustion rates for each tested samples.

From the profiles in Figure 3-8, it can be seen that there are similar characteristics of combustion, which is indicated by the same one peak of combustion. It shows that there is no significant different in chemical content of the washed sample compared to the original one. In order to compare the experimental result quantitatively, several combustion properties such as the ignition temperature (T_i), the peak temperatures (T_m) and the maximum combustion rates were obtained from the DTG burning profiles [5, 23]. Table 3-6 presented the ignition temperature (T_i), the peak temperatures (T_m) and the maximum combustion rates of the unwashed and washed HTT-180 hydrochars. The T_i associated with the point where the DTG profile encounters a sudden increase, while the T_m corresponds to the point where the combustion rate is at maximum [5].

Table 3-6. Combustion characteristics of the washed and unwashed HTT-180 hydrochar

Sample	HTT-180	HTW-180
T_i (°C)	267.5	277.5
T_m (°C)	285.3	297.4
DTG _{max} (mg/min)	4.01	2.96
Burn out temperature (°C)	476	457
Residue ^{db} (w.t. %)	4.3	1.1

It can be seen from Table 3-6 that the washing process increased the T_i and T_m values, shifting them to the higher temperature. According to Haykiri-Açma [23], the high T_m means the poor reactivity of the sample. Therefore, the increased T_m implied that washing lower the reactivity of the hydrochar. Compared to HTT-180 hydrochar, the reactivity of the washed hydrochar decreased, resulting in a higher T_i . The higher temperature at the peak center for the washed hydrochar clarifies that this fuel was harder to combust. These demonstrate that in the washing process, the possible accompanied removal of extractives, soluble organics and alkali metal components increased the heavy and difficult-to-combust components in the fuel, such as cellulose and lignin. The extractives are usually associated with the low temperature decomposition, very volatile, and is the less stable components in wood [24]. The elevated combustion temperature implies improved combustion safety, increased combustion efficiency and decreased pollutant emission. These combustion characteristics are significant improvements over unwashed hydrochar as a fuel [25, 23, 21].

3.3.6 FTIR Analysis

Further insight into the chemical composition of the material to compare the surface spectroscopy changes due to washing the hydrochars also may be obtained by FTIR-ATR. In Figure 3-9, a comparison on the surface spectroscopy of the unwashed HTT-180 hydrochar and washed HTT-180 hydrochar is presented. As previously noted, the peak around 2300 to 2400 cm^{-1} was attributed to uncontrollable CO_2 in the measurement environment.

Determination of the main functional groups for a given wave number was done based on previous reports [26–29]. As indicated in Figure 3-8, for the washed samples, the FTIR spectra are assigned into three regions representing the main identification peaks observed. It seems that there is no significant change shown in the FTIR adsorption peaks due to washing, as the plot is seen showing quite similar absorption bands. However, some minor changes can be observed from the FTIR spectra. Deng et al. [28] stated, that during washing, a fraction of inorganic salt, organic salt and organic compound would enter water.

In the first region, wide band at 3700 – 3000 cm^{-1} that attributed to O – H stretching vibrations [30] became weak compared to unwashed hydrochar. This absorption band is due to the O – H bond stretching [16, 28, 31, 32]. As appeared in Fig 3-9, the O – H stretching of carbohydrates sterols and diglycerides is decreased. He et al. [16] and Jenkins [33] have studied that significant sugars are extracted during washing. The hydrolysis of hemicelluloses during HTT breaks ester and ether bonds (mainly β -(1-4) glycosidic bonds resulting in products including oligomers like (oligo-) saccharides [27].

Weaker characteristics of the absorption band at about 1640 cm^{-1} were observed after washing, which indicates that some carboxylates might enter water. This band is due to the COO^- antisymmetric stretching of carboxylates [28]. The peak at 1720 cm^{-1} also associated with COO^- groups, which indicates the organic acids. There was an abundance removal of K^+ during washing, and these cations occurred mainly as carboxylates as the accompanying anions for K^+ . Other researcher reported that the production of carboxylic acids can be observed from the solid and liquid state products of HTC of biomass [27]. Therefore, these groups were present in the hydrochar sample, but modestly removed during washing.

In the last region, the peaks at around 790-800 cm^{-1} might correspond to the symmetric stretching of Si – O – Si [28], which is not changed due to washing. This means that Si is very stable, as already discussed in sub-chapter 3.3.4. There were no strong characteristic changes of absorption bands in the range between 900 and 650 cm^{-1} in the FTIR spectra. It seems that aromatic compounds hardly entered the water during washing.

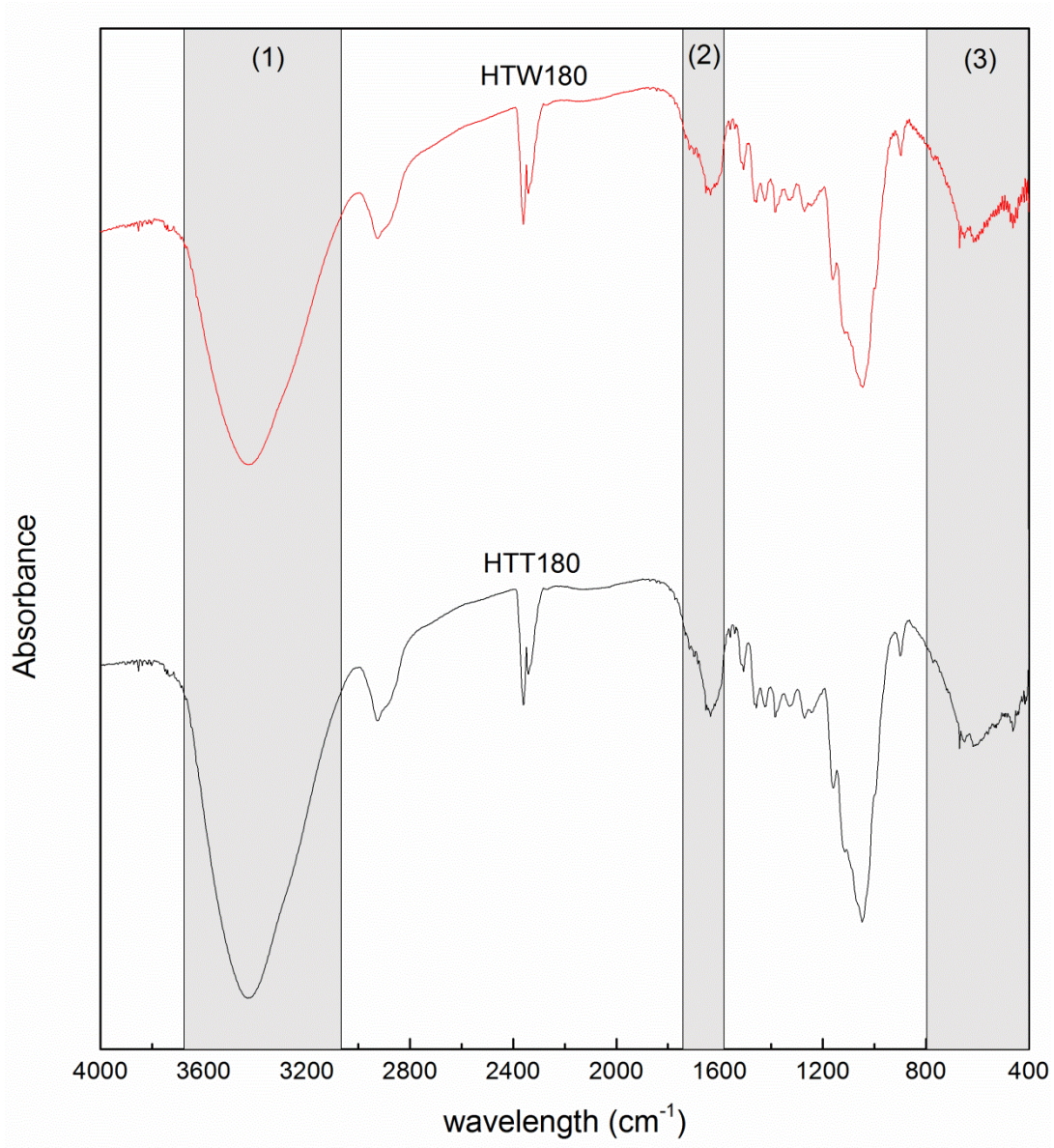


Figure 3-9. FTIR spectra of unwashed and washed HTT-180 hydrochar

3.4 Summary

This chapter discussed the results from the potassium removal experiment of raw-EFB by HTT and washing treatments. Batch-washing experiments were conducted where the samples were mixed with distilled water with the ratios of 1:5, 1:8, 1:10, 1:20 and 1:50 at the washing temperature of 60°C for 15 minutes. The summary of this chapter are as follows:

1. The results indicated that the major removal of potassium was attributed to the HTT process, with 92% potassium removal can be obtained after HTT combined with the water washing process. The combination also lowered the ash content and the chlorine content of EFB down to averagely 0.9% and 0.19%, respectively.

2. According to the results, it was found that 180°C was the optimum HTT temperature for the effective potassium removal.
3. Combination of HTT and the water washing improved the slagging and fouling indices, exhibiting positive results in the term of the deposition tendency, thus clarified that the removal of potassium may lead to the lower deposition tendency.
4. From the combustion analysis results, the elevated combustion temperature implies that washed hydrochars has lower reactivity compared to the unwashed, leading to improved combustion safety, increased combustion efficiency and decreased pollutant emission. These combustion characteristics are significant improvements over unwashed hydrochar.
5. The FTIR spectra suggested that some sugars and organic acids produced during HTT was extracted during washing experiment, along with the alkali elements.

In conclusion, the combination of HTT and the water washing may become a viable way to produce a clean fuel from EFB for combustion or co-combustion with coal.

References

1. Stemann, J., Erlach, B., Ziegler, F.: Hydrothermal Carbonisation of Empty Palm Oil Fruit Bunches: Laboratory Trials, Plant Simulation, Carbon Avoidance, and Economic Feasibility. *Waste and Biomass Valorization*. 4, 441–454 (2012).
2. Baxter, L.L., Miles, T.R., Jenkins, B.M., Milne, T., Dayton, D., Bryers, R.W., Oden, L.L.: The behavior of inorganic material in biomass-fired power boilers: field and laboratory experiences. *Fuel Process. Technol.* 54, 47–78 (1998).
3. Miles, T., Miles, T. jr, Baxter, L., Bryers, R.W., Jenkins, B.M., Oden, L.L.: Alkali Deposits Found in biomass power plant: A preliminary investigation of their extent and nature, Volume II. National Renewable Energy Laboratory, USA (1996).
4. Jensen, P. a., Sander, B., Dam-Johansen, K.: Removal of K and Cl by leaching of straw char. *Biomass and Bioenergy*. 20, 447–457 (2001).
5. Deng, L., Zhang, T., Che, D.: Effect of water washing on fuel properties, pyrolysis and combustion characteristics, and ash fusibility of biomass. *Fuel Process. Technol.* 106, 712–720 (2013).
6. Jensen, P. a., Sander, B., Dam-Johansen, K.: Pretreatment of straw for power production by pyrolysis and char wash. *Biomass and Bioenergy*. 20, 431–446 (2001).
7. Nakhshiniev, B., Gonzales, H.B., Yoshikawa, K.: Hydrothermal Treatment of Date Palm Lignocellulose Residue for Organic Fertilizer Conversion: Effect on Cell Wall and Aerobic Degradation Rate. *Compost Sci. Util.* 20, 245–253 (2012).
8. Kieseler, S., Neubauer, Y., Zobel, N.: Ultimate and Proximate Correlations for Estimating the Higher Heating Value of Hydrothermal Solids. *Energy & Fuels*. 27, 908–918 (2013).
9. Gil, M. V, Casal, D., Pevida, C., Pis, J.J., Rubiera, F.: Thermal behaviour and kinetics of coal/biomass blends during co-combustion. *Bioresour. Technol.* 101, 5601–8 (2010).

10. Muthuraman, M., Namioka, T., Yoshikawa, K.: A comparative study on co-combustion performance of municipal solid waste and Indonesian coal with high ash Indian coal: A thermogravimetric analysis. *Fuel Process. Technol.* 91, 550–558 (2010).
11. Tortosa Masiá, a. a., Buhre, B.J.P., Gupta, R.P., Wall, T.F.: Characterising ash of biomass and waste. *Fuel Process. Technol.* 88, 1071–1081 (2007).
12. Bakker, R.R., Jenkins, B.M., Williams, R.B.: Fluidized Bed Combustion of Leached Rice Straw. *Energy & Fuels.* 16, 356–365 (2002).
13. Jenkins, B.M., Bakker, R.R.: On the properties of washed straw. *Biomass and Bioenergy.* 10, 177–200 (1996).
14. Pellet Fuel Institute: PFI standard specification for residential/commercial densified fuel. Pellet Fuels Institute, Arlington, VA (2008).
15. Knudsen, J.N., Jensen, P. a., Dam-Johansen, K.: Transformation and release to the gas phase of Cl, K, and S during combustion of annual biomass. *Energy and Fuels.* 18, 1385–1399 (2004).
16. He, Z., Mao, J., Honeycutt, C.W., Ohno, T., Hunt, J.F., Cade-Menun, B.J.: Characterization of plant-derived water extractable organic matter by multiple spectroscopic techniques. *Biol. Fertil. Soils.* 45, 609–616 (2009).
17. Reza, M.T., Lynam, J.G., Uddin, M.H., Coronella, C.J.: Hydrothermal carbonization: Fate of inorganics. *Biomass and Bioenergy.* 49, 86–94 (2013).
18. Miles, T.R., Baxter, L.L., Bryers, R.W., Jenkins, B.M., Oden, L.L.: Alkali deposits found in biomass power plants, Vol 1. NREL. I, 1–122 (1995).
19. Zhao, H., Song, Q., Wu, X., Yao, Q.: Study on the Transformation of Inherent Potassium during the Fast-Pyrolysis Process of Rice Straw. *Energy & Fuels.* 29, 6404–6411 (2015).
20. Dayton, D.C., Jenkins, B.M., Turn, S.Q., Bakker, R.R., Williams, R.B., Hill, L.M.: Release of Inorganic Constituents from Leached Biomass during Thermal Conversion. 1977, 860–870 (1999).
21. Khan, A.A., de Jong, W., Jansens, P.J., Spliethoff, H.: Biomass combustion in fluidized bed boilers: Potential problems and remedies. *Fuel Process. Technol.* 90, 21–50 (2009).
22. Pronobis, M.: Evaluation of the influence of biomass co-combustion on boiler furnace slagging by means of fusibility correlations. *Biomass and Bioenergy.* 28, 375–383 (2005).
23. Haykırı-ac, H.: Combustion characteristics of different biomass materials. *Energy Convers. Manag.* 44, 155–162 (2003).
24. Grønli, M.G., Várhegyi, G., Di Blasi, C.: Thermogravimetric Analysis and Devolatilization Kinetics of Wood. *Ind. Eng. Chem. Res.* 41, 4201–4208 (2002).
25. Demirbas, A.: Combustion characteristics of different biomass fuels. *Prog. Energy Combust. Sci.* 30, 219–230 (2004).
26. Yuliansyah, A., Hirajima, T.: Efficacy of hydrothermal treatment for production of solid fuel from oil palm wastes. In: *Resource Management for Sustainable Agriculture. Resour. Manag. Sustain. Agric.* 296 (2012).
27. Reza, M.T.: *Upgrading Biomass by Hydrothermal and Chemical Conditioning.* University of Nevada, Reno (2013).
28. Deng, L., Che, D.: *Chemical, Electrochemical and Spectral Characterization of Water Leachates from Biomass.* (2012).
29. Kobayashi, N., Okada, N., Hirakawa, A., Sato, T., Kobayashi, J., Hatano, S., Itaya, Y., Mori, S.: Characteristics of Solid Residues Obtained from Hot-

- Compressed-Water Treatment of Woody Biomass. *Ind. Eng. Chem. Res.* 48, 373–379 (2009).
30. Sevilla, M., Maciá-Agulló, J.A., Fuertes, A.B.: Hydrothermal carbonization of biomass as a route for the sequestration of CO₂: Chemical and structural properties of the carbonized products. *Biomass and Bioenergy*. 35, 3152–3159 (2011).
 31. Sun, R.C., Tompkinson, J.: Comparative study of organic solvent and water-soluble lipophilic extractives from wheat straw I: Yield and chemical composition. *J. Wood Sci.* 49, 47–52 (2003).
 32. Che Man, Y.B., Setiowaty, G.: Application of Fourier transform infrared spectroscopy to determine free fatty acid contents in palm olein. *Food Chem.* 66, 109–114 (1999).
 33. Jenkins, B., Mannapperuma, J., Bakker, R.: Biomass leachate treatment by reverse osmosis. *Fuel Process. Technol.* 81, 223–246 (2003).

Chapter 4. Pelletized fuel from EFB hydrochar and washed EFB hydrochar

Abstract: In chapter 4, the comparison of the pellets produced from the hydrothermally treated EFB (HTT-EFB) and washed HTT-EFB was performed. Pelletization of biomass has been practiced widely to produce homogenous products with a high density. However, the study on the pelletization of the washed hydrothermally treated biomass is currently limited. The pelletization of the raw EFB, HTT-EFB and washed HTT-EFB was conducted using a single pellet making device. The experiment was performed in the room temperature under the pressure of 150 MPa. The physical property, the mechanical strength, the durability and the hydrophobicity of the produced pellets from each sample were evaluated. The SEM analysis was also performed to investigate the bonding mechanism within the pellets. From the results, washed HTT-EFB pellets showed a high mechanical strength and the durability comparable to HTT-EFB and raw EFB pellets. The pellets also showed the hydrophobic nature against the moisture exposure. However, washed HTT EFB pellets required higher energy for making pellet. From the analysis, it was found that the changes in the composition of EFB biomass by HTT and the washing process regulate the pelletization behavior and affects the bonding mechanism during the pelletization. In conclusion, the combination of the pelletization, HTT, and the washing co-treatment is promising for upgrading EFB into clean, energy dense, homogenous, friable, durable and hydrophobic solid fuel.

4.1 Introduction

With the increasing demand of energy fuel, EFB pellet is considered to be potential fuel for power generation in East Asia [1]. Pelletization may facilitate handling and transporting of EFB for domestic and international markets. In comparison to raw biomass, biomass pellets have obviously improved fuel quality.

However, conventional biomass pellets also still have many drawbacks, like the high moisture affinity and the relatively weak durability [2]. The pellets tend to absorb moisture from the surrounding humid air that leads to pellets disintegration and also provides an ideal environment for microbial and biochemical activities [3]. A low durability pellet tends to disintegrate easily into fines during handling and storage. Previous published literature has shown that pellets made from steam treated wood have better properties; such as increased dimensionally stable and less hygroscopic [4], higher breaking forces resistance [5].

After the pre-treatment of EFB by the hydrothermal treatment and the washing process, it was found that the raw-EFB was enhanced in term of its energy density, hydrophobicity, ash and alkali metal contents. To make a pellet that meet the European pellet standard, the ash content should be below 2%, and the chlorine content should be below 0.03%. The washed hydrochar produced in the previous chapter has met these requirements. However, the effect of the HTT and washing to the pelletization process and the produced pellet need to be investigated. The physical property, the mechanical strength, the durability and the hydrophobicity of the produced pellets from each sample were evaluated to compare with the pellet produced from hydrochar and washed hydrochar. The SEM analysis was also performed to investigate the bonding mechanism within the pellets.

4.2 Material and methods

4.2.1 Fuel preparation

The feedstock for pelletization was produced from the HTT experiment and washing experiment. The HTT experiment description had been done in the section 3.2.2 of the previous chapter and the detail of the washing experiment can be found in the section 3.2.3. The samples for the pelletization experiments are raw-EFB, hydrochars, and washed hydrochars.

4.2.2 Pelletization technique

In preparation for pelletization, the samples were conditioned to 10% moisture content in average to ensure enough moisture content was present to act as a binder and lubricant during the pelletization [6]. The samples was then wrapped in the aluminum foil and stored in a sealed plastic bag until pelletization.

The pelletization of the raw EFB, hydrochar and washed hydrochar were conducted using a single pellet making device. Basically, the pelletization unit consists of a cylindrical die with a piston (8 mm in diameter) made from stainless steel, and a removable electrical heater wrapped around the die cylinder. There is a removable plate at the bottom of the die which can be placed during compression and removed during extrusion of the pellet. The pelletization experiment set up is shown in Figure 4-1.

The experiment was performed in the room temperature, and the pressure used was 150 MPa (approximately 7.5 kN). Before making a pellet, the heater was turned on and set to the target temperature and maintained by the thermocouple attached to the temperature controller. Then, approximately 1 g of samples was manually loaded inside the die and then compressed to a preset pressure. The pressing was performed using an Autograph Universal Testing Machine AG-IS (Shimadzu, Japan). The displacement speed was set at 0.1 mm/min. After holding for 30 s at the maximum pressure, the

pressure was released and the plate was removed followed by pressing the formed pellet out from the die. The displacement for extrusion was set at the same speed and also using the same piston that used for the compression. The force-displacement data were logged during the compression-extrusion cycle of the pellet. The pellets were left undisturbed for 2 minutes and stored inside a sealed plastic bag for further measurements. More than 20 replicates were made from each treated and untreated EFB sample to ensure the reproducibility and consistency.



Figure 4-1. The pelletization unit set up

4.2.3 Characterization methods

4.2.3.1 Physical characterization

To calculate the pellet density, which is expressed by the ratio of the mass and the volume of the single pellet, a stereometric method was used. The basis of this method is the dimensions measurement of the pellet shape. The mass, length and diameter of each pellet were measured at once after extruded from the die cylinder to determine the initial pellet density. The length and diameter of each single pellet was measured using a digital caliper (As One, Japan), while the weight of the pellet was measured using an

analytical balance with 0.0001 g precision. These measurements were repeated after storing the pellets for 2 days. The energy density was calculated by multiplying the mass density with HHV of the pellet. HHV of the untreated and pretreated EFB (HTT and washed) has been discussed in Chapter 3.

4.2.3.2 Durability test

The durability test employed in this research was the abrasive resistance test. The abrasive resistance test in this study was performed by adopting the methodology designed for coal, called tumbler test or MICUM test (ASTM standard method D441-86 for). Five pellets were placed in a tumbling can. Then the samples were rotated for 80 min at 38 rpm. After rotating, the samples were screened using 2 mm sieve. The particles that screened out then weighed. The ratio of mass larger than 2 mm to initial mass for each batch of pellets demonstrates the indicator of abrasive resistance, or will be defined as the durability index.



Figure 4-2. The tumbler can set up in the laboratory

4.2.3.3 Compressive test

The compression strength of the pellet was evaluated using an unconfined compression tester shown in Figure 4-3. The cylindrical pellet was horizontally placed between two plates, bottom plate and a disc shape metal probe (10 cm in diameter) attached to a 50 kN load cell (see the right side of Figure 4-3). The force and displacement data were recorded using a data logger attached to the compression tester. The test was carried out at a compression rate of 1.6 mm/min, and stopped after pellet failure. The value of the compression strength was defined as a maximum force a pellet could withstand, before the fracture of the pellet.

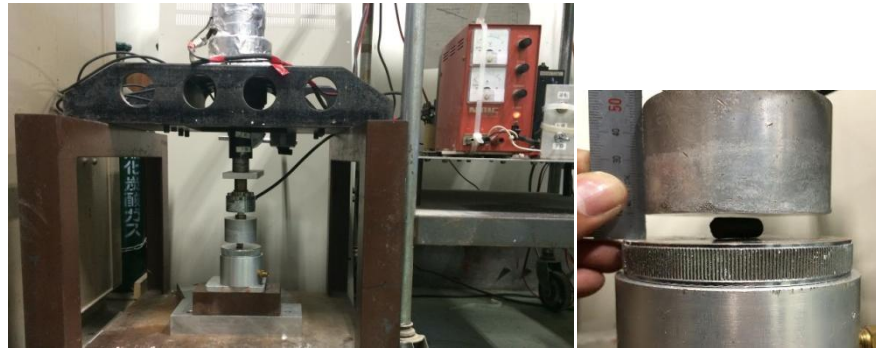


Figure 4-3. The unconfined compression tester

4.2.3.4 Equilibrium moisture content

The moisture uptake test was measured by exposing the pellet samples to a controlled environment. The static desiccators technique [7] was adopted in this study in order to create a controlled humidity. The technique was illustrated in Figure 4-4. The controlled humidity inside a chamber, a desiccator in this case, was maintained at a constant value by keeping the air equilibrium with an aqueous solution saturated with particular salt. NaCl (Wako pure chemical industries, Japan) solution was used to maintain humidity of 75 to 80% at 26 – 28 °C [8]. Prior to the moisture uptake test, the pellets were dried at 105°C for 24 h. A pair of pellets was placed in the Petri glass dish and put inside the desiccators for at least 5 h. The weight of the pellets was measured every 15 min for the first hour followed by every 1 h for the following 5 h. Three replicates were measured for the test.

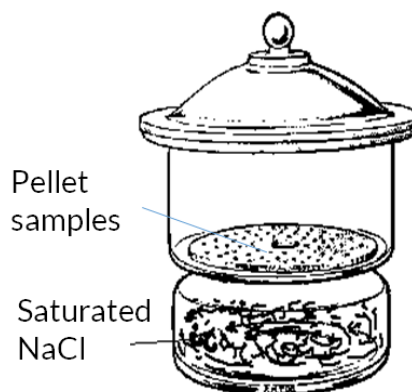


Figure 4-4. Static desiccators technique

4.2.3.5 SEM analysis

The JSM-6610LA scanning electron microscope (JEOL Co., Ltd. Japan) was used to study the changes in the fibrous structure as a result of pretreatment and the bonding mechanism of the pellets by fracture surface analysis. All the samples were cut then mounted onto the surface of standard SEM stub using a carbon tape. The samples were then placed into ion sputter coater MSP-1S (Shinkuu, Japan) where Pt-Pd was deposited

on the surface of sample to provide a conductive coating. Scanning electron microscopy (SEM) was performed using a voltage of 10 kV with magnification of 430 times for the images collection.

4.2.3.6 Lignocellulosic component analysis

The feedstocks for pelletization were measured for its lignocellulosic component (lignin, hemicelluloses, cellulose, and extractives). The milled EFB hydrochars were Soxhlet-extracted with acetone to determine the content of the extractives. The acid-insoluble lignin (Klason lignin) content of the feedstocks was determined using the method of Yoshihara et al. [9] with modified procedures as follows [10]: the prepared sample (0.5 g, as oven-dried weight) was primarily hydrolyzed with 72 % sulfuric acid for 2.5 h and further hydrolyzed with 4 % sulfuric acid at 121°C for 1 h. The sample was then filtered to obtain the residue and filtrate with a glass filter (1 GP 16). The weight of the residue was measured as acid-insoluble lignin. The amount of acid-soluble lignin was determined according to UV spectrophotometry at the wavelength of 205 nm (TAPPI Test Method: T222 om-11 [11]). The amounts of glucose and xylose were determined from the 1000 times diluted filtrate by using ion chromatography according to the procedures described in a previous study [12]. The system using Dionex ICS 3000 ion chromatograph (Dionex, Sunnyvale, CA, USA) consisted of a single pulp model (SP-1), an electrochemical detector (ED), an IonPac AS 7 column ($\varnothing 4\text{mm} \times 250\text{ mm}$), an IonPac AS 7 guard column ($\varnothing 4\text{mm} \times 50\text{ mm}$), and an auto sampler (AS).

4.3 Results and discussion

4.3.1 Lignocellulosic chemical composition of the pelletization feedstock

The lignocellulosic composition of the samples used in the pelletization experiment was analyzed and presented in the Table 4-1. Many researches had reported the correlation between the biomass lignocellulosic component and the produced pellet quality (strength and durability) as well as the pelletizing behavior [13–15]. Therefore, this analysis will be important to support the investigation on the phenomenon behind the pelletization process.

To be note, the glucose and xylose content presents in the Table 4-1 are representing the cellulose and hemicelluloses component of the biomass, respectively. During the biomass component analysis, the samples were pretreated by sulphuric acid hydrolysis for lignin and sugar measurement. After hydrolysis, cellulose will be decomposed mainly into glucose and hemicelluloses into xylose. The other sugars such as arabinose and mannose were not measured due to relatively small amount in the biomass.

As seen in the Table 4-1, raw-EFB comprises of higher content of cellulose compared to lignin and hemicelluloses. This is in agreement with the content of EFB from other

research [16]. After HTT process, the content of the hemicelluloses was decreased due to hydrolysis reaction that occurred during the HTT which can be obviously seen in Table 4-1. As discussed before in the previous chapter, hemicelluloses is the least thermally stable polymer among all three lignocellulosic polymers, and its solubilization in water starts at about 180°C under hydrothermal conditions [17, 18]. The hemicelluloses is relatively easy to be hydrolyzed into basic sugars. HTT at 180°C is seen only can decompose a partial hemicelluloses as can be observed from the small hemicelluloses decrease compared to the content in the raw-EFB in Table 4-1. The increment of the HTT temperature to 220°C could decompose almost all the hemicelluloses, which only leaving approximately 3% of hemicelluloses in the HTT-220 hydrochars. The significant reduction of the hemicelluloses content resulted in the relative increase of other component such as lignin and extractives. Moreover, the degradation of hemicellulose, cellulose, and extractives was found leaving a porous hydrochars with concentrated sugars and organic acids dissolved in water. The porous structures might absorb the dissolved sugars and furfurals during HTT so that the extractives percentage increases in the hydrochars [19].

Table 4-1. The lignocellulosic chemical composition of the raw EFB and treated hydrochars.

Samples	Chemical component (% of dry free-extractives weight)					Extractives (%)	Ash (%)
	Lignin		Total lignin	Carbohydrates			
	Acid-insoluble	Acid-soluble		Glucose (Cellulose)	Xylose (Hemicelluloses)		
EFB [16]	-	-	22.1	38.3	35.3	-	-
Raw-EFB	19.96	3.91	23.87	39.65	24.36	4.29	4.9
HTT-180	21.61	3.43	25.04	47.25	21.94	5.48	2.2
HTW-180	21.27	3.22	24.49	56.38	22.91	4.46	0.9
HTT-220	28.69	1.82	30.51	54.84	2.83	17.91	4.1
HTW-220	26.63	1.00	27.64	58.64	2.40	24.86	2.7

The subsequent washing experiment was not really given any significant changes to the structural organic component of the hydrochars compared to the changes resulted from the HTT process. The obvious change was observed in the removal of the ash content. In contrast with the HTW-180, the increase in the extractives content was seen for HTW-220 hydrochars. This might be because high content of significant water soluble sugars and organic compound from the hemicelluloses decomposition during HTT at 220°C are extracted during washing by water compared to the hydrochar from HTT 180°C. These differences in the feedstock composition will highly determine the produced pellet quality and the mechanism of the binding during pelletization.

4.3.2 Pellet characteristics

4.3.2.1 Appearance

The color of the raw EFB feedstock is less dark color than the hydrochars. The color became darker brown color as the HTT temperature increased. These color change was due to Maillard reactions of mono-saccharides and extractives degradation after steam treatment [15]. Figure 4-5 shows the physical appearance of the pellets made from raw-EFB, hydrochars, and washed hydrochars. As can be seen, the hydrochar pellets has smoother and glassy surface compared to raw-EFB pellets. It can also be seen that the surface of the hydrochar pellets were very compact and uniform without visible voids. Contrary, obvious voids and gaps were seen on the surface of the raw-EFB pellet. These gaps were reported to able to reduce the pellet resistance to deformation and promote the movement of the particles within matrix that leads to weak mechanical durability [2]. The bigger gaps were also indicating poor adhesion between the biomass particles [20].



Figure 4-5. The appearance of the pellets made from raw-EFB, hydrochars and washed hydrochars

The shiny surface that seen in the hydrochar pellets might be due to the lignin coating on the outer surface of the pellets [6]. The washed hydrochar pellets had shinier surface compared to hydrochar pellets. As had been described in the previous sub-chapter, the hydrochar and washed hydrochar had relatively more lignin, due to hemicelluloses degradation and removal of ash. The broken down of lignocellulosic matrix during HTT was also giving the lignin more accessible passage to come out during pelletization.

4.3.2.2 Particle size distribution

Particle size is known as an important influence of the pellet durability [14]. Commonly, finer particles lead to higher durability. The particle size distribution of all the samples is presented in Figure 4-6. Larger particle sizes were found for the raw-EFB. While smaller particle size portion was seen to increase with the increasing severity of HTT.

From the figure, HTT shifted the particle distribution into smaller size. The effect of washing was evidently seen for the hydrochar at HTT-220. Originally, the smaller particle size is already dominantly present in the HTT-220 hydrochar particles. However, since hemicelluloses removal increased the relative content of lignin at the HTT temperature of 220°C, the products become brittle and easy to break. Therefore,

the mixing process during washing experiment might break the hydrochar particles further, resulting in smaller size particles compared to the unwashed ones. On the other hand, washing process had only slight effect on the HTT-180 hydrochars.

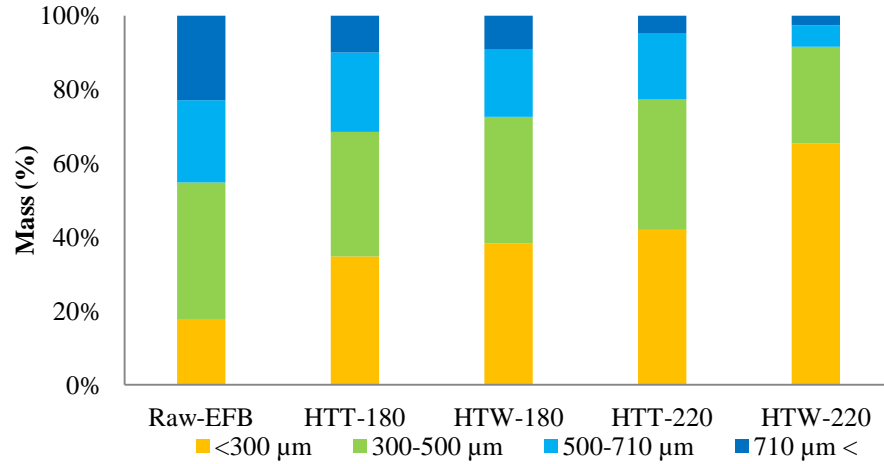


Figure 4-6. Particle size distribution of raw EFB, hydrochars and washed hydrochars

4.3.2.3 Mass and energy density of pellets

During measurement of the physical dimension of the pellets, the diameter and the length of the pellets were recorded 2 times; immediately after extrusion from the cylinder and after resting them for 24 h. Therefore, the initial density and relaxed (final) density could be calculated. The length expansion happened during the relaxation of pellets was also calculated. Figure 4-7 presents the initial and final pellet density, and also the expansion rate of all the pellet samples observed.

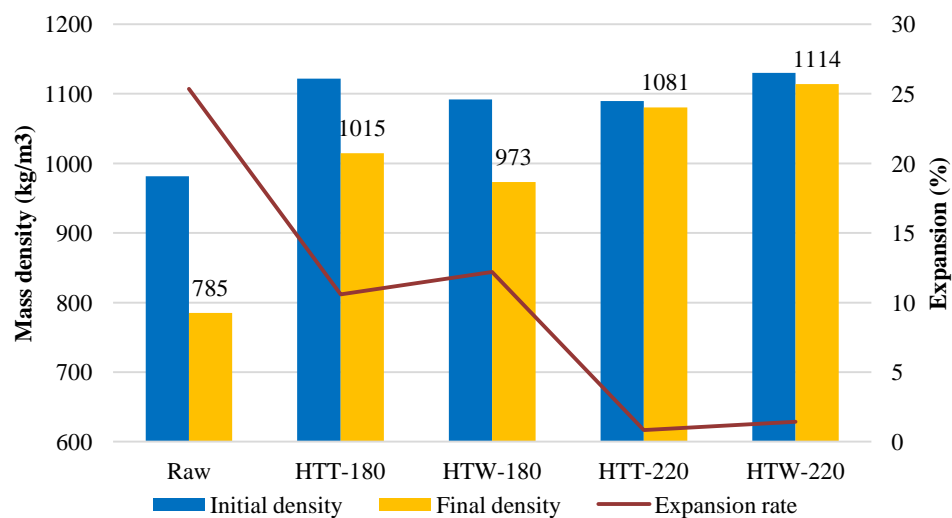


Figure 4-7. Initial, final density and expansion of all the pellet samples

The bulk density of the feedstock particles prior to pelletization were recorded at approximately 160 kg/m³ and 180-240 kg/m³ for raw-EFB and hydrochars, respectively. The initial pellet density of raw-EFB measured from mass and volume of a single pellet was 982 kg/m³, and the initial pellet density for HTT-180 hydrochar was 1122 kg/m³. The initial pellet density increased with the severity of HTT. This is also in line with the previous studies on the HT pretreated pellet [4, 21]. However, in this study, the initial pellet density of HTT-180 hydrochar decreased after the washing process, while it was increasing for HTT-220 hydrochars. The smaller particles of the washed HTT-220 hydrochar that has been discussed previously might be the reason of the higher mass density of the washed HTT-220 hydrochar compared to the washed HTT-180 hydrochar pellet. A similar trend was observed for the final pellet density measured after 1 day rest.

The pellet density of the raw-EFB decreased from 982 kg/m³ to 785 kg/m³ due to 25% length expansion, as can be seen in Figure 4-7. In contrast, for the hydrochar pellets, the expansion is less, particularly for the HTT-220 hydrochar pellet that only experienced a 0.84 % length expansion. The effect of the washing treatment was seen in the slight increase of 1 – 1.5% of the expansion rate for all the hydrochar pellets. Stelte et al. (2012) reported on the phenomenon where the biomass has tendency to expand after palletization, which is known as “spring back effect”[20, 22]. The expansion rate also can be a measure for the bonding quality between the biomass particles within a pellet. If there is poor adhesion, the particles do not bind well together and the pellet expands like a spring [20].

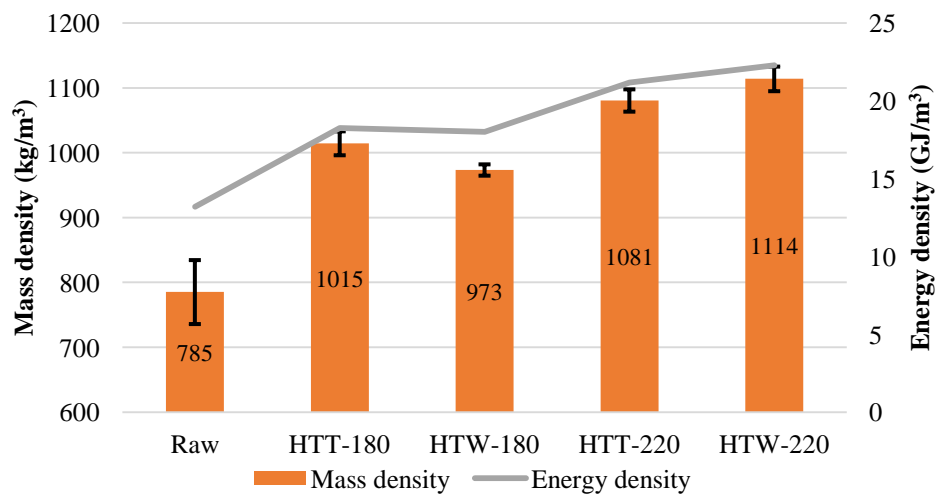


Figure 4-8. Mass and energy densities of all the pellet samples

Previous research reported that this less length expansion of hydrochar pellets confirmed the strong bonding between hydrochar particles and better durability of hydrochar pellets [2]. In other words, the HTT is able to reduce the “spring back effect” of the raw biomass. This effect may be caused by the hemicelluloses that usually acted as visco-elastic component in the biomass fiber matrix [15, 23]; thus this component

degradation during HTT reduced the stress relaxation of the component and lower the “effect”. In other theory, the increase in the available lignin caused by HTT is said to be responsible for the superior performance in the expansion test [5]. The lignin became available for binding by the disruption of lignocellulosic biomass during HTT. The pellets produced from hydrochars and washed hydrochars showed only limited expansion, exhibiting a consistent dimensional stability compared to the raw-EFB.

Figure 4-8 presents the energy density of all the pellet samples. It can be seen from the figure that the volumetric energy density (energy per volume) of raw-EFB pellets and hydrochar pellets increased significantly, ranging from 18.3 GJ/m³ to 22.3 GJ/m³, due to densification. There should be no change in HHV of samples before and after the pelletization. It was because most of lignocellulosic (hemicelluloses, cellulose and lignin) composition of biomass does not start reacting until the material temperature reaches 180°C [6, 21, 24], thus no compositional change should take place in biomass at the room temperature of pelletization. No external binding material was used during pelletization of raw and pre-treated EFB in this study; therefore, HHV remained relatively unaffected.

4.3.3 Mechanical strength and durability of pellets

The mechanical strength and durability test is a good way to know the pellet strength and quality in holding its shape without being disintegrate during transportation and storage. The compressive strength of pellet is the measure of internal bonding strength of the maximum force a pellet can withstand before its rupture during transportation and storage [21]. The durability is defined as the ability of pellet to remain intact during handling measured by the amount of fine particles generated after mechanical agitation [25].

4.3.3.1 Compressive strength

Figure 4-9 shows the typical curves of the compressive force against the displacement of the raw-EFB, hydrochar and washed hydrochar pellets. The compressive strength was presented in a normalized maximum load to the pellet length, since each resulted pellet has different length as shown in Figure 4-10.

As seen in Figure 4-9, the force that the pellet can withstand was higher for the treated pellets (both HTT and HTW) compared with the raw-EFB. However, when comparing the unwashed and washed pellet, the effect of washing was very obvious for the HTT-180 pellet; giving higher force resistance compared to the unwashed one. While, it was not so obvious in the case of HTT-220 pellets.

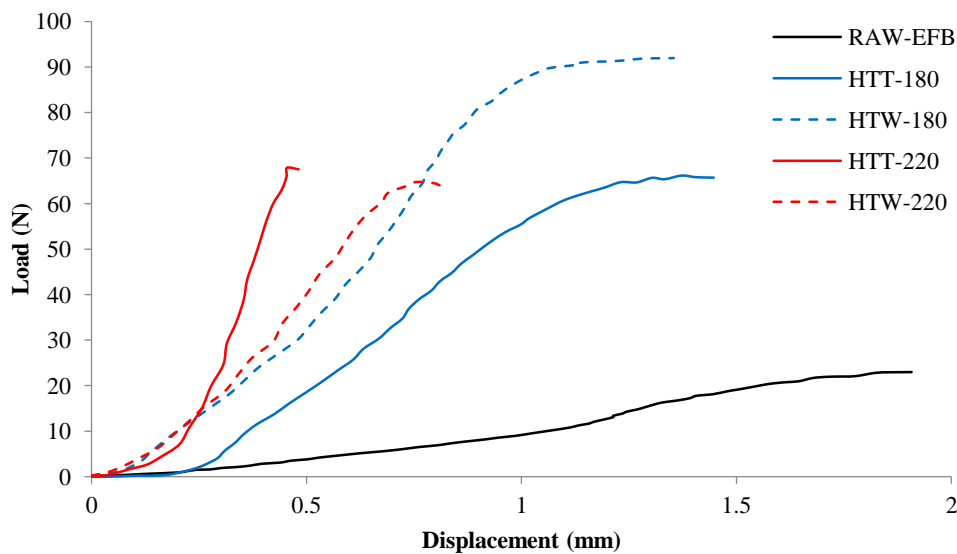


Figure 4-9. The compressive force versus displacement curves of the pellets prepared from raw EFB, hydrochars and washed hydrochars.

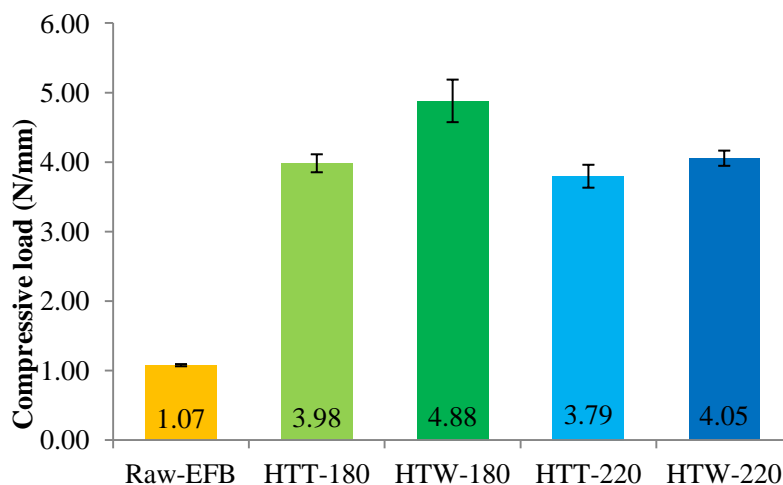


Figure 4-10. The compressive strength of the raw-EFB, hydrochar and washed hydrochar pellets

The maximum load required to break the pellet slightly decreased for the hydrochar pellet with the increasing of the HTT severity; 3.98 N/mm and 3.79 N/mm for HTT-180 and HTT-220 pellets, respectively. The increase of the lignin content caused by the thermal degradation of hemicelluloses contributed to the increase in the compressive strength [4, 26]. In HTT, the hydrolysis reaction depolymerizes the hemicelluloses into oligosaccharides or monosugars like xylose [27, 28]. The additional bonding strength of the hydrochar pellets possibly caused by the formation of highly branched polysaccharides by reverse reactions of monosugars during pelletization [4]. However, too high percentage of lignin present, as in the hydrochar produced from HTT-220, can act as a natural binder, but at the same time can make the pellets highly brittle [21, 24]. The less lignin in hydrochar pretreated at lower temperature (180°C) compare to higher

one (220°C) make the pellet more elastic; therefore it requires more compressive load to break the pellet [24]. The hemicelluloses degradation and the increase in the cellulose content might also result in more brittle pellet after HTT at a higher temperature.

Washing the hydrochar could increase the strength of the pellets. The highest compressive strength was obtained from the washed HTT-180 hydrochar with the maximum load of 4.88 N/mm. The higher strength of washed hydrochar pellets might be due to the removal of metal content during washing process that might exposed more lignin for binding, thereby increasing the pellet strength.

4.3.3.2 Durability

In this study, durability or abrasive resistance was estimated by using the tumbling can method. This method can determine the pellet quality in terms of the pellet durability index (PDI), or, simply percent durability [14]. The high PDI means high quality pellets. The PDI is defined as follows:

$$\text{PDI (\%)} = \frac{\text{mass of particles} > 2\text{mm after tumbling}}{\text{initial mass of particles}} \times 100 \quad (4-1)$$



Figure 4-11. The appearance of the pellets after tumbling; (a) HTT-180 hydrochar pellet and (b) HTT-220 hydrochar pellet

Figure 4-11 presents the appearance of the hydrochar pellets after the mechanical agitation by the tumbling can method. From Figure 4-11, it can be seen that the HTT-220 hydrochar pellets produced more fine particles compared to HTT-180 pellets. Only from this visual observation, it can be predicted that HTT-220 pellets seem to have lower durability than HTT-180 pellets.

Figure 4-12 shows the durability index of the pellets of the raw-EFB as well as the hydrochar and washed hydrochar pellets. It is interesting to find that all pellets has quite high index with more than 85%. Reza et al. (2012) reported the torrefied loblolly pine pellets to have 78.5% durability, much lower than the raw-EFB pellets produced in this

study. The durability index (PDI) of the raw-EFB was around 87.9%, and increased for the hydrochar pellets. The PDI was seen to decrease with the increase of the HTT temperature, for example, the PDI of HTT-180 was 98.4% and decreased to 91.8% for the HTT-220 pellet. The lower durability of the HTT-220 pellets was due to the higher amount of fine particles produced in HTT at a higher temperature, as has been discussed in the section 4.3.1.2. These compacted fine particles (<300 μm) are easy to disintegrate and tend to shatter when the external agitation were given during the tumbling experiment. The other reason is the brittle nature of the HTT-220 hydrochar which is due to high content of lignin. Previous researches reported that the abrasive resistance has been correlated to the particle distribution in biomass pellet [14, 29]. In those studies, higher amount of fines in pellet is considered to create more durable pellets. However, in this study, the higher fine particles together with the brittleness of the particles made the pellets to have a lower durability. Moreover, other study reported that at above threshold level of lignin plus extractive component of 34%, the pellet durability decreased [14]. From the chemical composition analysis in Table 4-1, the lignin plus extractives content for HTT -220 and HTW-220 hydrochars was higher than 34%, thus lower the strength and durability of the pellets.

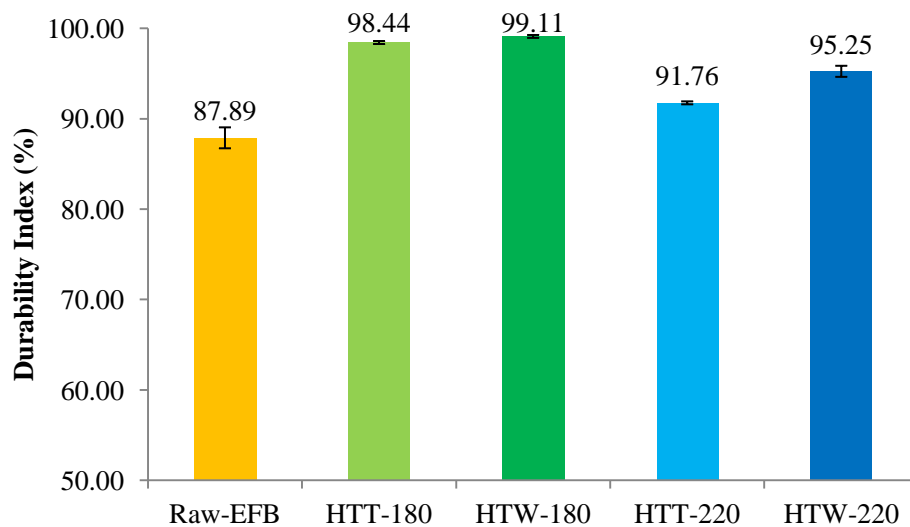


Figure 4-12. The durability index of raw-EFB, hydrochar and washed hydrochar pellets.

The washed HTT-180 hydrochar exhibited the highest durability among other pellets. It can be observed that washing enhanced the durability of the pellets. The trend is quite similar with the trend of the compressive strength meaning that the quality of the pellets can be evaluated well with these parameters. The reason that can explain the higher durability of washed HTT-180 hydrochar is the removal of extractives and ash content that contributed to the better bonding of the particles thus increase the durability. To meet the requirement of European pellet standard [30], the mechanical durability shall be $\geq 97.5\%$. Therefore, it was only pellets made from HTT-180 hydrochar and washed HTT-180 hydrochar that can meet the standard.

4.3.4 Hydrophobicity

The biodegradation of biomass pellets was strongly influenced by its moisture content. The moisture content of the biomass largely depends on the surrounding atmosphere but it also depends on the composition of biomass [7, 24]. From the previous chapter, it was found that HTT makes the hydrochar hydrophobic and the hydrophobic nature will increase with the treatment severity.

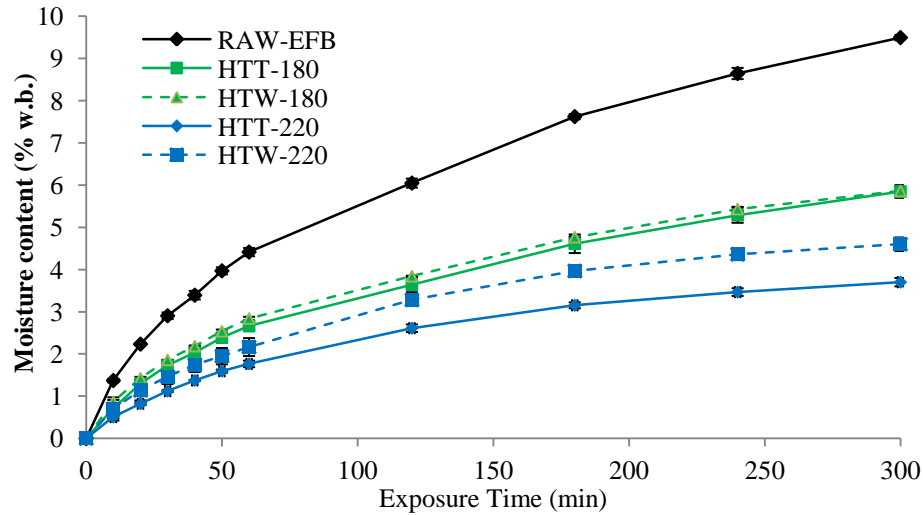


Figure 4-13. The moisture uptake of raw EFB, hydrochar and washed hydrochar pellets at 26-28°C and 75-80% relative humidity.

Figure 4-13 shows the moisture content of the pellets against the exposure time for 5 h. Pellet produced from the raw-EFB exhibited the highest moisture uptake of 9.49% after being exposed to the high humidity for 5 h, showing the hygroscopic behavior. On the other hand, the moisture uptake of the hydrochar pellets was seen decreased significantly compared to the corresponding raw-EFB pellet. The lowest moisture uptake was observed for the HTT-220 hydrochar pellet for which the increase of the moisture content is only 3.70% after 5 h exposure. The hydrochar pellets indeed presented the hydrophobic nature compared to the raw-EFB pellet. The hydrophobic nature of hydrochar is coming from the lignin content. Among the biomass component, hemicelluloses have the greatest capacity of water absorption, while lignin has only little tendency to absorb water [7, 21]. Therefore, the removal of hemicelluloses from the biomass will increase its hydrophobicity. Alternatively, the presence of pores on the surface of raw EFB pellets, as discussed in sub-chapter 4.3.1.1, might increase the tendency to absorb moisture content (free water) from the atmosphere [31]. These all reasons explained the high hydrophobicity of the hydrochar pellets compared to the raw-EFB.

In case of HTT-180 hydrochar, the unwashed and washed hydrochar has no difference in moisture uptake behavior. While, the washed HTT-220 hydrochar pellet showed slightly higher uptake by 1.1% than unwashed, exhibiting a lower moisture resistance. Hence, washing was seen to decrease the moisture resistance slightly. The possible reason for this phenomenon is that the introduction of water during washing experiment may reduce the hydrophobic nature of the hydrochar. However this is still a presumption, more investigation is needed to explain this behavior.

The moisture uptake test results indicated that the pretreated EFB pellets has a good resistance against moisture and highly hydrophobic in nature. Therefore, the pellets can be safely stored for long time without being afraid of biological deterioration. Moreover, the transportation cost will be less expensive, since there will be less water to transport along with the biomass [21].

4.3.5 Morphology of pellet and bonding mechanism

The morphology was studied using the SEM of the cross-section for each pellet. The morphology is important to investigate the bonding mechanism that works within the pellets. Figure 4-14 presented the SEM images of the cross-section of the pellet samples observed.

The binding forces that act between the individual particles in densified products have been categorized into five major groups [14]. They are (i) solid bridges, (ii) attraction forces between solid particles, (iii) mechanical interlocking bonds, (iv) adhesion and cohesion forces, and (v) interfacial forces and capillary pressure. Due to the application of high pressures and temperatures, solid bridges maybe developed by diffusion of molecules from one particle to another at the points of contact. Solid bridges may also be formed between particles due to the crystallization of some ingredients, chemical reaction, hardening of binders and solidification of melted components. Solid bridges are mainly formed after cooling/drying of densified products. Short-range forces such as molecular [valance forces (i.e., free chemical bonds), hydrogen bridges and van der Waals' forces], electrostatic, and magnetic forces can cause solid particles to adhere to each other if the particles are brought close enough together. During the compression process, fibers, flat-shaped particles and bulky particles can interlock or fold about each other resulting in interlocking bonds. Highly viscous binders (e.g., molasses and tar) adhere to the surfaces of solid particles to generate strong bonds that are very similar to those of solid bridges[6, 14].

The raw-EFB fibrous structure was bound to the other particles poorly with large inter-particle gaps, which is indicated in Figure 4-14 (a). This figure is indicating the poor adhesion between particles. Poor adhesion is due to the lack of strong binding force between inter-particles to minimize the expansion by stress relaxation in the raw-EFB [15]. The large gaps reduced the attractive force between adjacent particles, as Valance

forces are effective only if the inter-particle distance is about 10 \AA [6]. Van der Waals' forces also believed to make the most contribution to all intermolecular attractive effects and are partly responsible for the adhesion between particles less than 0.1 \mu m apart[6]. By applying high pressure, mechanical interlock may have taken place, forming a pellet with low durability[24]. Therefore, mechanical interlock is thought to be the main binding mechanism for the raw-EFB pellet.

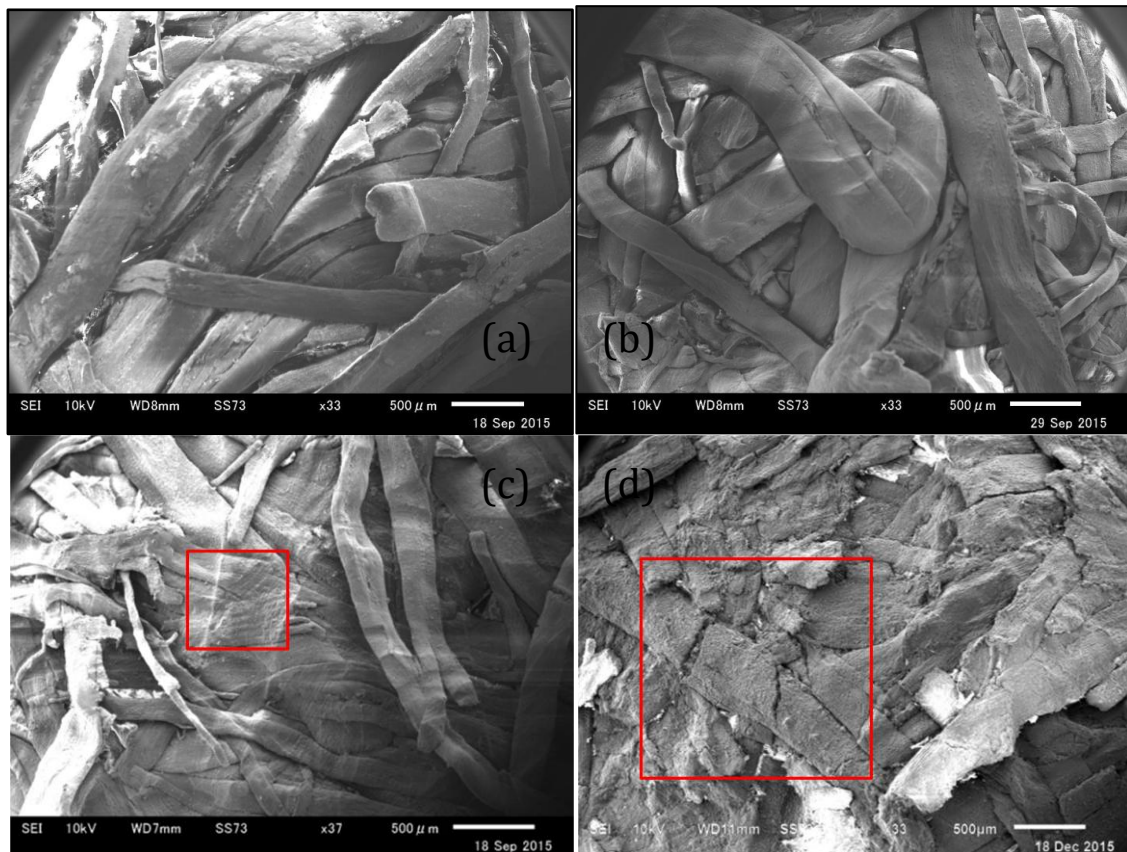


Figure 4-14. SEM images of the cross section of (a) raw-EFB pellet, (b) HTT-180 pellet, (c) HTW-180 pellet, and (d) HTT-220 pellet at low magnification (33-37x)

However, the treated EFB pellets, both hydrochar and washed hydrochar, showed smaller inter-particle distance, which is implying a good inter-particles adhesion, as depicted in Figure 4-14 (b), 4-14 (c) and 4-14(d). In the point of view of enlarged surface, it was attributed to the highly friable property of the hydrochars due to the increased lignin content. As the consequence of the high friability, the hydrochar broke down into small particles under the compressive force during the pelletization. Accordingly, the contact area between particles was enlarged compared to the raw-EFB pellet. The physico-chemical changes during HTT were obviously affecting the binding properties of the biomass particles.

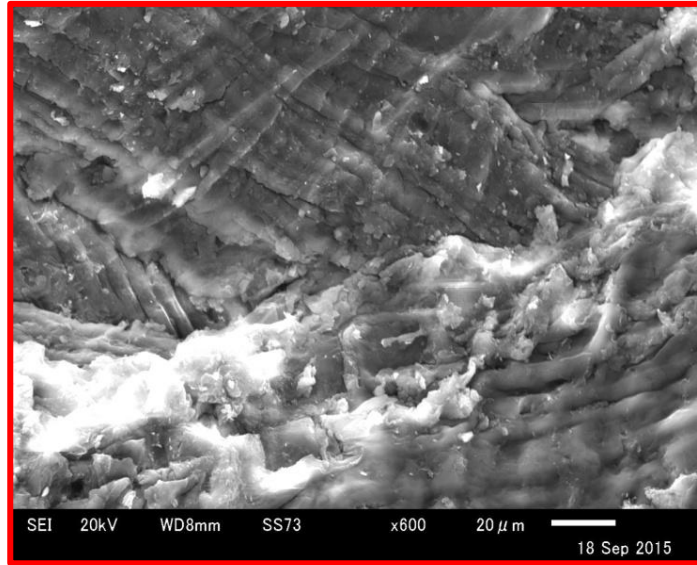


Figure 4-15. The magnification of SEM images of HTW-180 pellet

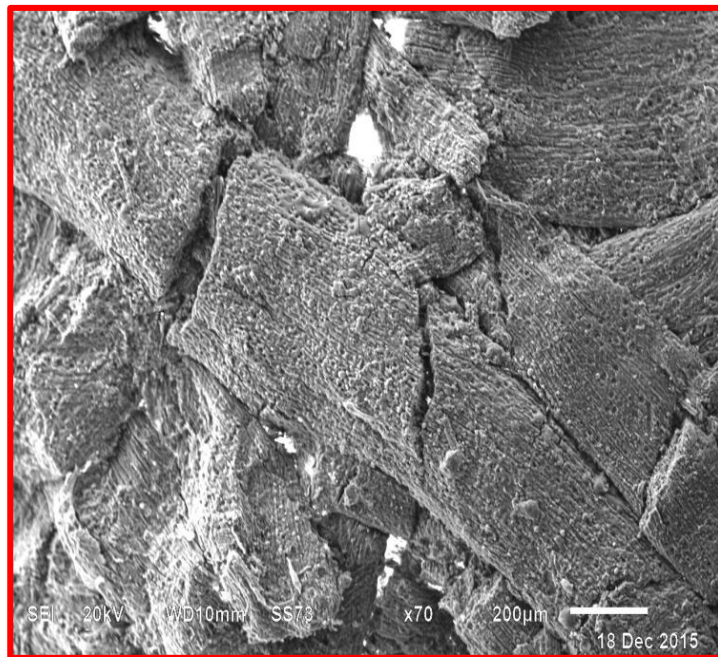


Figure 4-16. The magnification of SEM images of HTT-220 pellet

Due to the absence of high temperature pelletization in this study, the attraction forces between particles and the mechanical interlocking bonds are considered to be responsible for the main type of bonding in this pelletization of hydrochar. However, in this laboratory pelletization, pellets were made at 150 MPa pressure. Because of the application of high pressures, particles were brought close together causing inter-particle attraction forces, and the natural binding components in hydrochars were squeezed out from the cells, which made solid bridges bonding may also take place between the particles [6]. The solid bridge bonding mechanism can be observed in the

magnification SEM images of HTW-180 pellets and HTT-220 pellets (see Figure 4-15 and Figure 4-16). This caused the pellets to become strong and durable, which was also shown from their compressive strength and durability index value discussed earlier. The crack in the surface particles, as seen in Figure 4-17, may facilitate the access for the lignin to be squeezed out during the compression.

4.3.6 Energy input of compression of pellet

Figure 4-17 shows the typical curve of force versus displacement of the pellets during the compression to form pellets. The force applied was initially small over the first 15-30 mm displacement then followed by a rapid force increase for a short displacement of about 5-10 mm. At the increasing force from 0 to 1 kN, the raw-EFB particles seem to undergo a particle packing rearrangement, as seen from the larger area under the raw-EFB curve than that of hydrochar curve. It means that under this force range, the required compression energy is higher for raw-EFB than the hydrochar. The possible explanation for this is because the hydrochars has smaller particle size that leads to the easy compaction under the applied force [32]. However, at the further increase from 1 kN to 9 kN, the less steep slope in the plasticization region was seen for the hydrochar; therefore it required more energy to make a pellet compared to the raw-EFB.

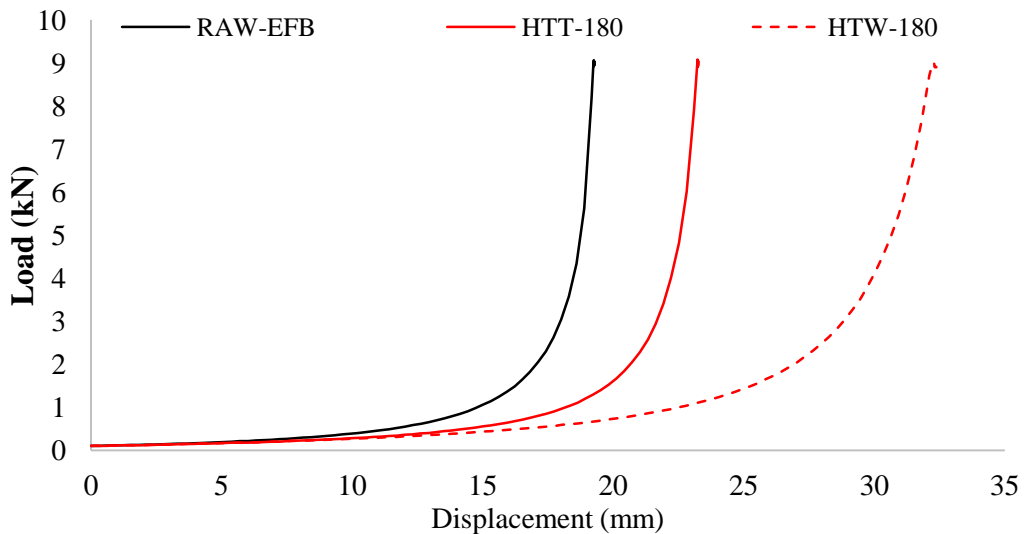


Figure 4-17. The typical force-displacement plot during the compression

In total, the required compaction energy for the hydrochar pellet is 25.0 J, while for the raw-EFB pellet is 18.62 J, as can be seen in Figure 4-18. The brittleness that coming from the increase in the crystallinity and acid-insoluble lignin of the hydrochars due to HTT can be a reason for the higher compaction energy required [4]. Among the three major components of biomass, cellulose has a crystalline structure with the highest modulus of elasticity. Hemicelluloses are the visco-elastic components of wood fiber which introduce viscous effect among the amorphous lignin and the crystalline structure of cellulose (rigid) in the fiber [15, 23]. The hydrolysis of hemicelluloses due to steam

treatment leads to an increase in brittleness of the samples [33]. Therefore, the energy to break the brittle particles was higher. Another reason to account for the increase in the compression energy is due to the friction between the rough hydrochar particles during the packing prior to the compression stage. Previous research reported that the coefficient of friction of steam-treated agricultural residues was significantly higher than the untreated particles [34].

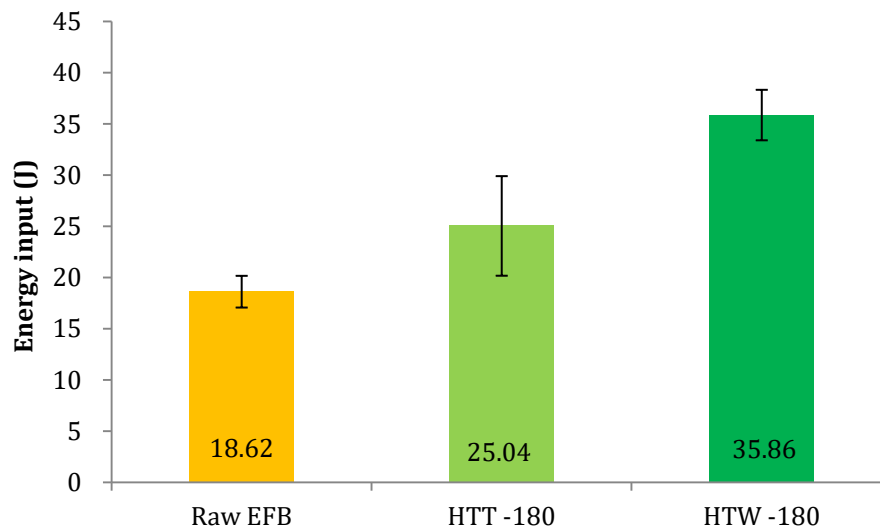


Figure 4-18. The compression energy required for making each pellet

The HTW-180 hydrochar exhibited the highest compression energy for making pellets. The required compression energy was 35.86 J. Water washing was found to reduce the extractive content of the biomass as well as increasing the relative amount of lignin in the hydrochar particles. Nielsen et al. (2010) suggested that the extractives act as plasticizers and lubricants, which minimize the energy required for compression [35]. Therefore, the removal of extractives from the HTT-180 hydrochars increases the energy requirement for the pelletization. The increase of the lignin content also leads to the elevated friability and increase the friction force during the compression; thus it also increased the compression energy.

4.3.7 High HTT temperature consideration

Higher HTT temperature $>220^{\circ}\text{C}$ ($230^{\circ}\text{C}\sim$) may decompose cellulose and further decompose lignin at higher HTT temperature ($>250^{\circ}\text{C}$). Other than hydrolysis and dehydration reactions, decarboxylation, condensation polymerization and aromatization reactions might also occur under such high temperature. Consequently, with increasing the temperature severity, a product with higher carbon content is produced. In the point of view of solid fuel properties, the hydrochar produced at such high temperature can give significant advantage or improvement like high energy dense product due to higher carbon content with lower oxygen and hydrogen content, giving a higher HHV. The

hydrochar samples produced at high temperatures contained atomic ratios close to that of lignite or even low rank coal. At the temperature of 240°C, hemicelluloses might completely decompose, and the cellulose and lignin component probably underwent only partial degradation, leaving a higher content of lignin in the hydrochars. High lignin content is preferable, if the subsequent pelletization process will employ the temperature higher than 100°C. It is because at its glass transition temperature (140°C), lignin will be soften and melted to provide liquid bridges joining, acting as natural binder during pelletization [24].

However, depending on the intended application of the products, higher temperature HTT might also give disadvantage to the final application of the solid fuel, particularly when we intend to produce it in the larger scale. In the large scale, higher HTT temperature means that higher pressure boiler will be needed. Moreover, too high boiler pressure is impractical in the commercial scale, due to increasing investment cost for pressure equipment as well as higher energy consumption generally [36]. The objective of HTT in our study focused on the improvement of the EFB biomass in term of potassium removal and pelletization (heatless and binderless to minimize cost) to produce clean and high quality pellets. In the point of view of pelletization process, the high lignin content hydrochar produced at high HTT temperature is not desirable since too high lignin content will make the hydrochar highly friable and highly brittle, thus reducing the durability and mechanical strength of the pellets which then lower the pellet quality as already discussed in the sub-chapter 4.3.2.

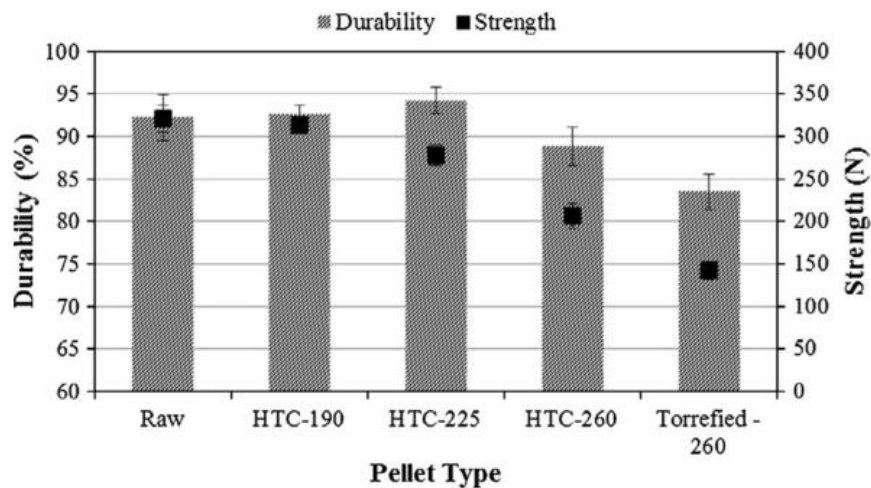


Figure 4-19. Effect of pre-treatment type on the durability and strength of pellets (adapted from [37])

PS Lam et al [15] reported that the elastic modulus is related to the chemical composition of the treated materials, and therefore the most severe steam treatment would cause a relatively large variation in mechanical properties of pellets. From the result in his study, a less severe treatment at 200°C would be the optimum temperature

to produce the hardest pellets with a lesser variation in mechanical properties. In addition, Figure 4-19 from a study by Kambo (2014) [37] showed that there is an optimum pre-treatment condition to produce a strong and durable pellet. In short, the most severe treatment did not mean that it will produce the strongest and the most durable pellets.

The advantage and disadvantage of the higher HTT reaction temperature is listed as follows:

Advantage:

1. Decompose cellulose, increased carbon content, decreased hydrogen, and increased energy density thus giving higher HHV.
2. In the high temperature pelletization, higher lignin might become a good binder and increase the durability and strength of the pellets.
3. The hydrochar samples produced at 260°C contained atomic ratios close to that of lignite

Disadvantage:

1. High energy consumption for the HTT process
2. Too high pressure is not practical in the commercial scale
3. In the point of view of heat-less pelletization process, higher HTT temperature will produce highly friable and highly brittle hydrochar, thus reducing the durability and mechanical strength of the pellets which then lower the pellet quality.
4. Low product mass yield

4.4 Summary

This chapter mainly discussed the effect of the HTT and washing co-treatment on the pelletization behavior and the properties of the produced pellets. The comparison of the pellets produced from the hydrochar and washed hydrochar was performed. The pelletization of the raw EFB, HTT-EFB and washed HTT-EFB was conducted using a single pellet making device. The experiment was performed in the room temperature under the pressure of 150 MPa. The result from the pelletization experiments can be summarized as follows:

1. From the appearance, the surface of the hydrochar pellets was very compact and uniform without visible voids. It means that the hydrochar pellets indicate better adhesion that lead to good mechanical durability compared to raw-EFB pellets.
2. The pellet mass density and the volumetric energy density were enhanced due to the pelletization for all the pellet samples. In addition, the hydrochar and washed hydrochar pellets have less length expansion that indicated a more stable dimension.
3. Washed hydrochar pellets show high mechanical strength, and durability compared to hydrochar and raw EFB pellets. However, the hydrochar pellets show the

hydrophobic nature against moisture exposure better than the washed hydrochar pellets.

4. The composition of biomass plays an important role in the bonding mechanism during the pelletization. The attraction forces between particles and the mechanical interlocking bonds are considered to be responsible for the main type of bonding in this pelletization of hydrochar.
5. The pretreated pellets required higher energy for making pellet (the compression energy input) compared to the raw-EFB. The washed hydrochar has the highest compression energy among other pellets.
6. The improvement in the mechanical strength and the moisture adsorption resistance of pre-treated pellets are attractive for outdoor storage for end-users.

In conclusion, combining densification, HTT and washing co-treatment is promising for upgrading biomass into clean, energy dense, homogenous, friable, durable and hydrophobic solid fuel.

References

1. Cocchi, M., Nikolaisen, L., Junginger, M., Goh, C.S., Hess, R., Jacobson, J., Ovard, L.P., Thrän, D., Hennig, C., Deutmeyer, M., Schouwenberg, P.P.: Global wood pellet industry market and trade study. IEA Bioenergy Task. 190pp (2011).
2. Liu, Z., Quek, A., Balasubramanian, R.: Preparation and characterization of fuel pellets from woody biomass, agro-residues and their corresponding hydrochars. *Appl. Energy*. 113, 1315–1322 (2014).
3. Lehtikangas, P.: Storage effects on pelletised sawdust, logging residues and bark. 19, 287–293 (2000).
4. Lam, P.S., Sokhansanj, S., Bi, X., Lim, C.J.: Energy Input and Quality of Pellets Made from Steam-Exploded Douglas Fir (*Pseudotsuga menziesii*). *Energy and Fuels*. 25, 1521–1528 (2011).
5. Shaw, M.D., Karunakaran, C., Tabil, L.G.: Physicochemical characteristics of densified untreated and steam exploded poplar wood and wheat straw grinds. *Biosyst. Eng.* 103, 198–207 (2009).
6. Kaliyan, N., Morey, R.V.: Natural binders and solid bridge type binding mechanisms in briquettes and pellets made from corn stover and switchgrass. *Bioresour. Technol.* 101, 1082–90 (2010).
7. Acharjee, T.C., Coronella, C.J., Vasquez, V.R.: Effect of thermal pretreatment on equilibrium moisture content of lignocellulosic biomass. *Bioresour. Technol.* 102, 4849–54 (2011).
8. Greenspan, L.: Humidity fixed points of binary saturated aqueous solutions. *J. Res. Natl. Bur. Stand. -A. Physic Chem.* 81A, (1977).
9. Yoshihara, K., Kobayashi, T., Fujii, T., Akamatsu, I.: A novel modification of klason lignin quantitative method. *Japan Tappi J.* 38, 466–475 (1984).

10. Ohi, H., Ju, Y., Kuroda, K.: Structural Analysis of Lignin by Pyrolysis-Gas Chromatography (VII). Conditions for Acid Hydrolysis of Wood Pulps and Characteristics of Acid-Insoluble Residues. *Japan Tappi J.* 51, 1578–1586 (1997).
11. Harsono, H., Samodra, A., Roni, P.: Preparation of dissolving pulp from oil palm empty fruit bunch by prehydrolysis soda-anthraquinone cooking method. *J. Wood Sci.* 62, 65–73 (2016).
12. Tanifuji, K., Takahashi, S., Kajiyama, M., Ohi, H., Nakamata, K.: Advantage of Acid Sulfite Cooking as Processes of Bioethanol Production. *Japan Tappi J.* 65, 494–505 (2011).
13. Castellano, J.M., Gómez, M., Fernández, M., Esteban, L.S., Carrasco, J.E.: Study on the effects of raw materials composition and pelletization conditions on the quality and properties of pellets obtained from different woody and non woody biomasses. *Fuel.* 139, 629–636 (2015).
14. Kaliyan, N., Vance Morey, R.: Factors affecting strength and durability of densified biomass products. *Biomass and Bioenergy.* 33, 337–359 (2009).
15. Lam, P.S., Lam, P.Y., Sokhansanj, S., Bi, X.T., Lim, C.J.: Mechanical and compositional characteristics of steam-treated Douglas fir (*Pseudotsuga menziesii* L.) during pelletization. *Biomass and Bioenergy.* 56, 116–126 (2013)
16. Aziz, M. a., Sabil, K.M., Uemura, Y., Ismail, L.: A study on torrefaction of oil palm biomass, (2012).
17. Bobleter, O.: Hydrothermal degradation of polymers derived from plants. *Prog. Polym. Sci.* 19, 797–841 (1994).
18. Garrote, G., Dominguez, H., Parajo, J.C.: Hydrothermal processing of lignocellulosic materials. *Holz als Roh- und Werkst.* 57, 191–202 (1999).
19. Sevilla, M., Fuertes, a. B.: The production of carbon materials by hydrothermal carbonization of cellulose. *Carbon N. Y.* 47, 2281–2289 (2009).
20. Stelte, W., Clemons, C., Holm, J.K., Ulrik, B.: Fuel pellets from wheat straw : The effect of lignin glass transition and surface waxes on pelletizing properties. *BioEnergy Res.* 5, 450–458 (2012).
21. Kambo, H.S., Dutta, A.: Strength, storage, and combustion characteristics of densified lignocellulosic biomass produced via torrefaction and hydrothermal carbonization. *Appl. Energy.* 135, 182–191 (2014).
22. Mani, S., Tabil, L.G., Sokhansanj, S.: Effects of compressive force, particle size and moisture content on mechanical properties of biomass pellets from grasses. *Biomass and Bioenergy.* 30, 648–654 (2006).
23. Assor, C., Placet, V., Chabbert, B., Habrant, A., Lapierre, C., Pollet, B., Perré, P.: Concomitant changes in viscoelastic properties and amorphous polymers during the hydrothermal treatment of hardwood and softwood. *J. Agric. Food Chem.* 57, 6830–7 (2009).
24. Reza, M.T., Lynam, J.G., Vasquez, V.R., Coronella, C.J.: Pelletization of biochar from hydrothermally carbonized wood. *Environ. Prog. Sustain. Energy.* 31, 225–234 (2012).

25. Gil, M. V, Oulego, P., Casal, M.D., Pevida, C., Pis, J.J., Rubiera, F.: Mechanical durability and combustion characteristics of pellets from biomass blends. *Bioresour. Technol.* 101, 8859–67 (2010).
26. González-Peña, M.M., Curling, S.F., Hale, M.D.C.: On the effect of heat on the chemical composition and dimensions of thermally-modified wood. *Polym. Degrad. Stab.* 94, 2184–2193 (2009).
27. Reza, M.T.: *Upgrading Biomass by Hydrothermal and Chemical Conditioning.* University of Nevada, Reno (2013).
28. Stemann, J., Putschew, A., Ziegler, F.: Hydrothermal carbonization: process water characterization and effects of water recirculation. *Bioresour. Technol.* 143, 139–46 (2013).
29. Biswas, A.K., Yang, W., Blasiak, W.: Steam pretreatment of *Salix* to upgrade biomass fuel for wood pellet production. *Fuel Process. Technol.* 92, 1711–1717 (2011).
30. ENplus: EN plus For Wood Pellets EN plus Handbook Part 3 : Pellet Quality Requirements. (2015).
31. Stelte, W., Clemons, C., Holm, J.K., Sanadi, A.R., Ahrenfeldt, J., Shang, L., Henriksen, U.B.: Pelletizing properties of torrefied spruce. *Biomass and Bioenergy.* 35, 4690–4698 (2011).
32. Lam, P.S., Lam, P.Y., Sokhansanj, S., Lim, C.J., Bi, X.T., Stephen, J.D., Pribowo, A., Mabee, W.E.: Steam explosion of oil palm residues for the production of durable pellets. *Appl. Energy.* 141, 160–166 (2015).
33. Angles, M.N., F, F., X, F., J, S.: Suitability of steam exploded residual softwood for the production of binderless panels . Effect of the pre-treatment severity and lignin addition. *Biomass and Bioenergy.* 21, 211–224 (2001).
34. Adapa, P., Tabil, L., Schoenau, G.: Grinding performance and physical properties of non-treated and steam exploded barley, canola, oat and wheat straw. *Biomass and Bioenergy.* 35, 549–561 (2011).
35. Nielsen, N.P.K., Gardner, D.J., Felby, C.: Effect of extractives and storage on the pelletizing process of sawdust. *Fuel.* 89, 94–98 (2010).
36. Funke, A., Ziegler, F.: Hydrothermal carbonization of biomass: A summary and discussion of chemical mechanisms for process engineering. *Biofuels, Bioprod. Biorefining.* 4, 160–177 (2010).
37. Kambo, H.S., Dutta, A.: Strength , storage , and combustion characteristics of densified lignocellulosic biomass produced via torrefaction and hydrothermal carbonization. *Appl. Energy.* 135, 182–191 (2014).

Chapter 5. Evaluation of the leachate for agricultural purpose

Abstract: Chapter 5 discusses about the possibility to use the leachate from the washing process of HTT-EFB for agricultural purpose. The properties of the leachate were analyzed for its macronutrient, pH and EC. The phytotoxicity effect of the leachate on the plant growth by means of seed germination was also performed and discussed in this chapter. The result showed that EC was acceptable for plant application. Considering the macronutrients amount, this leachate could not be used as a universal fertilizer, but primarily as an organic nutrient supplement. A proper dilution factor was found to reduce the phytotoxicity effect of the leachates to the plant growth.

5.1 Introduction

In the previous chapter, the washing treatment of the hydrochar was conducted following the HTT treatment. The washing process produced a substantial amount of washing water or leachates. In the large scale application, this washing water generally should be treated in the waste water treatment facility before discharge. Because the leachate is considered still rich in potassium content, which contains around 8% of potassium present in the raw-EFB biomass, it is thought that it will become a huge benefit to recycle the nutrient back to the soil and utilize the leachates for further application to fertilize the palm oil plantation.

Therefore, this chapter aims to investigate the possibility to utilize the washing water (or leachates) produced from the previous washing process of hydrochars for organic fertilizer or nutrient recovery. The properties of the leachate were analyzed for its macronutrient, pH and EC. The phytotoxicity effect of the leachate on the plant growth by means of seed germination was also performed and discussed in this chapter. The result will then be used to decide the safety approach when applying the leachate back to the palm oil plantation.

5.2 Material and methods

5.2.1 Washing treatment

The leachate was produced from the washing experiment that follows the HTT experiments. The washing process was applied for different hydrochars obtained from the HTT experiment. The washing experiment procedure has been explained in Chapter

3. Five samples; raw EFB, hydrochar produced at 100 °C (HTT- 100), HTT-150, HTT-180, and HTT-220 were used in the washing experiment. The biomass to distilled water ratio was 1 : 10. After the washing process, the mixture was separated using a vacuum filter. The liquid sample obtained after washing is designated as leachate in this chapter, and named as LW followed by the temperature in which the hydrochar was produced.

5.2.2 Analysis

5.2.2.1 pH and EC

The acidity and the electric conductivity is an important factor for liquid subjected to agricultural purpose. The pH and the EC values of the leachate were determined by using a pH meter (Laqua pH meter F-72, Horiba, Japan) and an EC meter (Laqua Cond meter DS-72, Horiba, Japan). The analyzer was depicted in Figure 5-1.



Figure 5-1. pH meter



Figure 5-2. TOC-L with unit TNM-L

5.2.2.2 Total carbon and total nitrogen

The total carbon (TC) and the total nitrogen (TN) of the produced leachate were analyzed by TOC analyzer (TOC-L) attached with TN unit (TNM-L) (Shimadzu, Japan). The analyzer is shown in Figure 5-2. The basic principle for quantization of the total carbon and the total nitrogen relies on the destruction of material via heat at elevated temperatures. The equipment was operated in the temperature range of 600°C – 800°C. All carbon forms are converted into CO₂, while nitrogen forms are changed into NO.

5.2.2.3 ICP analysis

The macronutrient elements contained in the leachate, in this case the potassium (K) and phosphorus (P), were determined using the ICP emission spectroscopy (ICPS-8100, Shimadzu, Japan). The filtered sample of around 20 ml was prepared for the analysis to prevent clogging in the ICP.

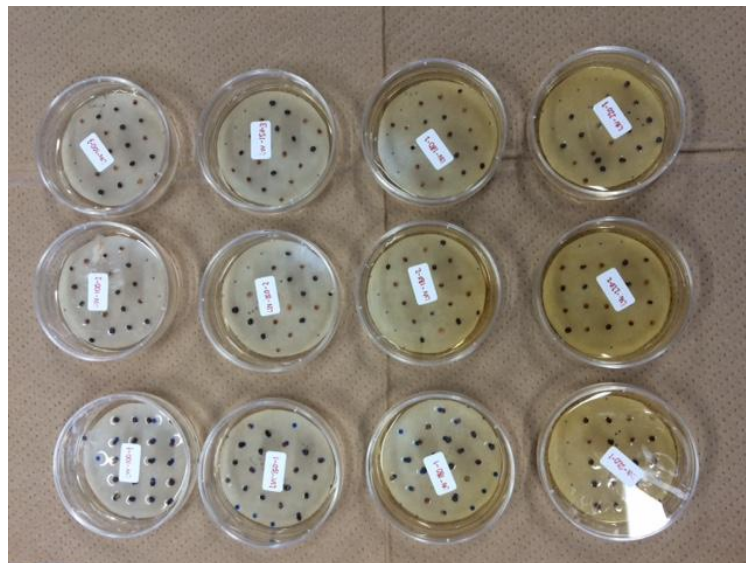


Figure 5-3. Seed germination test

5.2.2.4 Seed Germination

To evaluate the phytotoxicity of the liquid, a germination test was performed. Twenty seeds of komatsuna (*Brassica rapa* var. *perviridis*) were placed in a petri dish containing special filter paper (Tanepita, FHK, Japan), added with 3 ml distilled water as control, or the leachate samples. The leachate samples were diluted to different solutions. The petri dishes were then incubated at 25°C for 96 hours in the dark room. Three replicates were set out for each treatment, including distilled water that was used as a control as presented in Figure 5-3.

After incubated, germinated seeds were counted, and the root and the shoot length were measured. The GI was then calculated using the Germination Index formula [1] as follows:

$$\text{Germination index (GI)} = \frac{S_i \times \text{MRL}_i}{S_c \times \text{MRL}_c} \times 100 \quad (5-1)$$

Where,

S_i = average number of seed germinated in the sample

S_c = average number of seed germinated in the control

MRL_i = average of the root length in the sample

MRL_c = average of the root length in the control

Data were analyzed statistically using ANOVA provided by Data Analysis ToolPack of the Excel and means were compared by Fisher's Least Significant Difference (LSD) test at 5% probability level to determine the significant difference among the various treatment [2].

5.3 Results and discussion

5.3.1 pH and EC of the leachate

The leachate is intended to be use for fertilizing the palm oil plantation. The properties of the leachate were expected to have similar properties of that of mature compost to be applied to the plants. The variations in pH and EC are known to be useful parameters for monitoring the composting process [3]. In addition, pH and EC are considered important compost parameters because they can affect the quality and suitability of the final product for plant growth. The compost pH value ranging from 5.5 to 8.5 is considered to be acceptable and the EC value higher than 1.5 dS/m and 4.0 dS/m are considered to be the upper limit values for growing media and tolerable by plants of medium sensitivity, respectively [1, 4]. The pH and EC values of the leachate produced from washing the hydrochars are shown in Table 5-1.

The increase in the acidity in leachate product was observed with the increase of the HTT temperature, as shown in Table 5-1. pH is near neutral value for leachate coming from hydrochar produced at lower temperature (LW-100). Considering that the distilled water was originally neutral, the acidic condition of the leachates was possibly occurred due to the formation of organic acids that typically took place during the HTT process [5]. The organic acids might be still left in the hydrochar pores, and enter water during the washing process. During HTT, the degradation of hemicellulose, cellulose and extractives produces concentrated sugars and organic acids. These produced sugars and organic acids inside the hydrochar will be extracted during washing and will decrease pH of the leachates. This organic acid extraction finding has also been discussed in

FTIR section in Chapter 3. From Table 5-1, it can be seen that LW-220 has pH as low as 5.24. It was found that more severe decomposition that occurred at a higher HTT temperature will result in more formation of organic acids, thus increases the acidity of the leachate from higher temperature hydrochar. As stated previously, the optimum pH value for plants to take up nutrients that applied to the root zone and foliage is ranging from 5.5- 8.5 [1]. Therefore it can be seen, that only LW-100 and LW-150 is considered acceptable to be applied for plants without dilution.

Table 5-1. The pH and EC values of leachates obtained from washing of hydrochars

Sample	pH		EC(dS/m)	
	average	SD	average	SD
LW-100	6.76	0.09	1.44	0.03
LW-150	6.30	0.08	1.55	0.01
LW-180	5.42	0.02	1.41	0.01
LW-220	5.24	0.03	1.49	0.04

The EC value is usually measured because it reflects salinity of the composting product and its suitability for plant growth [2]. From Table 5-1, it can be noticed that the EC values of the leachates are in the range of 1.41 to 1.55 dS/m, and there is no clear trend in the EC values data. The EC of the leachates were mainly due to the extraction of salt or alkali metal, and the soluble organic ions during washing experiment. The alkali metals would have caused a rise in salinity[5]. The EC value of 1.5 dS/m is considered acceptable [1], because too high concentration of soluble organics can reduce growth because the ions contributing to high EC could compete with fertilizer nutrients for plant uptake. Except for LW-150, the other leachates cannot be considered acceptable for plant growth. Since low pH and high EC may harm to the plant growth, the dilution of the leachates might be a good way to ease the risk when applying as liquid organic fertilizer.

5.3.2 Macronutrient of the leachate

Plants need macronutrients, essential elements required in relatively large amounts, for plant growth. Among them, nitrogen (N), phosphorous (P) and potassium (K) are considered as the primary macronutrients. The macronutrients content in the leachates produced from hydrochar washing were also analyzed, and presented in Table 5-2.

Nevertheless, the macronutrients concentration shown in Table 5 is comparatively not so significant compared with those of commercial liquid fertilizers. The N content in the raw-EFB apparently very low, only 0.6% wt. The HTT process might solubilize some nitrogen from the hydrochars. Therefore, the only source of the nitrogen in the leachates is organically bound N presents in the hydrochar, that commonly hard to be leached out. It can be concluded that the low nitrogen content in liquid residue is attributed to the low initial nitrogen content in raw EFB.

Table 5-2. The macronutrients and the TC values of the hydrochar leachates

Sample	TN (ppm)		P (ppm)		K (ppm)		TC (ppm)	
	average	SD	average	SD	average	SD	average	SD
LW-100	151.2	32.9	6.880	0.06	531.2	3.58	737.3	38.7
LW-150	154.0	25.8	5.820	0.07	491.7	6.22	763.9	10.5
LW-180	235.8	19.8	8.070	0.14	516.6	5.04	1775	39.7
LW-220	203.7	29.4	8.440	0.06	503.6	8.58	1629	17.0

Compared to TN, the potassium (K) content is still quite high. This is due to the extraction of the soluble K^+ during washing. The lignocellulosic breakdown and the porous structure of the hydrochar enlarged the surface area contacted with water, thus enhancing the diffusion of K to water. The phosphorus (P) content is very low in all leachates. Considering its application as fertilizer, the amounts of N, P and K applied with this leachate would only cover a part of crops need, so this leachate could not be used as a universal fertilizer, but primarily as an organic nutrient supplement. The additional organic fertilizer rich in N might be required to increase the nutrient concentration.

5.3.3 C/N ratio

The C/N ratio is an essential agronomic parameter of the final compost product, which plays an important role in release of the nutrients to the soil [6]. A mature compost should have a C/N ratio below 25 and the best ones are preferable below 10 [7]. The C/N ratio is the first important aspect for determining the quality of fertilizers, if the C/N ratio is over than 25, the microbes in soil will surely take the nitrogen for its growth thus the plants will insufficiently absorb nutrient from fertilizers. In addition, if organic fertilizer has the C/N ratio larger than 20:1 (low nitrogen), soil microbes cannot obtain enough nitrogen and cause a loss of plant available nitrogen (deficiency) called immobilization. Therefore the C/N ratio below 10 is preferable so that the balance of nitrogen for microbe's activity and plant growth will be adequately sufficient.

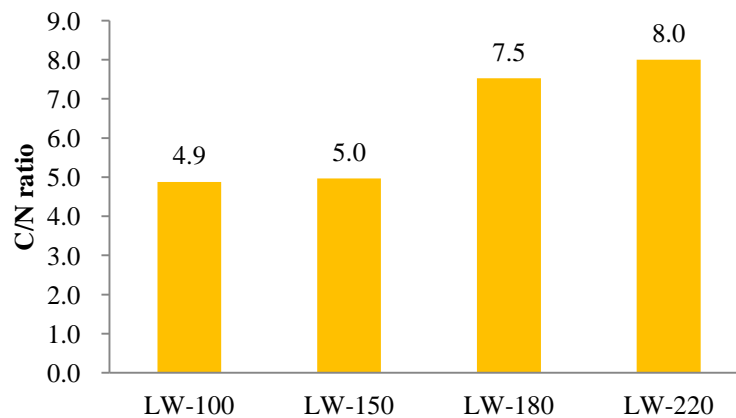


Figure 5-4. The C/N ratio of all the leachate samples

As the HTT temperature increased, more carbon compounds was found in leachates, presented as the total carbon content (TC) listed in Table 5-2. The higher TC in the leachates from the higher temperature hydrochar washing might be due to the sugars, organic acids and their derivatives under the treatment temperature high enough for hemicelluloses and cellulose degradation.

The C/N ratios of the leachates from washed hydrochars are illustrated in Figure 5-4. The C/N ratios trend to be also positively correlated with the increasing HTT temperature, which resulted in the higher C/N ratio, as can be seen in Figure 5-4. The calculated C/N ratios for these leachates are highly determined by the TC content, since the TN content is relatively similar. All leachate samples showed the C/N ratio below 10, with the highest C/N ratios was observed at 8.0 for LW-220, means that the ratios were acceptable. The leachates nutrient content allowed the balance of nitrogen for microbe's activity and considered adequately sufficient for plant growth

5.3.4 Phytotoxicity

It is important to consider the safety requirement since the produced liquid is intended to be used for use in the palm oil plantation. The evaluation of the toxicity by the biological testing was conducted for screening the suitability of waste for agricultural application. The seed germination and the plant growth bioassay are the most common techniques used to evaluate compost phytotoxicity [8]. A seed germination test has been used as rapid, simple, reliable, and reproducible techniques to indicate the damaging effect of land application of animal manure, compost and sewage sludge on the plant growth [9].

Table 5-3. Effect of leachates from washed hydrochars on the germination of Komatsuna seedlings

Dilution	Germination Index (GI)			
	LW-100	LW-150	LW-180	LW-220
No dilution	15.4 ± 22.5ab	29.1 ± 50.4abc	5.3 ± 9.1a	0.0 ± 0.0a
10 times	91.1 ± 17.7bcd	82.2 ± 30.6abcd	123.8 ± 22.3d	145.9 ± 2.5d
20 times	103.5 ± 20.0cd	99.9 ± 22.1cd	119.5 ± 9.5d	131.8 ± 31.3d

The results are the means of three replicates ± standard error. Value followed by the same letter(s) do not differ significantly according to LSD test ($\alpha=0.05$).

The detail of the effect of the leachates from washing process of the hydrochars on the Komatsuna seed is shown in Table 5-3. It was found that using the leachates without dilution in the germination test resulted in the poor germination. The germination index of all the leachates was lower than 30%. Low germination was thought to be due to a too high carbon concentration in the leachates that attributed to the soluble organics and other compounds. The formation of potentially toxic substances like phenols, furfurals

and their derivatives might occur during HTT process, and leached out during washing treatment. At a higher temperature, more organic acids, soluble salts and excessive ions were also dissolved which then could cause fertilizer burn and seed damage. The acidity that has been explained earlier might also contribute to the lower GI.



Figure 5-5. Seed germinated using leachates from washed hydrochars (left: 10 times dilution, right: 20 times dilution)

Dilution to lower concentration has a tendency to increase GI which implies the decreasing of the harmful effect of leachates. Table 5-3 shows that all leachates with 10 times dilution (TC range from 70-180 ppm) gave GI higher than 80%, even GI 145.9% can be obtained from seed germinated by leachate LW-220. It is found that for compost as a reference, GI of $\geq 80\%$ is considered to be phytotoxic free [10]. Therefore the leachates diluted by 10 times did not show any detrimental effect as seen in Figure 5-5.

It is interesting to find that GI of all the 20-times diluted leachates was close to $\geq 100\%$, but in the case of LW-180 and LW-220, GI was lower than the 10 times diluted leachates. Too high dilution might reduce the concentration of the nutrient content in the leachates, particularly the N and P concentrations. Actually, the N and P contents of LW-180 and LW-220 was quite high, however the high TC inhibited the germination.

When the dilution applied, in the case of 10 times dilution, toxic effect is disappeared and the higher nutrient content enhanced the germination. As a result, GI was higher than the 20 times dilution leachates.

Therefore, the dilution factor is one of important keys in the safe application of liquid fertilizer coming from EFB. However, excessive dilution is also not desirable since it will lower the essential nutrient needed for plant growth. The optimized dilution factor should be calculated in order to find the point where it can suppress the phytotoxic effect while maintained enough nutrient for the plants.

5.4 Summary

The evaluation of the leachates produced from the washing treatment of hydrochars has been performed. The properties of the leachate were evaluated by analyzing its macronutrient, pH and EC. The phytotoxicity of the leachate by means of seed germination was also performed. The results were summarized as follows:

1. Only the pH value of LW-100 is acceptable, while the EC value is acceptable for all the leachate samples. The dilution of the leachates might be a good way to ease the risk when applying as fertilizer.
2. Considering its amounts of N, P and K macronutrients, this leachate could not be used as a universal fertilizer, but primarily as an organic nutrient supplement. The additional organic fertilizer rich in N might be required to increase the nutrient concentration.
3. All leachate samples showed the C/N ratio below 10, which is acceptable. The leachates nutrient content allowed the balance of nitrogen for microbe's activity and considered adequately sufficient for the plant growth
4. From the germination test results, the 10 times dilution is enough to safely apply the leachates back to the plantation.
5. The proper dilution factor was able to suppress the phytotoxic effect of the leachates, and the optimized dilution should be calculated to maintain enough nutrient for the plants.

In conclusion, the leachates from the washing process can be applied back to the plantation with a proper dilution factor. This can eliminate the need of water treatment to treat the washing water and reduce the cost of the treatment.

References

1. Silva, M.E.F., Lemos, L.T., Bastos, M.M.S.M., Nunes, O.C., Cunha-Queda, A.C.: Recovery of humic-like substances from low quality composts. *Bioresour. Technol.* 128, 624–32 (2013).
2. Fang, M., Wong, J.W.: Effects of lime amendment on availability of heavy metals and maturation in sewage sludge composting. *Environ. Pollut.* 106, 83–89 (1999).
3. Hosseini, S.M., Aziz, H.A.: Evaluation of thermochemical pretreatment and continuous thermophilic condition in rice straw composting process enhancement. *Bioresour. Technol.* 133, 240–247 (2013).
4. Nakhshiniev, B., Biddinika, M.K., Gonzales, H.B., Sumida, H., Yoshikawa, K.: Evaluation of hydrothermal treatment in enhancing rice straw compost stability and maturity. *Bioresour. Technol.* 151, 306–313 (2014).
5. Funke, A., Ziegler, F.: Hydrothermal carbonization of biomass: A summary and discussion of chemical mechanisms for process engineering. *Biofuels, Bioprod. Biorefining.* 4, 160–177 (2010).
6. Fornes, F., Belda, R.M., Lidón, A.: Analysis of two biochars and one hydrochar from different feedstock: focus set on environmental, nutritional and horticultural considerations. *J. Clean. Prod.* 86, 40–48 (2015).
7. Ahmad, Z., Yahiro, Y., Kai, H., Harada, T.: Factors affecting immobilization and release of nitrogen in soil and chemical characteristics of the nitrogen newly immobilized IV. Chemical nature of the organic nitrogen becoming decomposable due to the drying of soil. *Soil Sci. Plant Nutr.* 19, 287–298 (1973).
8. Bernal, M.P., Alburquerque, J.A., Moral, R.: Composting of animal manures and chemical criteria for compost maturity assessment. A review. *Bioresour. Technol.* 100, 5444–5453 (2009).
9. Kapanen, a, Itävaara, M.: Ecotoxicity tests for compost applications. *Ecotoxicol. Environ. Saf.* 49, 1–16 (2001).
10. Tam, N.F.Y., Tiquia, S.: Assessing Toxicity of Spent Pig Litter Using a Seed Germination Technique. *Resour. Conserv. Recycl.* 11, 261–274 (1994).
11. California Compost Quality Council: Compost maturity index. , California (2001).

Chapter 6. Conclusions and Recommendation

6.1 Conclusions

In this thesis, the study on production of clean and durable pellets from palm oil empty fruit bunch by combination of the hydrothermal treatment (HTT) and the washing treatment has been conducted. The outline of this thesis is illustrated in Figure 6-1. Each chapter has its own objective to be realized.

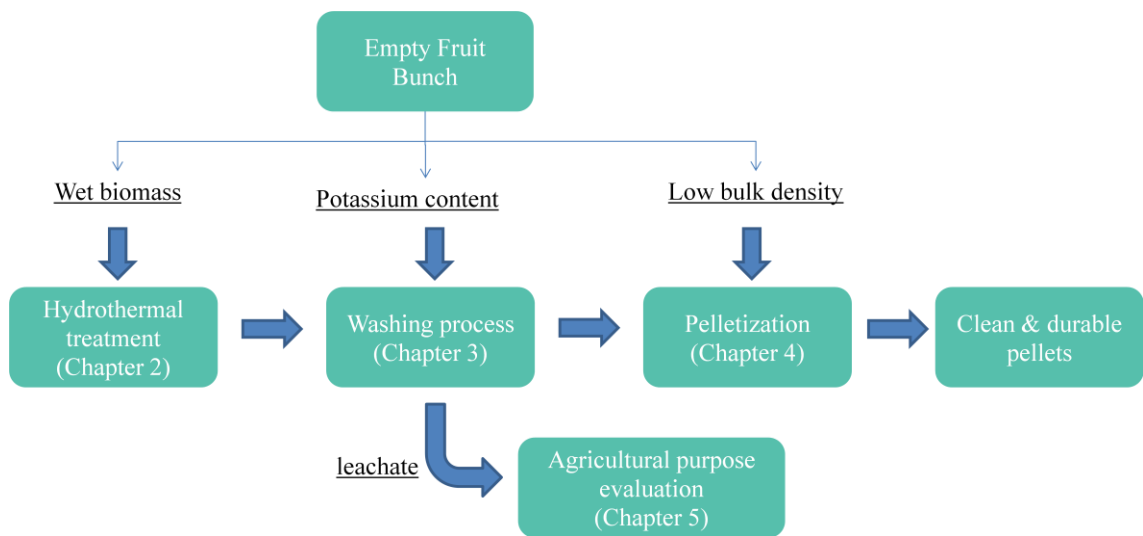


Figure 6-1. Outline of this research

In this section, the general conclusions are drawn regarding the work reported in the previous chapters. The conclusions both in each study can be summarized as follows:

1. Chapter 2, *Hydrothermal upgrading of empty fruit bunch*, showed that the fuel qualities of the product was improved after HTT; such as a higher carbon content, a higher energy density, lower O/C and H/C ratios compared with the raw feedstock. The calorific value of the hydrochar is equal to low-grade sub-bituminous coal. The main reaction pathways that might occur during the HTT process at a mild temperature were the dehydration and the hydrolysis. Considering the energy consumption and fuel property, HTT at 180°C is found to be most favorable for large-scale production of solid fuel from EFB.
2. Chapter 3, *Low potassium fuel from empty fruit bunch via hydrothermal treatment and water washing*, reported that the major removal of potassium was attributed to the HTT process. The 92% potassium removal can be achieved by the HTT and washing co-treatment. The combination also lowered the ash content and the chlorine content of EFB down to 0.9% and 0.19%, respectively. It was found that

180°C was the optimum HTT temperature for the effective potassium removal. Combination of HTT and the water washing improved the slagging and fouling indices, exhibiting positive results in the term of the deposition tendency, thus clarified that the removal of potassium may lead to lower deposition tendency.

3. Chapter 4, *Pelletized fuel from EFB hydrochar and washed EFB hydrochar*, explained that pellets treated by the HTT and washing has better quality; such as high mechanical strength, high durability and resistance to the atmospheric moisture. In addition, it also has lower ash and alkali metal contents. It was found that the changes in the composition of EFB biomass by HTT and the washing process regulates the pelletization behavior and affects the bonding mechanism during the pelletization.
4. Chapter 5, *Evaluation of the leachates for agricultural purpose*, showed that the leachate has an acceptable EC value and acceptable C/N ratio for agriculture. The leachate can be regarded as organic nutrient supplement. Therefore, the leachates from the washing process can be applied back to the plantation with a proper dilution factor. This can eliminate the need of water treatment to treat the washing water and reduce the cost of the treatment.

Finally, the combination of the pelletization, HTT, and the washing co-treatment is promising for upgrading abundant EFB biomass into clean, energy dense, homogenous, friable, durable, and hydrophobic solid fuel that is ready for domestic and international markets, while dealing with the waste EFB problem in the plantation.

6.2 Recommendations

In order to commercialize the integrated process of HTT, the washing treatment and the pelletization, and to better understand the real combustion application of the pellet fuel, the following works are recommended for further studies:

1. In this study, the only dominant variable is considered to be the HTT reaction temperature. Nevertheless, other variables are negligible. To design the HTT process and commercialize it, all the variables need to be considered and optimized. From the previous results, hydrochar produced at 180°C is by far the most promising for bigger scale application considering its energy consumption. The HTC process requires energy to make solid fuel, and it will be extremely useful to study the techno-economic analyses of the bigger scale HTT process to prove the usability of this process.
2. In this study, the gaseous products were ignored, but the gaseous products might have some volatile organic components, which should be considered accordingly. In

this work, the gaseous products were not considered. A detailed study on gaseous products should be conducted to reveal whether they contain high value products

3. In Chapter 3, only the behavior and removal of potassium is considered in the washing treatment. The investigation of other inorganics may give understanding of the all inorganic behavior during HTT and washing. The ash forming elements other than potassium might have a catalytic effect in the combustion and have effect in the ash deposition tendency of the fuel.
4. The pellets were prepared under only one set of operating conditions, which could be optimized by changing the pelletization pressure or temperature. More investigation needs to be conducted for better optimization.
5. Firing or co-firing the pellet fuel with coal in existing coal power plants might be commercially advantageous. Therefore, the combustion test in the lab scale and real combustor (fixed bed or fluidized bed) should be conducted to evaluate the combustion characteristics in the real application. This also can be a good way to investigate and to do validation on the fouling and slagging behavior of the treated pellet fuel in the real combustor.
6. For the overall process systems to produce clean and durable pellets, the studies on the large scale application including the life cycle and socio-economic analyses should be conducted as well.